DEVELOPMENT OF PHOTOREFRACTIVE POLYMERS:

EVALUATION OF PHOTOCONDUCTING AND

ELECTRO-OPTIC PROPERTIES

Thesis submitted to

Cochin University of Science and Technology

in partial fulfillment of the requirements
for the award of the degree of

DOCTOR OF PHILOSOPHY
in Physics
Under the Faculty of Science

by

Kishore V. C.
Applied Optics Division
Department of Physics
Cochin University of Science and Technology
Kochi - 682022, Kerala, India

June 2008

Development of Photorefractive Polymers: Evaluation of Photoconducting and Electro-optic Properties
Ph.D. thesis in Optics

Submitted by,

Kishore V. C.
Dept of Physics
Cochin University of Science and Technology
Kochi - 22, Kerala, India
vckishore@gmail.com

Research Supervisors
Dr. C. Sudha Kartha
Reader, Dept. of Physics
Cochin University of Science and Technology
Kochi - 22, Kerala, India
csk@cusat.ac.in

Dr. K. Sreekumar
Reader, Dept. of Applied Chemistry
Cochin University of Science and Technology
Kochi - 22, Kerala, India
ksk@cusat.ac.in

Front cover : A photorefractive polymer sandwich device.

അച്ഛനുമമ്മയ്ക്കും...

to my parents...

CERTIFICATE

Certified that the work presented in the thesis entitled "Development of Photorefractive Polymers: Evaluation of Photoconducting and Electro-optic Properties" is a bonafide research work done by Mr. Kishore V. C. under our guidance at the Department of Physics, Cochin University of Science and Technology, Kochi, India, and has not been included in any other thesis submitted previously for the award of any degree.

Kochi-22
June, 2008

Dr. C. Sudha Kartha
(Supervising Guide)

Dr. K. Sreekumar
(Co-Supervising Guide)

DECLARATION

I hereby declare that the work presented in this thesis entitled "Development of Photorefractive Polymers: Evaluation of Photoconducting and Electro-optic Properties" is based on the original research work done by me under the guidance of Dr. C. Sudha Kartha, Department of Physics, Cochin University of Science and Technology, Kochi, India and co-guidance of Dr. K. Sreekumar, Department of Applied Chemistry, Cochin University of Science and Technology, Kochi, India, and has not been included in any other thesis submitted previously for the award of any degree.

Kochi-22
June, 2008

Kishore V. C.

Preface

Photorefractive effect was termed an unwanted light induced refractive index inhomogeneity in electro-optic crystals, in 1966. But soon after the initial observation, F. S. Chen et.al. were able to demonstrate holographic recording in the electro-optic crystal $LiNbO_3$ utilizing the photorefractive effect. Research further revealed that this reversible refractive index change was caused by the creation of an internal space charge field which modulates the refractive index of the crystal through electro-optic effect. Thus the basic requirements for observing photorefractive effect was understood, the material must be capable of generating carriers on illumination with light and these carriers must arrange themselves so that a space charge field is created. The next requirement is the electro-optic effect so that refractive index modulation can be achieved in response to the space charge field. Photorefractivity was observed in polymers in 1991 by S. Ducharme et. al. and the latest development is the invention of a 3D updatable holographic display in 2008 by Sava Tay et. al. Photorefractive polymers are proposed materials for reversible holographic data storage. Many groups around the world are actively working in this area. The photoconductor Poly(N-vinyl carbazole) has been the photoconducting host usually reported in all photorefractive composites.

In this thesis, an attempt was made to develop a low cost photorefractive polymer. The steps to achieve the aim was formulated based on the requirements for photorefractive effect. Photoconductivity and electro-optic effect has to be achieved in a single polymer. The experiments conducted for attaining these and the results obtained are elaborated in the different chapters of the present thesis.

Chapter 1 gives the basics of photorefractive effect in polymers. As required by the mechanism, both photoconductivity and electro-optic effect has to be studied. An introduction to the basics of photoconductivity in polymers and various types of photoconducting systems are given. The electro-optic effect is also explained, emphasizing the molecular properties that determines the electro-optic response of the molecules. This chapter also gives the details of the experiential techniques, all of which were setup based on literature information.

In **Chapter 2**, two kinds of photoconducting polymers are given. One is molecularly doped poly(methyl methacrylate) (PMMA) and another based on Poly(2-methacryloyl-1-(4-azo-1'-phenyl) aniline-co-styrene). Molecularly doped poly(methyl methacrylate) was prepared by dispersing the

molecules Aniline and 2,4,6-trinitrophenol (TNP) in PMMA. Aniline is an electron donor while TNP is an electron acceptor. The formation of a charge transfer (CT) complex was evident from the electronic absorption spectrum of the dispersed polymer compared to the neat polymer and the other molecules alone. Temperature dependent current-voltage measurements and room temperature photocurrent measurements were carried out. The spectral dependence of the photoconductivity was also studied. Photoconductive sensitivity, defined as the change in conductivity per incident light intensity, of the molecularly doped PMMA was not sufficient to observe photorefractive effect according to literature values. In addition, molecularly doped systems are liable to phase separation and more stable systems are required to maintain optical quality and stability when molecules are added to the system to give an electro-optic effect. In view of this, single component photoconductors were selected for the study.

The next molecule, is a co-polymer of (2-methacryloyl-1-(4-azo-1'-phenyl) aniline and styrene. It is a non-conjugated polymer but contains electron rich molecular units as pendant to the main chain of the polymer. Optical absorption of the molecule start from 650 nm and peaks in the ultraviolet. The molecule was highly fluorescent but when an electron acceptor molecule C_{60}, was used as dopant, the fluorescence intensity was reduced by $\sim 40\%$. This could be due to the ultra-fast electron transfer reaction reported to occur in C_{60} doped polymers. Photocurrent measurement was done on the single component polymer and the polymer doped with the sensitizer C_{60}. Doping the polymer with C_{60} increased the photocurrent yield in the low energy tail of the absorption spectrum of the polymer. The photoconductive sensitivity of the polymer was evaluated and found to be comparable to the values reported for photorefractive polymers.

Chapter 3 describes the studies on a series of polybenzoxazines, which are photoconductive enough to be suitable for photorefractivity. The molecules were Poly(6-tert-butyl-3,4-dihydro-2H-1,3-benzoxazine, Poly(6-tert-butyl-3-methyl-3,4-dihydro-2H-1,3-benzoxazine) and Poly(6-tert-butyl-3-phenyl-3,4-dihydro-2H-1,3-benzoxazine). Other than C_{60}, the electron acceptor molecules 2,4,6-trinitrophenol (TNP) and 7,7,8,8-tetracyano quinodimethane (TCNQ) were also tried to get an enhancement in photoconductivity. Spectrally resolved photocurrent measurements were done on all molecules in the sandwich cell configuration. Temperature dependence of dark conductivity was also examined. TCNQ and TNP were used as electron acceptors but they were found to be less efficient than the molecule

C_{60}. Out of the three polymers studied, Poly(6-tert-butyl-3-phenyl-3,4-dihydro-2H-1,3-benzoxazine) doped with C_{60} was found to be a highly efficient photoconductive system. Spectral response of photocurrent for this system spanned the entire visible region of the spectrum. It was decided to use this molecule for the development of photorefractive composites.

A series of p-nitroaniline derivatives were examined for possible use as electro-optic molecules for photorefractivity. **Chapter 4** describes the detailed studies done on these molecules. The ground state dipole moment of the molecules was estimated using the Debye Guggenheim method. The excited state dipole moment of the studied molecules was estimated using the solvatochromic method and the value was used to calculate the first hyperpolarizability of the molecules. Solvatochromic effect is the change in the position, intensity, and shape of absorption or emission bands of a molecule due to the change in polarity of the solvent. The analysis was based on a method proposed by Ravi et. al. and used the solvent polarity parameter E_N^T proposed by Reichardt. The figure of merit of the studied molecules were estimated based on the values of first hyperpolarizability and the ground state dipole moment. Out of the ten molecules studied, three molecules possessing relatively higher values for the figure of merit were selected for electro-optic studies.

Chapter 5 deals with the discussion of experiments carried out to determine the electro-optic coefficients possible with the p-nitroaniline derivatives studied in the previous chapter. The molecules were dispersed in poly(methyl methacrylate) and the glass transition temperature of the composite was estimated using differential scanning calorimetry. The composite was sandwiched between two ITO plates and electrically poled at 10V/μm near the glass transition temperature of the composite, so that an alignment of the chromophores could be achieved for higher second order susceptibilities. The samples were studied in the transmission geometry using a modulated ellipsometric technique. The electro-optic coefficients were determined but was found to be small compared to usual photorefractive chromophores in use. Also, these molecules showed phase separation when doped in PMMA to more than 20 wt%. This was a serious limitation for their application to photorefractive polymers where chromophore loading of up to 50 wt% is usually employed to get high efficiency photorefractive polymers.

The polymer Poly[3-methacrloyl-1-(4-nitro-4-azo-1-phenyl)phenylalanine-co-methacrylate was examined next. This molecule possess chiral prop-

erties which is reported to help in maintaining a non-centrosymmetric fashion. This property may result in high electro-optic coefficients. Sandwich cells of this molecule was prepared and examined to evaluate the electro-optic coefficient before poling. Electro-optic coefficient of 4.75pm/V was obtained in this material at a wavelength of 632.8 nm.

In **Chapter 6**, details of the attempts made to prepare a possible photorefractive polymer and also the details of the beam coupling experiment done are given. Based on the studies done in the previous chapters, combinations of different molecules were tried for preparing a photorefractive polymer. The effect was observed in the composite Poly(6-tert-butyl-3-phenyl-3,4-dihydro-2H-1,3-benzoxazine) doped with C_{60} along with the known electro-optic molecule Disperse Red 1 (DR 1). The photorefractive devices for experiments were prepared by melting a vacuum treated powder of the composite on a patterned ITO glass cell. The Photoconductivity of the prepared composite was also studied along with tests for electro-optic effect. Photoconductive sensitivity of 1.25 x 10^{-10} S cm/W was obtained. The refractive index modulation was dominated by the orientational birefringence. This meant that the reorientation of the doped molecules was significant due to the low glass transition temperature (33^0C) of the composite. Two beam coupling experiments were carried out on this composite to test for photorefractive effect. Beam coupling was observed in the composite. The photorefractive gain obtained was 8.8 cm^{-1} at 62.5 V/μm. This was smaller than the absorption loss (73 cm^{-1}) in the device so that an effective gain could not be achieved.

The thesis is concluded by giving the main results of this work and steps for improving the observed photorefractive effect to the level of an application in **Chapter 7**.

Publications in peer reviewed journals

1. Photoconductivity in molecularly doped poly(methyl methacrylate) sandwich cells, V. C. Kishore, R. Dhanya, C Sudha Kartha, K Sreekumar and Rani Joseph, Journal of Applied Physics, Vol 101, 063102 (2007).

   (This article was selected also for inclusion in Virtual Journal of Nanoscale Science & Technology - April 2, 2007, Volume 15, Issue 13).

2. On the Dipole Moments and First-order hyperpolarizability of N, N-bis(4-bromobutyl)-4- nitrobenzenamine, V. C. Kishore, R. Dhanya,

K Sreekumar, Rani Joseph and C Sudha Kartha, Spectrochimica Acta Part A, 2007 (Accepted, in press).

3. Spectral distribution of photocurrent in poly(6-tert-butyl-3-methyl-3,4-dihydro-2H-1,3-benzoxazine), V. C. Kishore, R. Dhanya, K. Sree kumar, Rani Joseph and C. Sudha Kartha, Synthetic Metals, 2008 (Accepted, in press).

4. Ground state and excited state dipole moments of alkyl substituted para-nitroaniline derivatives. Dhanya R, Kishore V C, Rani Joseph, Sudha Kartha C and Sreekumar K. Spectrochimica Acta Part A, 2008 (Accepted, in press).

Conference Presentations

1. Photophysical and electrochemical investigations on photoconducting poly (6-tertiary-butyl-3, 4-dihydro-2H-1, 3- benzoxazine) Dhanya R., Kishore V.C., Sreekumar K., Sudha Kartha C., Rani Joseph. International conference POLYCHAR-16, Feb. 17-22, 2008, Lucknow, India (Won IUPAC Best student poster award and Prof. Brar best student poster award).

2. The photocurrent action spectrum of poly(6-tert-butyl-3-methyl-3,4-dihydro-2H-1,3-benzoxazine)/poly(methyl methacrylate) blend, V. C. Kishore, R. Dhanya, K Sreekumar, Rani Joseph and C Sudha Kartha. International conference POLYCHAR-16, Feb. 17-22, 2008, Lucknow, India.

3. Electric field dependence of thermal activation energy in poly(4TBU)/poly(methylmethacrylate) blend, Kishore V. C., Dhanya R., Sreekumar K., Rani Joseph and C. Sudha Kartha, International Workshop on the Physics of Semiconductor Devices (IWPSD-2007), Dec. 16-20, 2007, IIT Bombay, Mumbai, India.

4. Photoconduction in Polymethyl methacrylate/4-tertiary butyl phenol formaldehyde resin blend. R. Dhanya, V. C. Kishore, C. Sudha Kartha, K Sreekumar and Rani Joseph, International Conference Photonics 2006, Hyderabad 12-16 Dec. 2006.

5. Solvatochromatic Study of the Ground and Excited State Dipole Moments of N, N-bis(4-(2-ethylamino) butyl)-4-nitrobenzenamine. V. C. Kishore, R. Dhanya, C Sudha Kartha, K Sreekumar and Rani

Joseph, International Conference Photonics 2006, Hyderabad 12-16 Dec. 2006.

6. Photoconductivity in molecularly doped PMMA at low electric fields. V. C. Kishore, R. Dhanya, Cheranellore Sudha Kartha, Krishnapillai Sreekumar and Rani Joseph, International Conference on Optoelectronic Materials and Thin films for Advanced Technology, Cochin - 24-27 Oct. 2005.

7. Three-Dimensional Self -Written Optical Waveguide in a photopolymer, C. P. Jisha, Beena Mary John, V. C. Kishore, V.C. Kuriakose, K. Porsezian and C. Sudha Kartha. International Conference on Optoelectronic Materials and Thin films for Advanced Technology, Cochin - 24-27 Oct. 2005.

8. Low field extrinsic photoconductivity in Aniline doped PMMA, Kishore V. C., R. Dhanya, Cheranellore Sudha Kartha, K. Sreekumar and Rani Joseph, International Conference on Optics & Optoelectronics, Dehradun - 12-15, Dec. 2005.

Acknowledgements

First and foremost I would like to thank my teacher and guide Dr. C. Sudha Kartha. Right from my M.Sc. project days, when I came up with a simple but successful recording configuration (we still use it!) and a hologram on a photopolymer material for the first time in our lab, she was there with constant inspiration. I am thankful for the immense freedom she offered me during the course of this work. I am also grateful to her for the keen interest and critical yet constructive comments.

I would like to express my sincere gratitude to Prof. Rani Joseph and Dr. K. Sreekumar, my co-guides, for their timely help, support, prayers, love and able guidance throughout my work. I would also like to thank Prof. K. P. Vijayakumar, from whom I learned the basics of research.

I gratefully acknowledge the financial assistance given by the Department of Science and Technology (DST), Govt. of India. I also thank Cochin University of Science and Technology (CUSAT) for providing me fellowship during the initial stages of this research work.

I would like to thank Head, Dept. of Physics for permitting me to use all facilities available in the department without any restrictions or delay. I am thankful to all my respected teachers in the Dept. of Physics for their kind attitude and support. I am also thankful to all the office and library staff, past and present, of the Department of Physics for the help and cooperation I received from them.

I extend my sincere thanks to Head, Dept. of Polymer Science and Rubber Technology for permitting me to use the facilities in the department. I am also thankful to all members of the Dept. of PS&RT for their kind attitude towards me. I would also like to thank Dr. Gireesh Kumar, Dept. of Applied Chemistry for the permission to do experiments in his lab.

I would like to thank Murali sir of the Dept. of Instrumentation for the assistance I received during the course of my work, especially with the instrumentation part of the experiments. I am thankful to Mr. Joshi for his able assistance.

I would like to thank all my friends in the Department of Physics for their timely help. I express my sincere thanks to Deepa K. G., R. Jayakrishnan, R. Sreekumar, Tina S., Sajeesh, Anitha, Pramitha, Vimalkumar, Angel Susan, Nimmy, Rajesh C S, Jaffer, Poornima, Rajesh Menon, Rajesh Mon, Sreeroop, Subrahmanyan, Amarnath, Saji, Joshy sir, Senoy and

Manu Punnen John. I also thank my seniors Dr. Ramkumar S, Dr. Paulraj M, Dr. Teny Theresa John and Dr. P. M. Ratheesh Kumar.

I reserve my gratitude to Vinu Namboory and Ajimsha R. S. They were always there to listen, help and support me in every possible way. I would like to thank Jisha, Chitra Nayak and R. Radhakrishnan.

I am thankful to Dhanya, her abilities in synthesis definitely requires a word of appreciation. I am thankful for the support she extended to me. I would also like to thank Kapil and Kiran, my younger brothers, for their understanding and help. I would like to thank my parents, my loving parents, for always being there for me. I am thankful for their never ending patience.

Finally, I thank **Him** for the blessings showered onto me.

Kishore V. C.

CONTENTS

CHAPTER

ONE

Photorefractive Polymers - An Introduction

The photorefractive effect was observed for the first time in $LiNbO_3$ and $LiTiO_3$ crystals, and reported as an unwanted refractive index inhomogeneity caused by light.[1] The first paper stated *"The effect, although interesting in its own right, is highly detrimental to the optics of nonlinear devices based on these crystals"*. Soon after the first observation, holographic storage was demonstrated in $LiNbO_3$ using 488nm wavelength and a diffraction efficiency of 40% was obtained.[2] The refractive index modulation was shown to be by an internal space charge field produced due to the generation and subsequent diffusion of charges following laser illumination.[3] Now, years after, scientists have realized 3D holographic dynamic displays based on photorefractive materials.[4] This chapter tries to give an introduction to this interesting topic and outlines the mechanisms and necessary theoretical insight.

1.1 The photorefractive effect

The term photorefraction represents a light induced change of the refractive index, but the term is reserved only for the above mechanism as other physical or chemical reasons can also cause a light induced refractive index modulation. Photorefractive effect in an organic crystal[5] was reported in

1990 and the effect was reported in a polymer composite in 1991.[6] As required by the unique mechanism, the photorefractive effect is observed in materials possessing both photoconductivity and electro-optic response. The basic mechanism is schematically shown Fig. 1.1. If a photorefractive material is illuminated by a non-uniform pattern of light produced by the interference of two mutually coherent optical fields, charge generation will take place at the brighter areas of the pattern.[7] Due to the concentration gradient, or due to the presence of an external electric field, the generated charges (those surviving geminate recombination) move towards the darker regions. In a photorefractive polymer material, one charge is highly mobile than its counter charge. In most of the organic materials, the hole mobility is greater. Thus the electron is considered localized near the generation site while the hole migrates and get trapped in the darker regions. The resulting charge distribution will produce an internal space charge field. The final step is the alteration of the local refractive index of the medium by this space charge field due to electro-optic effect.[8]

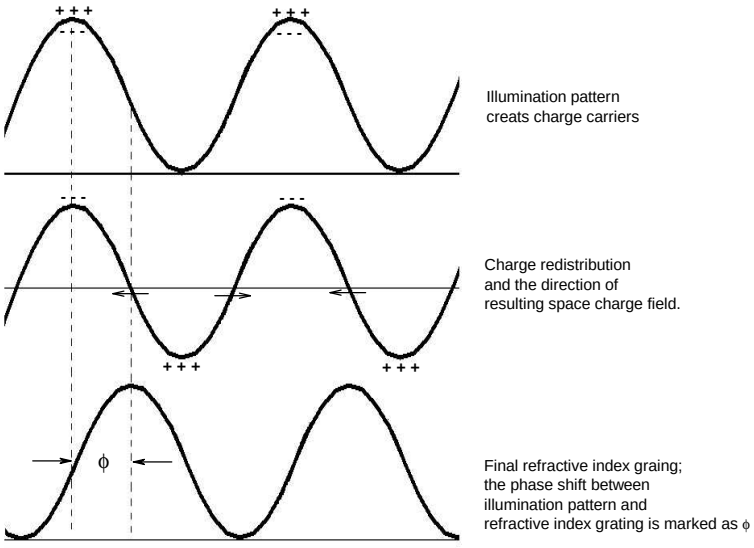

Figure 1.1: Illustration of the photorefractive grating formation.

Photorefractive media can store a replica of the incident non-uniform in-

tensity pattern as a refractive index grating. So many applications have been proposed in the literature using photorefractive materials. Multiplexed data storage,[9] holographic filters,[10] neural networks[11] are a few examples of demonstrated applications.

1.1.1 A model of the photorefractive effect

The Kukhtarev model which was originally developed for the photorefractive effect in inorganic crystals is considered to be the standard model of photorefractive effect. This model is also applicable to photorefractive polymers. The description provided here is based on the book by H. S. Nalwa et. al.[12]

If two mutually coherent laser beams of intensity I_1 and I_2 interfere in a medium, the result is an interference pattern with an intensity distribution given by,

$$I(x) = I_0[1 + mcos(\frac{2\pi x}{\wedge})] \tag{1.1}$$

where $I_0 = I_1 + I_2$ is the sum of the incident intensities, $m = 2\sqrt{I_1 I_2}/(I_1 + I_2)$ is the fringe visibility and $\wedge$ is the periodicity of the interference pattern which is dependent on the angle of incidence of the two beams.[13]

$$\wedge = \frac{\lambda_0}{2nsin(\frac{\theta_2 - \theta_1}{2})} \tag{1.2}$$

Here n is the refractive index of the medium, λ_0 is the optical wavelength in vacuum, and θ_1 and θ_2 are the internal angles of incidence.

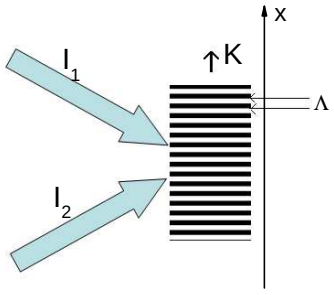

Figure 1.2: Formation of interference fringes by two coherent laser beams.

Following the creation of this periodic interference pattern in the photorefractive medium is the generation of excess charge carriers at the bright areas. The carriers, ideally one type of carrier, migrate from high intensity regions to darker regions of the fringes. The carrier generation and transport processes are discussed in Section 1.4. At darker regions, the optical excitation is negligible and these charges get trapped. Thus a periodic space charge field is generated which resembles the fringe pattern. The amplitude of the space charge field is given by,[12]

$$E_{sc} = m \left[\frac{(E_0^2 + E_D^2)}{(1 + E_D/E_q)^2 + (E_0/E_q)^2} \right]^{1/2} \tag{1.3}$$

E_0 is the component of the applied electric field along the direction of the grating vector. E_D is called the diffusion field, given by $\mathrm{E}_D = \mathrm{K}k_b\mathrm{T}/\mathrm{e}$ and $\mathrm{E}_q = \mathrm{eN}_T/\mathrm{K}\epsilon\epsilon_0$ is called trap limited field. In these equations, K is the grating vector, k_b is the Boltzmann constant, T is the temperature, ϵ is the dielectric constant, ϵ_0 is the permittivity of vacuum, N_T is the density of traps and e is the elementary charge. As shown in Fig. 1.1 there is a phase shift ϕ between the incident pattern and resulting space charge field. This phase shift is the result of the migration of the charges and is given by,

$$\phi = arctg \left[\frac{E_D}{E_0} \left(1 + \frac{E_D}{E_q} + \frac{E_0^2}{E_D E_q} \right) \right] \tag{1.4}$$

Final step is the modulation of the refractive index by an electro-optic effect. If the index modulation is purely due to the linear electro-optic effect, the refractive index modulation is given by,

$$\triangle n(x) = -\frac{1}{2} n^3 r_{eff} E_{sc}(x) \tag{1.5}$$

Here n is the average refractive index of the material and r_{eff} is the effective electro-optic coefficient. The electro-optic effect is discussed in Section 1.5.1. The model described here was modified by Schildkraut et. al. to incorporate some of the important features of carrier generation and trapping in polymers.[14] In this model, an additional trap level was introduced from which carriers can be thermally released.

1.2 The two beam coupling effect

The unique property that makes photorefractive effect different from other mechanisms capable of creating gratings is the phase shift between the incident pattern and the resulting grating. This phase shift is unique to photorefractive effect due to the very nature of the grating formation mechanism itself.[7,15] Due to this phase shift there exists an asymmetric energy exchange between two mutually coherent beams interacting inside a photorefractive medium.[16] This energy exchange is considered to be the signature of photorefractive effect.[17]

The beam which gains intensity is termed as the gain beam and the other beam is called the pump beam. The change in intensity of each beam along the z axis can be obtained from the coupled wave analysis and are given by the following equations.[17]

$$\frac{\partial I_1^{0.5}}{\partial z} = -\left(\frac{\pi \triangle n}{\lambda}\right)(I_2)^{0.5} \tag{1.6}$$

$$\frac{\partial I_2^{0.5}}{\partial z} = -\left(\frac{\pi \triangle n}{\lambda}\right)(I_1)^{0.5} \tag{1.7}$$

The energy exchange in a photorefractive medium is described by the gain coefficient Γ given by,[18]

$$\Gamma = \frac{4\pi}{\lambda}(\hat{e}_1.\hat{e}_2^*), \triangle n sin(\phi) \tag{1.8}$$

where $\hat{e}_i$ are the polarization vectors of the interfering beams. The gain factor γ_0, defined as the gain beam intensity with the pump beam on divided by its intensity with the pump beam off, is evaluated first. The gain factor and gain coefficient Γ are related according to,[18]

$$\Gamma = \frac{1}{l}[lnb\gamma_0 - ln(1 + b - \gamma_0)], \tag{1.9}$$

where $b = I_2/I_1$ is the ratio of the intensities of the interacting beams and l is the interaction length inside the medium. The direction of energy transfer depends on the sign of the gain coefficient and the refractive index modulation ($\triangle n$).

1.3 Photorefractive polymer classes

The photorefractive effect was observed for the first time in $LiNbO_3$ and $LiTiO_3$ crystals. The effect in an organic crystal was reported in 1990[5] with the subsequent report of the observation in a polymer in 1991.[6] As photoconductivity and electro-optic response are among the requirements of photorefractive effect, a variety of reports came in the literature demonstrating the photorefractive effect in polymeric systems that possess both these properties. Among the various classes of photorefractive polymers, the guest-host systems offer the maximum flexibility and tunability of properties as each active component of such a system is simply doped in to a selected polymer host.[19] The main drawback of these systems is the phase separation of the doped components. In some systems molecules capable of showing both photoconductivity and electro-optic response, which are termed as bifunctional molecules, are doped to reduce the chances of phase separation and to increase the overall stability of the system. The molecule 1,3-dimethyl-2,2-tetramethylene- 5-nitrobenzimidazole can act as a bifunctional molecule and a system with this molecule and poly(methyl methacrylate) as host showed a diffraction efficiency of 7% and a two beam coupling gain of 34 cm^{-1}.[20]

Photorefractive polymer systems were also reported with an electro-optic polymer as host and charge transporting molecules as dopant. In fact, the first reported photorefractive system belong to this class. In this, the electro-optic polymer bisphenol-A-diglycidylether 4-nitro-l,2-phenylenedia mine was made photoconductive by doping with the hole-transport agent (diethylamino)benzaldehyde diphenylhydrazone.[6] Another approach was to use a charge transporting polymer as host for electro-optic molecules. The highest diffraction efficiency (near 100%) was reported for such a guest-host polymer system.[16] Here, the active molecules were 2,5-dimethyl-4-(4-nitrophenylazo)anisole as electro-optic chromophore, Poly(N-vinyl carbazole) as charge transport polymer, N-ethylcarbazole as plasticizer and 2,4,7-trinitro-9-fluorenone as sensitizer. Phase separation and stability issues made the introduction of another type of photorefractive systems in

which all the required components are chemically attached to the polymer.[21] These polymers, called fully functionalized polymers, are stable against phase separation.[22] The main disadvantage is the preparation of the polymer itself as lengthy and complicated procedures may be required for the synthesis.

The following sections discusses the basic processes of carrier generation, transport, trapping and electro-optic effect along with some theoretical aspects. Experimental techniques, all of which were set up based on literature, are discussed in later sections.

1.4 Photo-induced carrier generation and transport

Photoconductivity refers to the increase in electrical conductivity when a material is exposed to electromagnetic radiation of appropriate energy. Photoconducting materials are usually insulators in the absence of light but become more conductive upon irradiation with light, which means that excess movable charge carriers are generated in the material on exposure to light. Thus a photoconductor must,[23]

- Absorb light to create pairs of charge carriers (electrons and holes), which can be separated under an electric field of required magnitude. In the ideal case, each absorbed photon creates an electron-hole pair.
- Permit transport of the carriers under the applied electric field towards the appropriate electrodes.

Photogeneration of carriers in polymers is believed to be a multi-step process involving the creation of intermediate states rather than direct generation of carriers following absorption of light. The photogeneration and transport of carriers in organic photoconductors have been of great interest for application in xerography.[24]

1.4.1 Carrier generation in polymers

The initial process is the absorption of a photon at the charge generation site. The absorbed energy leads to the formation of an excited state, which is stable for a characteristic life time. The excited state may have a high electric dipole moment in a suitable material due to charge separation, this is called a charge transfer (CT) state. If unperturbed, the excited species may relax back to the initial state releasing the absorbed energy as a photon of light. It can also undergo a non-radiative relaxation by giving away the energy to collective thermal modes within the material.[25,26]

The next step is the creation of coulombically bound pair of charges from the excited species, the efficiency of which is called the primary quantum yield of bound pairs. The two opposite charges of the bound pair can undergo recombination. If an initially generated electron-hole pair recombine, the process is termed as geminate recombination. If the pair that recombine was generated independently, the process is bimolecular recombination.[27] The bound pair can be separated by the energy from a thermal environment, or from an applied field.[26] The model proposed by Onsager in 1934 addresses the mathematics of field assisted escape from geminate recombination. In the case of organic semiconductors, geminate recombination proceeds via the recreation of the first excited state (CT_1) and the relaxation of this state to the relatively unpolar ground state, CT_0. The life time of the CT_1 state determines the rate of relaxation and it is electric field dependent.[26,28] Figure 1.3 is a pictorial representation of the discussed processes.

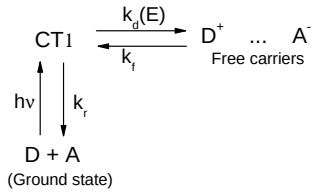

Figure 1.3: Representation of the steps towards carrier generation and recombination in organic media as per the model of Braun.[28] k_d, k_r and k_f are the rate constants associated with each process.

The binding energy of the initial charge separated state (CT_1) is given by,[26]

$$\triangle E \approx \frac{e^2}{4\pi\epsilon\varepsilon_0 a} \tag{1.10}$$

Here, a is the separation between the bound charges. ϵ, ε_0 and e are the dielectric constant, permittivity of free space and the electronic charge respectively.

If the material supports the creation of excitons, there exists a possible alternative route to a CT_1 state, i.e., through the creation of an exciton. An exciton can be considered as a distortion of the electronic states that persists long enough so that diffusion of the energy contained within it can be possible. An exciton can also be considered a species with absorption spectrum different from the molecule in the ground state and show fluorescence and stimulated emission.[29] The exciton can dissociate at impurity sites, interfaces with asymmetric ionization potentials or it can be dissociated by a strong electric field.[30,31] The exciton can diffuse to the site with a different electron affinity, at which a CT_1 state can be formed as the exciton decays.[26] This is shown schematically in Fig. 1.4.

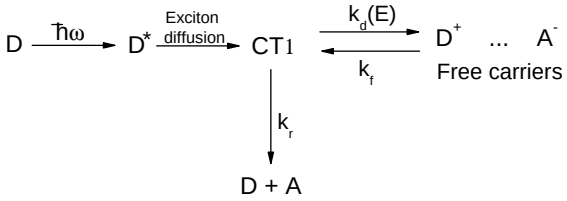

Figure 1.4: The model of Goliber and Perlstein describing the creation of the CT_1 state through the generation and diffusion of an exciton.

The creation of CT_1 state is efficient if the exciton diffusion length (l) defined by Eq. 1.11 is longer than the distance to the site of ionization potential mismatch or impurity.

$$l = \sqrt{D\tau} \tag{1.11}$$

Here, D is the diffusion coefficient of the exciton and τ is the lifetime of the exciton. If L is the thickness and α, the absorption coefficient, in the limit L >> l (thick film) and α^{-1} >> l (low absorption), CT_1 states are photogenerated with a rate proportional to the product of absorption coefficient, diffusion length and the intensity absorbed.[26]

1.4.2 Carrier transport in polymers

The second requirement for photoconductivity is the transport of created charge carriers by the medium. In organic materials, the electronic interaction between the molecules constituting the solid is weak and the relative dielectric constant (ε) is low. The weak interaction implies narrow valence, conduction and exciton bands. The low dielectric constant makes coulombic interactions to play a major role.[32] In contrast to inorganic crystalline semiconductors, where charge transport proceeds through well defined bands, in organic semiconductors carrier transport proceeds via hopping within a positionally random (positional disorder) and energetically disordered system of localized states.[33] The terms positional and energetic disorder implies that the distance between hopping sites and the energy required to hop from one localized state to the other vary significantly.

The photogenerated or injected carrier move within the transporting medium in the general direction of the applied electric field. Carriers reside in localized states (traps) most of the time and are released only if sufficient energy is available to hop to the next available transport state.[34] This is the reason for the extremely small mobilities observed in photoconducting polymers. Usually the carrier mobility is low and is in the range 10^{-2} to 10^{-8} cm^2/Vs. Carrier mobility in polymers can be determined using the time of flight (TOF) technique described in Section 1.6.1.[35] Mobility in polymers is field and temperature dependent due to the very nature of the transport process itself. Gill's model proposes that temperature and field dependence of mobility must be $\log \mu \propto 1/T$ and $\log \mu \propto E^{1/2}$. In another model due to Bässler, the temperature dependence has the form $\log \mu \propto 1/T^2$ and field dependence $\log \mu \propto E$.[32]

1.4.3 Carrier trapping

Carrier traps are electrically active defects or sites capable of immobilizing a moving carrier. Traps are usually classified in terms of their location (interfacial and bulk), depth (deep and shallow) and origin (extrinsic and intrinsic).[36] These states have high influence on the carrier mobility in a transporting polymer. According to the classical semiconductor theory, states below the conduction band, which are able to capture electrons are electron traps and states above the valence band which can capture holes are hole traps. Both hole and electron traps are located between the conduction and valence band edges of the semiconductor.[37] In the case of organic semiconductors where no well defined conduction or valence bands are available, transport occurs by hopping between localized states. These localized states can be either trap states or transport states. For distinguishing a transport state from a trap state, the concept of transport energy was introduced.[38,39] It describes the energetic position of transport levels through which hopping takes place. If the energetic position of a localized state is below the transport energy, it will be considered as a trap. States above the transport energy are transport states through which hopping occurs.

In polymers, addition of molecules with ionization potential lower than the polymer host will give rise to hole trapping. Holes will remain trapped at these locations until an electron from a neighboring electron rich unit gains sufficient energy and move to the trap. It is reported that at higher number densities such trap states can form alternate transport levels.[40]

1.4.4 Photoconductivity

In photoconductors, electrons and holes, are generated by the action of light. Only polymers capable of both generating charge carriers upon exposure to light and transporting them through the bulk are true photoconductors. The charge generation may also take place in an adjacent photoactive layer, and the carrier may be injected into a polymer which act as a charge transporting material only.[24] In most amorphous organic

media it is hole transport that is most significant.[41] A hole (an electron vacancy) can move through the material while the negative charge remains immobilized and bound to the site of creation, which is therefore an anion.

If a photoconductor is irradiated with appropriate radiation, carrier generation and recombination will take place. After reaching an equilibrium, the steady state carrier density will be,[23]

$$n_0 = G\tau \tag{1.12}$$

Here G is the rate at which carriers are photogenerated within the photoconductor and τ is the average time between generation and recombination of a carrier (recombination time). The corresponding photoconductivity is given by,

$$\sigma_{ph} = n_0 e\mu = G\tau e\mu, \tag{1.13}$$

where e is the electronic charge and μ is the mobility, which is defined as the velocity of the carrier in unit electric field. If the electrical contacts provided to the photoconductor are ohmic in nature, the steady state carrier density will not be affected by the application of an external voltage to measure the light induced change in conductivity.[23] The steady state photocurrent density is given by,

$$J_{ph} = \sigma_{ph} E = G\tau e\mu E \tag{1.14}$$

In the above equation, E is the electric field applied to the photoconductor. The number of generated charges per absorbed photon is called the internal quantum efficiency and is given by Eq. 1.15.[14]

$$\Phi_{int} = \frac{hc}{e\lambda ln(\alpha)L}\frac{J_{ph}}{I} \tag{1.15}$$

Here I is the intensity of incident light, L is the thickness of the photoconductor, α is the absorption coefficient and λ, the wavelength of light. The material parameter of interest is the change in conductivity per incident light intensity, called the photoconductive sensitivity. If I_{ph} is the photocurrent, P_0 the light power density, A the illuminated area and V the applied voltage, photoconductive sensitivity (S) is given by,[42]

$$S = \frac{I_{ph}L}{P_0 AV} \tag{1.16}$$

Photoconductive sensitivity has the unit S.cm/W. Most of the polymers are photoconducting only in the ultraviolet and thus suitable dyes are used to extend their spectral sensitivity to the desired region. The photoconductor poly(N-vinyl carbazole) (PVK) has been the subject of intense studies as it could give good photocurrents when doped with the electron acceptor 2,4,7,-trinitro-9-fluorenone (TNF).[24,43] Fig. 1.5 shows the chemical structure of these molecules.

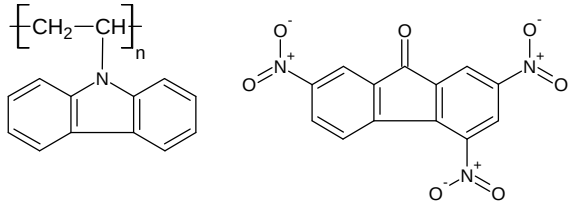

Figure 1.5: Structure of (a) Poly(N-vinyl carbazole) and (b) 2,4,7,-trinitro-9-fluorenone.

1.4.5 Role of photosensitizer molecules

Polymers studied for photorefractive application must not be strongly absorbing at the wavelength region of operation. This requirement is met by the use of polymers with wider optical gaps. A wide gap between the highest occupied molecular orbital (HOMO) and lowest unoccupied molecular orbital (LUMO) lead to optical absorption near the ultra-violet region of the spectrum. As strong absorption lies outside the visible region, charge photogeneration at the wavelength of interest is brought about by the addition of small concentrations of molecules with appropriate HOMO and LUMO levels compared to the host polymer.[24] Lower HOMO and LUMO levels than the host matrix are preferred for this purpose. These molecules are called photosensitizers. Details of the molecules examined in the present work for photosensitizing the polymer are given in Section 1.4.6.

Photoinduced charge transfer initiated by a sensitizer depends on many

factors. The following condition must be satisfied for an efficient charge transfer.[44]

$$I_{D^*} - A_s - U_c \leq 0 \tag{1.17}$$

Here, I_{D^*} is the ionization potential of the excited state of the polymer (donor), A_s electron affinity of the sensitizer molecule and U_c denotes the coulomb attraction of the separated radicals. Polarizability of the surrounding matrix plays an important role here.[45] This condition alone may not ensure an efficient charge transfer. The morphology of the polymer which introduce a large separation between the donor and the acceptor or a potential barrier which prevent the separation of the electron-hole pair are two other factors which may prevent an energetically allowed charge transfer process.[44] Depending upon the polymer host, the sensitizer needs to be either an electron acceptor or an electron donor. If the host is hole transporting, the sensitizer must be an acceptor which forms radical cations on photo-excitation. The charge transport is due to a series of electron transfer processes between charged and neutral units or transport is essentially a series of oxidation/reduction steps of molecular units involved. Charge generation, transport and trapping are the important requirements for photorefractive effect. The next requirement is refractive index modulation through electro-optic effect. Section 1.5 deals with the origin of this nonlinear optical effect in molecular systems.

1.4.6 Sensitizer molecules for photoconductivity

Most of the photoconducting polymers of interest are sensitive only in the ultra-violet (UV) region of the spectrum. Sensitizer molecules are used to extend the photocurrent generation ability of a given polymer to longer wavelengths. Important sensitizers are phthalocyanines, squaraines, azo dyes, perylene dyes, and thiapyrylium salts.[24,46] The charge-transfer (CT) complexes formed between a donor like and an acceptor like molecules or moiety comprises an important class of sensitizers. The well known PVK:TNF complex is an example.[43] A molecule or atom with low ioniza-

tion potential can be considered as an electron donor. Electron acceptors are atoms or molecules which posses a positive electron affinity.[47] These molecules are termed according to the type of molecular orbital donating or accepting electrons, e.g. σ and π donors or acceptors.

All molecules used in the present research study are strong electron acceptor molecules, their chemical structure are shown in Fig. 1.6.

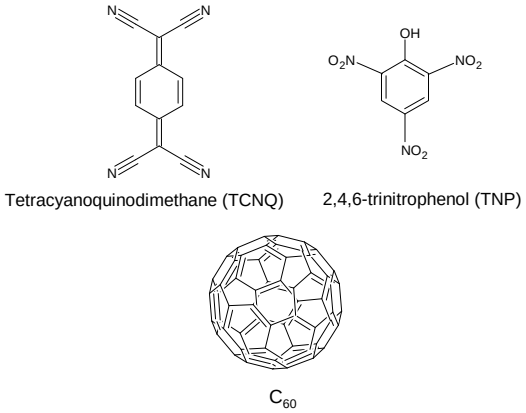

Figure 1.6: Structure of the electron acceptor molecules

The electron affinity (EA) of 7,7,8,8-tetracyanoquinodimethane (TCNQ) was given to be 2.83 eV.[48,49] The ionization potential (IP) of TCNQ was reported to be 7.8 eV.[50] From the experimental value of the optical gap (2.85 eV), the LUMO of this molecule can be calculated to be 4.95 eV. This value is consistent with the reported solid state electron affinity (4.5eV)[51] of TCNQ assuming 0.45eV for the binding energy of the exciton. The gas phase electron affinity of 2,4,6-trinitrophenol (TNP) was reported to be 1.9 eV.[52] The value of electron affinity in solid phase will be higher than this value.[45] There are also reports of even lower values for the EA of TNP.[53] It is assumed that the electron affinity of TNP in the solid phase is above 1.9 eV. The onset of absorption of TNP is at 461 nm, which corresponds to an optical gap of 2.69 eV. Thus the Highest Occupied Molecular Orbital (HOMO) level of TNP must be below 5.1 eV. The theoretical value of the ionization potential of TNP is 11.7 eV.[54] The actual electron affinities and ionization potentials differ depending on the polarizability of the

surrounding matrix.[45]

Optical absorption spectra of the electron acceptors used in this work are given in Fig.1.7.

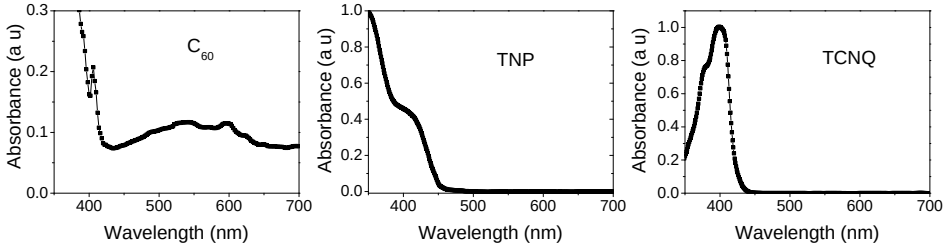

Figure 1.7: Absorption spectra of the electron acceptor molecules C_{60}, TNP and TCNQ in chloroform.

The HOMO and LUMO energy level values of C_{60} are 6.2eV and 3.6eV respectively.[55] This molecule and its more soluble derivative PCBM ([6,6]-phenyl C_{61}-butyric acid methyl ester) are among the important electron acceptor molecules for organic photovoltaic devices.[56,57] The capability of electron transfer from C_{60} to organic molecules has been the subject of intense research and it was found that photoinduced charge transfer happens on a time scale of picoseconds.[58] Different optoelectronic devices have been demonstrated based on fullerene-semiconducting polymer heterojunctions.[59]

1.5 Nonlinear Optical Effects in Molecular Systems

Nonlinear optics deals with the nonlinear response of a material when it interacts with the electric field of light. In the absence of perturbing fields, the charge distribution in a medium is in equilibrium so that electrical neutrality is maintained. When it interacts with intense light, such as from a laser, the charge distribution gets modified under the influence of the strong electric field, and the medium is said to be polarized.[60] The polarization is dependent on the applied electric field and is given by equation 1.18.

$$P_i = P_i(0) + \varepsilon_o \chi_{ij}^{(1)} \mathbf{E}_j + \varepsilon_o \chi_{ijk}^{(2)} \mathbf{E}_j \mathbf{E}_k + \varepsilon_o \chi_{ijkl}^{(3)} \mathbf{E}_j \mathbf{E}_k \mathbf{E}_l + ... \qquad (1.18)$$

Where $\chi^{(n)}$ are the nth order electric susceptibilities determining the strength of the linear and higher order nonlinear effects. Equation 1.18 gives the induced polarization in the bulk of the medium which has its origin in the molecular dipoles in the medium. At the microscopic level, the dependence of the dipole moment of a molecule on the electric field is given by equation 1.19.

$$\mu_i = \mu_i(0) + \alpha_{ij} \mathbf{E}_j + \beta_{ijk} \mathbf{E}_j \mathbf{E}_k + \gamma_{ijkl} \mathbf{E}_j \mathbf{E}_k \mathbf{E}_l + ... \qquad (1.19)$$

where α, β and γ are the polarizability, first hyperpolarizability and second hyperpolarizability respectively. It is the magnitude of these quantities which determine the strength of the nonlinear optical effects in molecular systems. They are the microscopic analogues of the susceptibilities $\chi^{(n)}$.[60,61] The subscripts i, j, k etc. refer to relevant molecular axes. The even order effects are absent in systems possessing centrosymmetry in the bulk.

1.5.1 The Electro-optic effect

Electro-optic effect refers to an electric field induced change in refractive index. If only one field of magnitude E is applied to a medium in which the polarizations can be represented by equations 1.18 and 1.19, the refractive index can be represented by,[62]

$$n(E) = n - \frac{1}{2} r n^3 E - \frac{1}{2} S n^3 E^2 + ... \qquad (1.20)$$

In eq. 1.20, n is the refractive index of the medium, r and S are the coefficients determining the linear (Pockels) and second order (Kerr) electro-optic effects. They are tensor quantities of rank three (3^3 components) and four (3^4 components) respectively.[63] The electro-optic tensor elements can be expressed in terms of the second order nonlinear susceptibility $\chi_{IJK}^{(2)}(-\omega; 0, \omega)$ as $r_{IJK} = -8\pi\chi_{IJK}^{(2)}(-\omega; 0, \omega)/n^4$.[64] Pockels effect

can be observed only in non-centrosymmetric media. The coefficient r is related to the molecular first hyperpolarizability β and an order parameter $< cos^3(\phi) >$ by equation 1.21.

$$r = \frac{2Nf(\omega)\beta cos^3(\phi)}{n^4} \tag{1.21}$$

Here N is the number density of the molecules (chromophores) with nonlinear optical properties, $f(\omega) = (n^2 + 2)/3$ is the Lorentz-Lorentz correction factor which relates the external electric field of electromagnetic wave to the field in the medium. The term $< cos^3(\phi) >$ represents the averaged value of the angle of rotation of the dipole moments of chromophores.[17] It is given by,

$$< cos^3(\phi) >= \frac{f(0)E_p\mu_g}{5kT} \tag{1.22}$$

Here f(0) is the Onsager correction factor relating the external applied field (E_p) to the local field inside the polymer,[65] μ_g is the ground-state dipole moment of the chromophore, k is the Boltzmann constant and T is the temperature in Kelvin scale. The order parameter is zero for centrosymmetric media.[17]

1.5.2 Push-pull chromophores for nonlinear optical effects

It is known that organic molecules with electron donor and acceptor groups possess high nonlinear optical properties. As evident from equation 1.21, molecules with high values for the first order hyperpolarizability β, can give rise to large electro-optic effect. For a molecule to show nonlinear optical effects, the basic requirements are polarizability, asymmetric charge distribution and an acentric crystal packing.[66] The general structure of an organic nonlinear optical chromophore is shown in Fig 1.8. There is a donor type group and an acceptor type group connected through a π bridge. The large second order susceptibilities of these types of organic molecules arise from a strong charge transfer between the donor and acceptor units.[67,68]

Figure 1.8: The general structure of an organic nonlinear optical chromophore.

At the molecular level, the parameters that can be changed are the relative electron affinities of the donor and acceptor groups and the length and nature of the conjugated segment connecting the donor to the acceptor. The presence of a strong dipole moment in the ground state is an indication that the molecule is having an asymmetric charge distribution. A non-centrosymmetry must be maintained in the bulk for second order effects to be seen. Most of the molecules with large first hyperpolarizability also have a strong permanent dipole moment and an ensemble of such molecules will tend to align antiparallel in pairs, leaving no macroscopic second order susceptibility. Poling techniques[69] are usually employed to break the centrosymmetry of the systems under study. Polymers doped with such chromophores have shown to possess high electrooptic (EO) coefficients.[70] Hydrogen bond directed aggregation may also be a potential method to achieve non-centrosymmetry.[71]

1.5.3 Figure of merit of push-pull chromophores

The role of a push-pull molecule in a photorefractive guest host system is to provide refractive index modulation in response to an electric field. The refractive index modulation in inorganic PR crystals is mainly due to the linear electro-optic effect.[72] For polymeric photorefractive materials, contributions arise also from Kerr electro-optic effect and the reorientation of the chromophores in response to an electric field.[13] The latter mechanism, called orientational birefringence, can induce very large refractive index modulation in photorefractive polymers with low glass transition temperatures. The ability of a chromophore molecule to induce refractive index change is expressed as the figure of merit[72] defined by Equation 1.23

$$FOM = \frac{1}{M}\left[9\mu_g\beta + \frac{2\mu_g^2\triangle\alpha}{k_BT}\right] \tag{1.23}$$

Where M is the molecular mass, μ_g is the ground state dipole moment, β is the first order hyperpolarizability, $\triangle\alpha$ is the anisotropy in linear polarizability, k_B is the Boltzmann constant and T is the absolute temperature. In systems with low glass transition temperature (T_g) where the molecules are relatively free to rotate, the chromophores can reorient in the applied/generated electric field. Due to the anisotropy in polarizability of the chromophores, such a reorientation will induce refractive index anisotropy which is termed as orientational birefringence.[65] The first term in equation 1.23 represents the contribution from the linear electrooptic effect and the second term represents the contribution of orientational birefringence (OB).

If the molecules are embedded in a polymer host with high T_g and poled, the dominant component to the refractive index modulation will be from the Pockels effect. In this case, the figure of merit can be assumed to be,[17]

$$FOM_{PEO} = 9\mu_g\beta_0 \qquad where, \quad \beta_0 = \frac{6\mu_{ge}^2\triangle\mu}{E_{ge}^2} \tag{1.24}$$

Here μ_{ge} is the transition dipole moment between the ground and excited states, $\triangle\mu$ is the difference between the dipole moments in the excited and ground states, and E_{ge} is the transition energy. Thus magnitude of the refractive index modulation achievable in a guest host system is determined by the figure of merit of the nonlinear optical chromophores,[17] present in the host. This is further related to the molecular second order susceptibility (β) and the ground state dipole moment (μ_g) of the dopant.

1.6 Experimental details

The following sections deal with the details of the experimental techniques employed in this work to study the charge carrier generation, transport

and electro-optic phenomena in polymers under study. The approach was to study the photoconductivity and electro-optic effect in pure polymer or blends and then to select systems with higher performance and suitable spectral response for photorefractivity. All experimental setups were fabricated in house and the verification of the results was done by measuring the parameters of known materials and comparing it with reported values.

1.6.1 Time of flight experiment

The time-of-flight (TOF) technique is used to measure the mobility of the careers in the polymer.[73] In this, the molecule under study is sandwiched between two electrodes, of which one is transparent to allow illumination of the sample. In some cases, a carrier generation layer is used to photogenerate and inject carriers to the polymer being studied. Illumination of the sample using a highly absorbed pulse of light through one transparent electrode creates a sheet of charge carriers, which drift under the electric field. The duration of the pulse should be lower than the time taken by the carriers to reach the other electrode. Current through the sample is monitored as the potential drop across a load resistor connected in series with the sample and power supply using an oscilloscope. The time taken for the arrival of carriers at the other electrode is noted from an abrupt decrease in the excess current after the excitation. If t_r is the time taken by the carriers under an electric field of magnitude E = v/d, where v is the applied voltage and d the thickness, the mobility, which is defined as the velocity under unit electric field, can be calculated using Equation 1.25.

$$\mu = \frac{d}{t_r E} \tag{1.25}$$

The arrangement for a TOF measurement is shown in Fig 1.9. In our experiment, a thin layer of evaporated Selenium was given on the ITO substrate to serve as a carrier generation layer prior to drop casting the polymer. The laser was a pulsed Nd:YAG (Quanta Ray) with 10 ns pulse width and 532 nm second harmonic emission. The signal was detected across a metal film resistor using a storage oscilloscope (TDS

210, Tektronix).

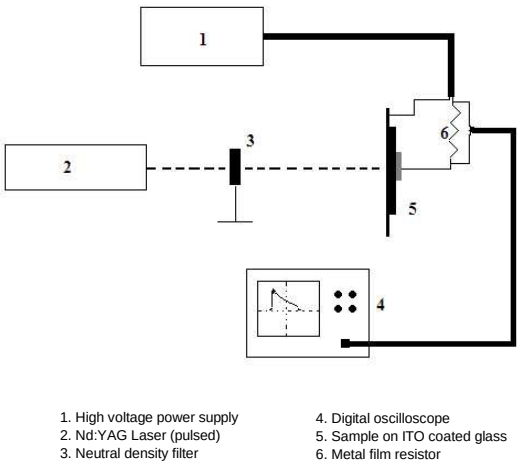

Figure 1.9: Experimental arrangement for Time-of-Flight mobility measurement.

The pulse energy of the laser was adjusted so that total charge generated was below 0.05CV, C is the capacitance of the device and V is the voltage applied. Also, care was taken to ensure that the time constant (RC) of the circuit was less than the drift time of the carriers.

1.6.2 Current-voltage characteristics

Current-Voltage (I-V) characteristics and its temperature dependence in an organic semiconductor based device can give important information about the molecule being studied.[74] A Keithley 236 Source-Measure Unit was used to apply voltage to the sandwich cell and to record the current. The measurements were done by keeping the sandwich cell thermally clamped to the cold head of a closed cycle liquid helium cryostat which was equipped with an auto-tuning temperature controller (LakeShore 321).

The electrical conductivity, defined as the ratio of the current density to the electric field strength, is given by equation 1.26.

$$\sigma = \frac{I}{V}\frac{d}{A} \tag{1.26}$$

where I is the current, V is the voltage applied, d is the thickness and A is the effective area of the polymer between the electrodes.

The electrical conductivity of polymers is highly dependent on the extent of disorder in the system. Three regimes of conductivity are usually identified based on the extent of disorder. They are metallic regime, critical regime, and insulating regime.[75] In the insulating regime, the low temperature dc conductivity is usually described by the variable range hopping (VRH) model.[75] According to this, the dc conductivity has a temperature dependence given by,[76]

$$\sigma_{dc}(T) = \sigma_0 e^{-(\frac{T_0}{T})^{\gamma}} \tag{1.27}$$

Here σ_0 is a prefactor value of the conductivity, T_0 is a characteristic temperature T, the absolute temperature and the exponent γ depends on the dimensionality of hopping conduction. The value of γ are 1/4, 1/3, or 1/2 for three-dimensional, two-dimensional, or one-dimensional hopping, respectively. The value of the exponent can also go above 0.5, in which case, the hopping transport is said to occur between the so called super-localization states of the polymer.[76]

1.6.3 Steady state photocurrent measurement

Photocurrent measurement in the steady state involves measuring the steady state current through the sandwich cell with and without light. A Keithley 236 Source Measure Unit was used for the experiment. A DC voltage is applied to the sandwich cell which is kept in dark and the resulting current is measured with time. After the dark current through the cell is stabilized, light is allowed to fall on the electrode area. Due to the photoinduced change in conductivity, the current increases suddenly and reaches a steady state. After reaching the steady state, light is cut off and the measurement of current is continued till the dark value of current is reached. If I_D and I_L are the steady state current values, prior to illumination and after illumination respectively, the photosensitivity of the polymer device can be written as,

$$I_{ph} = \frac{I_L - I_D}{I_D} \tag{1.28}$$

The experiential arrangement is shown schematically in Fig. 1.10.

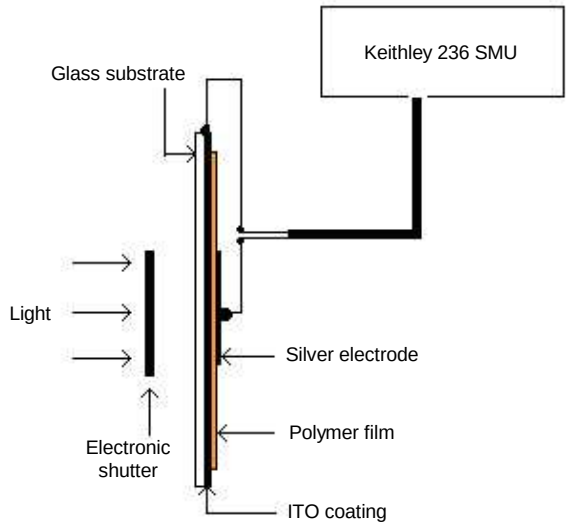

Figure 1.10: Experimental setup for steady state photocurrent measurement.

1.6.4 Modulated photocurrent detection

In this method, the illumination is modulated using a mechanical chopper.[77] The chopped light induces an alternating photocurrent in the circuit due to the carrier generation and subsequent loss. This induces an alternating voltage across a load resistor. The voltage is then fed to a lock-in-amplifier which is locked to the chopper frequency. The experimental setup is shown in Fig. 1.11. This method directly gives the value of photocurrent and the signal to noise ratio is higher due to the use of modulated detection.

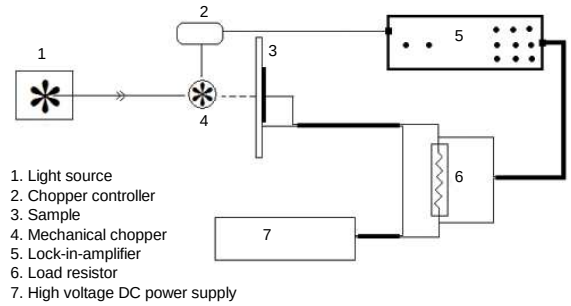

Figure 1.11: Setup for modulated photocurrent detection

In this work, the modulation frequency was selected between 20 and 30Hz and is specified along with the results. The photoconductive sensitivity, defined as the change in conductivity per unit light intensity, was calculated using equation 1.16.

The light source used for spectrally resolved measurement of the photocurrent was the dispersed output of a Fluoromax - 3 Fluorimeter, in which, a 150W Xenon lamp was the source. All measured spectra have been corrected for the spectral distribution of the lamp shown in Fig. 1.12.[77]

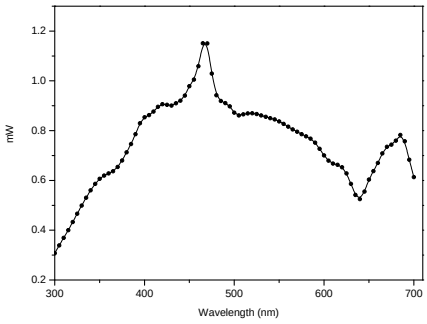

Figure 1.12: Spectral intensity distribution of the Xe lamp.

The photocurrent action spectra given in this thesis are for 1 mW incident power. The lock-in-amplifier was model SR830 (Stanford Research Systems), mechanical chopper was model SR540 (Stanford Research Systems) and High Voltage power supply model was model PS350

(Stanford Research Systems). The load resistor was a metal film resistor for increased stability.

1.6.5 Cyclic voltammetry

Cyclic voltammetry (CV) can be used to determine the oxidation and reduction potentials of a molecule. In this technique, the molecule is dissolved in a solvent with higher oxidation/reduction potential and used as the electrolyte of a cell. A potential sweep is applied to the electrode and the corresponding faradaic current (current due to redox reaction) is measured. The potential of the electrode is controlled and referenced to a standard. In the present case, Ag/AgCl was the reference electrode.

Experiments were done in a three electrode BASi epsilon electrochemical cyclic voltameter. The measurement was carried out at room temperature in dimethylformamide solution containing 0.1 M tetrabutylammonium chloride as supporting electrolyte with a glassy carbon working electrode. The instrument was calibrated with the standard ferrocene/ferrocenium redox system.

1.6.6 Determination of electro-optic coefficient

The electro-optic coefficient of the composites were studied in the transmission mode ellipsometric method[65,78] which is a modification of the reflection geometry proposed independently by Teng & Man[79] and Schildkraut.[80] Most of the experimental techniques rely on the measurement of the electric field induced phase shift between the two orthogonal components of electric field vector of the light wave after passing through the sample. The experimental arrangement for the electro-optic coefficient measurement is shown in Fig. 1.13.

Light from a He-Ne laser (632.8nm) was polarized at 45^0 and passed through a Soliel Babinet Compensator (SBC-VIS, Thorlabs), the sample and the analyzer. The angle (α) between the sample normal and the laser beam was 45^0, but could be increased if required for higher modulation.

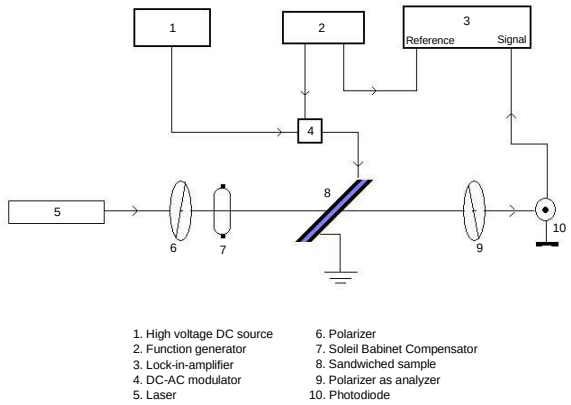

Figure 1.13: Experimental arrangement for electro-optic measurements

The phase difference between the E_x and E_y components of the electric field vector of the beam could be varied by the SBC, before the sample. An alternating voltage (variable from 30Hz to 1.5kHz) is applied to the sample to induce electro-optic effect and the transmitted intensity was detected with the photodiode (PDA55-EC, Thorlabs) and a lock-in-amplifier (SR830, Stanford Research). The alternating voltage was produced by switching the DC voltage from the PS350 (Stanford Research) power supply using a solid state rely model M221, which was generously supplied by Solid State Optronics Inc, USA. A function generator (DS340, Stanford Research) was used for driving the rely. The high frequency limit (1500Hz) of the experiment was set by the switching time of this rely. A storage oscilloscope (TDS210, Tektronix) was used to monitor the waveform and to measure the magnitude of the high voltage ac signal produced by the rely.

Initial measurement of the intensity of transmitted beam was done by varying the phase shift introduced by the SBC without any electric field. Then an ac electric field was applied. Maximum modulated intensity was obtained when the phase shift between E_x and E_y components was $\pi/2$ or $3\pi/2$.[79,81] Fig. 1.14 shows the typical variation of the transmitted intensity and the modulated intensity with the phase shift introduced by the SBC. The position of the compensator was fixed at the maximum

modulated intensity position and intensity of modulations in transmitted light was measured with applied field.

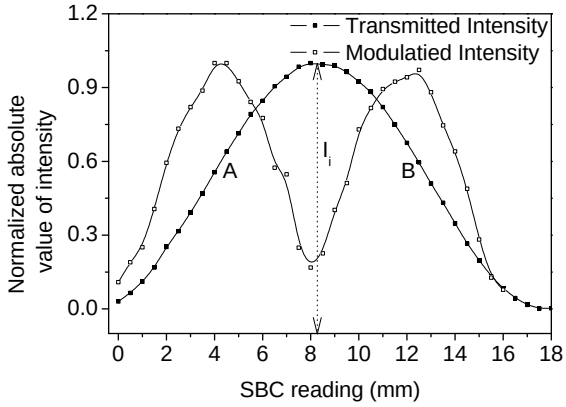

Figure 1.14: Variation of the transmitted intensity and the modulated signal with SBC introduced phase shift.

The field dependence of index of refraction for x and y polarization directions is different. This introduces a field dependent phase difference between the two polarization components. As the polarizers are crossed, the transmitted intensity depends on this phase difference denoted by ψ_{xy}. The transmitted intensity will be,

$$I_t = I_i sin^2\left(\frac{\psi_{xy} + \psi_{SBC}}{2}\right) \tag{1.29}$$

In equation 1.29, ψ_{SBC} represents the phase difference introduced by the SBC and I_i, the incident intensity. If ψ_{SBC} is fixed at $\pi/2$, the intensity depends only on ψ_{xy}. The position corresponding to $\psi_{SBC} = \pi/2$, is marked as A in Fig. 1.14. At this position, application of an ac electric field will produce small oscillations in I_t due to the alternating value of ψ_{xy} in response to the field.

For high T_g poled polymers, the electro-optic coefficient r_{33} is given by the following expression.[78]

$$r_{33} = \frac{3I_m\lambda n[n^2 - sin^2(\alpha)]^{\frac{1}{2}}}{I_i\pi n^3 V_{ac} sin^2(\alpha)} \tag{1.30}$$

This expression neglects the effect of field induced birefringence in low T_g polymers.[78] Thus for this class of polymers, the experiment has to be done in such a manner that the rod like chromophores can not follow the ac field. This can be done either by applying a DC field superimposed with an AC field to probe the modulation or the experiment can be performed at high frequencies. In low T_g polymers, electro-optic response functions are also used.[78] The above equation assumes the validity of Kleinmann symmetry. This means that the components of the susceptibility tensors $\chi^{(2)}$ and $\chi^{(3)}$ are invariant under change of subscripts.[82] The experiments were performed with 632.8 nm light, far from the absorption edge of the composites so that the above assumption is valid.

1.6.7 Electric poling

The linear electro-optic effect requires a finite value for the second-order susceptibility. This further requires that the polymer system must not be centrosymmetric. This condition is ensured by orienting the chromophores in such a way that the system does not possess a center of symmetry. Usually, electric field poling is used for aligning the chromophores and to bring about a macroscopic second order susceptibility.[69]

Electric field poling can be done either in the contact mode or in non-contact mode. Corona poling[83,84] is a non-contact method which has the advantage of reaching high electric field strengths while controlling the current through the sample. Contact poling[85] has the disadvantage of higher degree of sample breakdown due to the current flow through the sample.

Both corona poling and contact poling must be performed at elevated temperatures. Usually, the polymer is brought to its glass transition temperature and the poling field is applied. Under the high field, the chromophores undergo rotation in the general direction of the electric field. After poling, the system is returned to room temperature while maintaining the applied field so that the chromophores do not reorient to generate a centrosymmetry.[84] A macroscopic second order susceptibility can also be achieved using optical poling.[86–88]

The degree of polar order in the sample is usually expressed as an order parameter.[84] Poling leads to a change in absorbance and this change can be used to estimate the polar order in the system. The order parameter ϕ can be estimated as 1-($A_\perp/A_0$), where A_0 is the absorbance of the unpoled film and and $A_\perp$ is that of the poled film taken with the electric field of the probing light perpendicular to the poling direction.[84,89]

1.6.8 Role of plasticizing agents

Plasticizers are used to reduce the glass transition temperature of the polymer so that its flexibility is enhanced. The plasticizer acts similar to a solvent. These molecules are inserted between the polymer chains thereby pushing them apart which causes a reduction in the intermolecular cohesive forces. The plasticizers used in the present work were Ethyl carbazole (ECZ) and Dioctylphthalate (DOP). The structure of these molecules are shown in Fig. 1.15. Plasticizing a photorefractive system with ECZ was reported as a method to improve the photorefractive performance.[90]

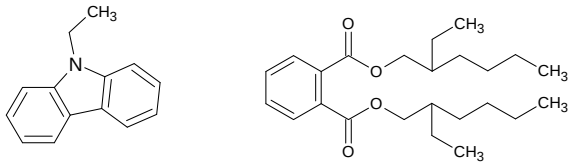

(a) (b)

Figure 1.15: Structure of the plasticizers (a) Ethyl carbazole and (b) Dioctylphthalate.

1.7 Aim and outline of the thesis

The photorefractive effect is an important property that makes a material suitable for a variety of optical applications. In this work, an attempt was made to study some potential new materials as photoconducting hosts and electro-optic materials for photorefractive polymer systems. The strategy was to study photoconductivity and electro-optic effect separately and

then make composites using well performing molecules. As most of the molecules examined in the present work were not considered in the past for these applications, studies were done with a view to gain maximum possible information about each of them, so that they can be considered for other applications also.

The second chapter deals with photoconductivity, one of the main requirements for photorefractivity. This chapter describe the study of photoconductivity in two polymer systems. One of them belongs to the class of molecularly doped polymers which are considered to be the simplest photoconducting systems. Poly(methyl methacrylate) was used as host for making this photoconducting system. Another system was the polymer Poly(2-methacryloyl-1-(4-azo-1'-phenyl)aniline-co-styrene) sensitized with the molecule C_{60}. Photoconductive sensitivity of this system was found to be of the order of typical photorefractive systems. The third chapter is about three polybenzoxazines which were studied for photoconductivity. One of these polymers was found to be highly sensitive when doped with C_{60}.

Solvatochromic study of some p-nitroaniline derivatives as nonlinear optical chromophores for electrooptic functionality is described in chapter four. Aim was to select molecules with higher values for the photorefractive figure of merit. The ground and excited state dipole moments and the first hyperpolarizability were estimated. Electro-optic effect, the second requirement for photorefractivity, is discussed in chapter five. Sixth chapter deals with the preparation of photorefractive composites. Many possibilities were tried to find a well performing composite out of the molecules examined. The results of two beam coupling experiment are given in this chapter. Chapter seven outlines the main results of the work and throws some light on future prospects.

References

[1] A. Ashkin, G. D. Boyd, J. M. Dziedzic, R. G. Smith, A. A. Ballman, J. J. Levinstein, and K. Nassau, "Optically-Induced Refractive Index Inhomogeneities in $LiNbO_3$ and $LiTaO_3$," Appl. Phys. Lett. **9,** 72–74 (1966).

[2] F. S. Chen, J. T. LaMacchia, and D. B. Fraser, "Holographic Storage in Lithium Niobate," Appl. Phys. Lett. **13,** 223–225 (1968).

[3] F. S. Chen, "Optically Induced Change of Refractive Indices in $LiNbO_3$ and $LiTaO_3$," J. Appl. Phys. **40,** 3389–3396 (1969).

[4] S. Tay *et al.*, "An updatable holographic three-dimensional display," Nature **451,** 694–698 (2008).

[5] K. Sutter, J. Hulliger, and P. Gunter, "Photorefractive effects observed in the organic crystal 2-cyclooctylamino-5-nitropyridine doped with 7,7,8,8-tetracyanoquinodimethane," Solid State Commun. **74,** 867–870 (1990).

[6] S. Ducharme, J. C. Scott, R. J. Twieg, and W. E. Moerner, "Observation of the Photorefractive Effect in a Polymer," Phys. Rev. Lett. **66,** 1846–1849 (1991).

[7] S. J. Zilker, "Materials Design and Physics of Organic Photorefractive Systems," Chem. Phys. Chem. **1,** 72–87 (2000).

[8] O. Ostroverkhova, D. Wright, U. Gubler, W. E. Moerner, M. He, AngelaSastre-Santos, and R. J. Twieg, "Recent Advances in Understanding and Development of Photorefractive Polymers and Glasses," Adv. Funct. mater. **12,** 1–9 (2002).

[9] G. J. Steckman, R. Bittner, K. Meerholz, and D. Psaltis, "Holographic multiplexing in photorefractive polymers," Opt. Commun. **185,** 13–17 (2000).

[10] V. M. Petrov, S. Lichtenberg, J. Petter, T. Tschudi, A. V. Chamrai, V. V. Bryksin, and M. P. Petrov, "Optical on-line controllable filters based on photorefractive crystals," J. Opt. A: Pure Appl. Opt. **5,** S471–S476 (2003).

[11] Y. Frauel, G. Pauliat, A. éVilling, and G. Roosen, "High-Capacity Photorefractive Neural Network Implementing a Kohonen Topological Map," Appl. Opt. **40,** 5162–5169 (2001).

[12] B. Kippelen, K. Meerholz, and N. Peyghambarian, "An Introduction to Photorefractive Polymers," In *Nonlinear Optics of Organic Molecules and Polymers*, S. Miyata and H. S. Nalwa, eds., pp. 467–480 (CRC Press, 1997).

[13] W. E. Moerner, A. Grunnet-Jepsen, and C. L. Thompson, "Photorefractive Polymers," Annu. Rev. Mater. Sci. **27,** 585–623 (1997).

[14] T. K. Däubler, L. Kulikovsky, D. Neher, V. Cimrová, J. Hummelend, E. Mecher, R. Bittner, and K. Meerholz, "Photoconductivity and Charge-Carrier Photogeneration in Photorefractive Polymers," In *Nonlinear Optical Transmission Processes and Organic Photorefractive Materials*, C. M. Lawson and K. Meerholz, eds., Proceedings of the SPIE **4462,** 206–216 (2002).

[15] P. Cheben, F. del Monte, D. J. Worsfold, D. J. Carlsson, C. P. Grover, and J. D. Mackenzie, "A photorefractive organically modified silica glass with high optical gain," Nature **408,** 64–67 (2000).

[16] K. Meerholz, B. L. Volodin, Sandalphon, B. Kippelen, and N. Peyghambarian, "A photorefractive polymer with high optical gain and diffraction efficiency near 100%," Nature **371,** 497–499 (1994).

[17] A. V. Vannikov and A. D. Girishina, "The Phtorefractive Effect in Polymeric Systems," Russ. Chem. Rev. **72,** 471–488 (2003).

[18] B. Kippelen, K. Meerholz, and N. Peyghambarian, "An Introduction to Photorefractive Polymers," In *Nonlinear Optics of Organic Molecules and Polymers*, S. Miyata and H. S. Nalwa, eds., p. 484 (CRC Press, 1997).

[19] K. Yokoyama, K. Arishima, T. Shimada, and K. Sukegawa, "Photorefractive Effect in a Polymer Molecularly Doped with Low-Molecular-Weight Compounds," Jpn. J. Appl. Phys. **33,** 1029–1033 (1994).

[20] S. M. Silence, J. C. Scott, J. J. Stankus, W. E. Moerner, C. R. Moylan, G. C. Bjorklund, and R. J. Twieg, "Photorefractive Polymers Based on Dual-Function Dopants," J. Phys. Chem. **99,** 4096–4105 (1995).

[21] M. S. Bratcher, M. S. DeClue, A. Grunnet-Jepsen, D. Wright, B. R. Smith, W. E. Moerner, and J. S. Siegel, "Synthesis of Bifunctional Photorefractive Polymers with Net Gain: Design Strategy Amenable to Combinatorial Optimization," J. Am. Chem. Soc. **120,** 9680–9681 (1998).

[22] W. You, L. Wang, Q. Wang, and L. Yu, "Synthesis and Structure/Property Correlation of Fully Functionalized Photorefractive Polymers," Macromolecules **35,** 4636–4645 (2002).

[23] M. Stolka, "Photoconductive Polymers," In *Special Polymers for Electronics and Optoelectronics*, J. A. Chilton and M. T. Goosey, eds., pp. 284–285 (Chapman & Hall, London, 1995).

[24] K.-Y. Law, "Organic Photoconductive Materials: Recent Trends and Developments," Chem. Rev. **93,** 449–486 (1993).

[25] P. J. Melz, "Photogeneration in Trinitrofluorenone-Poly(N-Vinyl carbazole)," J. Chem. Phys. **57,** 1694–1699 (1972).

[26] D. West and D.J.Binks, *Physics of Photorefraction in Polymers*, No. 6 in *Advances in Nonlinear Optics* (CRC PRESS, New York, 2005).

[27] J. W. Kerr and G. H. S. Rokos, "Bimolecular recombination and reciprocity in xerographic photoconductors," J. Phys. D: Appl. Phys. **10,** 1151–1160 (1977).

[28] C. L. Braun, "Electric field assisted dissociation of charge transfer states as a mechanism of photocarrier production," J. Chem. Phys. **80,** 4157–4161 (1984).

[29] V. Gulbinas, Y. Zaushitsyn, H. Bässler, A. Yartsev, and V. Sundström, "Dynamics of charge pair generation in ladder-type poly(para-phenylene) at different excitation photon energies," Phys. Rev. B **70,** 035215–035222 (2004).

[30] V. I. Arkhipov, H. Bässler, M. Deussen, E. O. Göbel, R. Kersting, H. Kurz, U. Lemmer, and R. F. Mahrt, "Field-induced exciton breaking in conjugated polymers," Phys. Rev. B. **52,** 4932–4940 (1995).

[31] V. I. Arkhipov and H. Bässler, "Exciton dissociation and charge photogeneration in pristine and doped conjugated polymers," Phys. Stat. Sol. (a) **201,** 1152–1187 (2004).

[32] H. Bässler, "Charge Transport in Random Organic Semiconductor," In *Semiconducting Polymers - Chemistry, Physics and Engineering*, G. Hadziioannou and P. F. van Hutten, eds., p. 365 (Wiley-VCH Verlag GmbH, Germany, 2000).

[33] V. I. Arkhipov, P. Heremans, E. V. Emelianova, and H. Bässler, "Effect of doping on the density-of-states distribution and carrier hopping in disordered organic semiconductors," Phys. Rev. B. **71,** 045214–045221 (2005).

[34] V. I. Arkhipov, P. Heremans, E. V. Emelianova, G. J. Adriaenssens, and H. Bässler, "Charge carrier mobility in doped semiconducting polymers," Appl. Phys. Lett. **82,** 3245–3247 (2003).

[35] M. Weitera and H. Bässler, "Transient photoconductivity and charge generation in thin films of π-conjugated polymers," J. Lumin. **112,** 363–367 (2005).

[36] A. A. Alagiriswamy and K. S. Narayan, "Determination of trap states in ladder type polymers," Synth. Met. **116,** 297–299 (2001).

[37] R. F. Pierret, in *Advanced Semiconductor Fundamentals*, R. F. Pierret and G. W. Neudeck, eds., (Pearson Education, London, 2003), Vol. VI, p. 110.

[38] V. Arkhipov, J. Reynaert, Y. Jina, P. Heremansa, E. Emelianova, G. Adriaenssens, and H. Bässler, "The effect of deep traps on carrier hopping in disordered organic materials," Synth. Met. **138,** 209–212 (2003).

[39] D. Monroe, "Hopping in Exponential Band Tails," Phys. Rev. Lett. **54,** 146–149 (1985).

[40] G. G. Malliaras, V. V. Krasnikov, H. J. Bolink, and G. Hadziioannou, "Control of charge trapping in a photorefractive polymer," Appl. Phys. Lett. **66,** 1038–1040 (1995).

[41] H. Kang, K. Kim, M. Kim, K. Park, K. Kim, T. Lee, J. Joo, K. . Kmi, D. Lee, and J. Jin, "Electrical and optical characteristics of various PPV derivatives (MEH-PPV, CzEH-PPV, OxdEH-PPV)," Curr. Appl Phys. **1,** 443–446 (2001).

[42] S.-H. Park, K. Ogino, and H. Sato, "Synthesis and characterization of a main-chain polymer for single component photorefractive materials," Synth. Met. **113,** 135–143 (2000).

[43] T. K. Däubler, R. Bittner, K. Meerholz, V. Cimrová, and D. Neher, "Charge carrier photogeneration, trapping, and space-charge field formation in PVK-based photorefractive materials," Phys. Rev. B. **61,** 13515–13527 (2000).

[44] C. Brabec, H. Johannson, F. Padinger, H. Neugebauer, J. Hummelen, and N. Sariciftci, "Photoinduced FT-IR spectroscopy and CW-photocurrent measurements of conjugated polymers and fullerenes blended into a conventional polymer matrix," Sol. Energy Mater. Sol. Cells **61,** 19–33 (2000).

[45] R. W. Lof, M. A. van Veenendaal, B. Koopmans, H. T. Jonkman, and G. A. Sawatzky, "Band gap, excitons, and Coulomb interaction in solid C_{60}," Phys. Rev. Lett. **68,** 3924–3927 (1992).

[46] E. Hendrickx, B. Kippelen, S. Thayumanavan, S. R. Marder, A. Persoons, and N. Peyghambarian, "High photogeneration efficiency of charge-transfer complexes formed between low ionization potential arylamines and C_{60}," J. Chem. Phys. **112,** 9557–9561 (2000).

[47] A. M. A. El-Sayed, H. F. M. Mohamed, and A. A. A. Boraei, "Positron annihilation studies of some charge transfer molecular complexes," Radiat. Phys. Chem. **58,** 791–795 (2000).

[48] C. E. Klots, R. N. Compton, and V. F. Raaen, "Electronic and ionic properties of molecular TTF and TCNQ," J. Chem. Phys. **60,** 1177–1178 (1974).

[49] R. N. Compton and C. D. Cooper, "Negative ion properties of tetracyanoquinodimethan: Electron affinity and compound states," J. Chem. Phys. **66,** 4325–4329 (1977).

[50] T. L. Kunii and H. Kuroda, "Ionization potentials and electron affinities of carbo- and heterocyclic π-conjugated molecules," Theor. Chim. Acta. **11,** 97–106 (1968).

[51] M. Pfeiffer, A. Beyer, T. Fritz, and K. Leo, "Controlled doping of phthalocyanine layers by cosublimation with acceptor molecules: A systematic Seebeck and conductivity study," Appl. Phys. Lett. **73,** 3202–3204 (1998).

[52] J. R. Miller, "Tunneling Reactions of Trapped Electrons with Added Electron Acceptors in Alcohol Glasses at 77 K," J. Phys. Chem. **82,** 767–774 (1978).

[53] M. M. Ayad, M. Gaber, and S. A. Azim, "Electrical and Spectrophotometric Properties of Charge-transfer Complexes of Some Anthracene Derivatives," Thermochim. Acta **147,** 57–64 (1989).

[54] P. C. Chen and C. C. Huang, "Theoretical calculation of the molecular structure of picric acid," J. Mol. Struct. (Theochem) **282,** 287–290 (1993).

[55] J. Y. Lee and J. H. Kwon, "Enhanced hole transport in C_{60}-doped hole transport layer," Appl. Phys. Lett. **88,** 183502–183504 (2006).

[56] J. Yang, A. Garcia, and T.-Q. Nguyen, "Organic solar cells from water-soluble poly(thiophene)/fullerene heterojunction," Appl. Phys. Lett. **90,** 103514–103517 (2007).

[57] R. Könenkamp, J. Erxmeyer, and A. Weidinger, "Photoconduction in fullerene films," Appl. Phys. Lett. **65,** 758–760 (1994).

[58] L. Smilowitz, N. S. Sariciftci, R. Wu, C. Gettinger, A. J. Heeger, and F. Wudl, "Photoexcitation spectroscopy of conducting-polymer-C_{60} composites: Photoinduced electron transfer," Phys. Rev. B **47,** 13835–13842 (1993).

[59] N. S. Sariciftci, D. Braun, C. Zhang, V. I. Srdanov, A. J. Heeger, G. Stucky, and F. Wudl, "Semiconducting polymer-buckminsterfullerene heterojunctions: Diodes, photodiodes, and photovoltaic cells," Appl. Phys. Lett. **62,** 585–587 (1993).

[60] P. Yeh, *Introduction to Photorefractive Nonlinear Optics*, 1st ed. (John Wiley & Sons, Inc., New York, 1993), pp. 2–3.

[61] A. Samoc, M. Samoc, M. Woodruff, and B. Luther-Davies, "Poly(p-phenylenevinylene): An Attractive Material for Photonic Applications," In *Photonic Polymer Systems - Fundamentals, Methods, and Applications*, D. L. Wise, G. E. Wnek, D. J. Trantolo, T. M. Cooper, and J. D. Gresser, eds., pp. 373–375 (Marcel Dekker, Inc., New York, 1998).

[62] B. E. A. Saleh and M. C. Teich, *Fundamentals of Photonics* (John Wiley & Sons, Inc., New York, 1991), pp. 697–698.

[63] B. E. A. Saleh and M. C. Teich, *Fundamentals of Photonics* (John Wiley & Sons, Inc., New York, 1991), pp. 713–714.

[64] B. Kippelen, K. Meerholz, and N. Peyghambarian, "An Introduction to Photorefractive Polymers," In *Nonlinear Optics of Organic Molecules and Polymers*, S. Miyata and H. S. Nalwa, eds., p. 476 (CRC Press, 1997).

[65] B. Kippelen, Sandalphon, K. Meerholz, and N. Peyghambarian, "Birefringence, Pockels, and Kerr effects in photorefractive polymers," Appl. Phys. Lett. **68,** 1748–1750 (1996).

[66] S. K. Yesodha, C. K. S. Pillai, and N. Tsutsumi, "Stable polymeric materials for nonlinear optics: a review based on azobenzene systems," Prog. Polym. Sci. **29,** 45–74 (2004).

[67] J. L. Oudar and D. S. Chemla, "Hyperpolarizability of the nitroanilines and their relations to the excited state dipole moment," J. Chem. Phys. **66,** 2664–2668 (1977).

[68] J. L. Oudar, "Optical nonlinearities of conjuagted molecules. Stilbene derivatives and highly polar aromatic compounds," J. Chem. Phys. **67,** 446–457 (1977).

[69] M. Tsuchimori, O. Watanabe, and A. Okada, "Temporal Stability of Second-Order Optical Nonlinearity of Polyurethane: Influence of Poling Conditions," Jpn. J. Appl. Phys. **40,** 6396–6400 (2001).

[70] L. M. Hayden, G. F. Sauter, F. R. Ore, and P. L. Pasillas, "Second-order nonlinear optical measurements in guest-host and side-chain polymers," J. Appl. Phys. **68,** 456–465 (1990).

[71] M. C. Etter, "Encoding and Decoding Hydrogen-Bond Patterns of Organic Compounds," Acc. Chem. Res. **23,** 120–126 (1990).

[72] O. Ostroverkhova and W. E. Moerner, "Organic Photorefractives: Mechanisms, Materials, and Applications," Chem. Rev. **104,** 3267–3314 (2004).

[73] D. West, M. Rahn, C. Im, and H. Bässler, "Hole transport through chromophores in a photorefractive polymer composite based on poly(N-vinyl carbazole)," Chem. Phys. Lett. **326,** 407–412 (2000).

[74] W. Wang, T. Lee, and M. A. Reed, "Mechanism of electron conduction in self assembled alkanethiol monolayer devices," Phys. Rev. B. **68,** 035416–035422 (2003).

[75] Y. Long, Z. Chen, N. Wang, Y. Ma, Z. Zhang, L. Zhang, and M. Wan, "Electrical conductivity of a single conducting polyaniline nanotube," Appl. Phys. Lett. **83,** 1863–1865 (2003).

[76] A. Sarkar, P. Ghosh, A. K. Meikap, S. K. Chattopadhyay, S. K. Chatterjee, and M. Ghosh, "Alternate and direct current conductivity of conducting polyaniline dispersed with poly vinyl alcohol and blended with methyl cellulose," J. Appl. Phys. **97,** 113713–113717 (2005).

[77] V. C. Kishore, R. Dhanya, C. S. Kartha, K. Sreekumar, and R. Joseph, "Photoconductivity in molecularly doped poly(methyl methacrylate) sandwich cells," J. Appl. Phys. **101,** 063102–063105 (2007).

[78] Sandalphon, B. Kippelen, K. Meerholz, and N. Peyghambarian, "Ellipsometric measurements of poling birefringence, the Pockels effect, and the Kerr effect in high-performance photorefractive polymer composites," Appl. Opt. **35,** 2346–2354 (1996).

[79] C. C. Teng and H. T. Man, "Simple reflection technique for measuring the electro-optic coefficient of poled polymers," Appl. Phys. Lett. **30,** 1734–1736 (1990).

[80] J. S. Schildkraut, "Determination of the electrooptic coefficient of a poled polymer film," Appl. Opt. **29,** 2839–2841 (1990).

[81] D. H. Park, C. H. Lee, and W. N. Herman, "Analysis of multiple reflection effects in reflective measurements of electro-optic coefficients of poled polymers in multilayer structures," Opt. Express **14,** 8866–8884 (2006).

[82] M. Goodwin, D. Bloor, and S. Mann, "Nonlinear materials," In *Special Polymers for Electronics and Optoelectronics*, J. A. Chilton and M. T. Goosey, eds., p. 134 (Chapman & Hall, London, 1995).

[83] P. Qi-Wei, F. Chang-Shui, Q. Zhi-Hui, G. Qing-Tian, W. Xiang-Wen, S. Wei, and Y. Jin-Zhong, "Thermally Stable Guest-Host Polyetherketone Poled Polymer for Electro-Optical Applications," Chin. Phys. Lett. **19,** 1125–1127 (2002).

[84] D. M. Burland, R. D. Miller, and C. A. Walsh, "Second-Order Nonlinearity in Poled-Polymer Systems," Chem. Rev. **94,** 31–75 (1994).

[85] F. Michelotti and E. Toussaere, "Pulse poling of side-chain and crosslinkable copolymers," J. Appl. Phys. **82,** 5728–5744 (1997).

[86] G. Xu, J. Si, X. Liu, Q. Yang, P. Ye, Z. Li, and Y. Shen, "Permanent optical poling in polyurethane via thermal crosslinking," Opt. Commun. **153,** 95–98 (1998).

[87] K. Kitaoka, N. Matsuoka, J. SI, T. Mitsuyu, and K. Hirao, "Optical poling of phenyl-silica hybrid thin films doped with azo-dye chromophore," Jpn. J. Appl. Phys. **38,** L1029–L1031 (1999).

[88] A. Apostoluk, C. Fiorini-Debuisschert, and J.-M. Nunzi, "All Optical Poling in Polymers and Applications," In *Photoreactive Organic Thinfilms*, Z. Sekkat and W. Knoll, eds., pp. 333–361 (Academic Press, London, 2002).

[89] O. Sugihara, S. Kunioka, Y. Nonaka, R. Aizawa, Y. Koike, T. Kinoshita, and K. Sasaki, "Second-harmonic generation by Cerenkov-type phase matching in a poled polymer waveguide," J. Appl. Phys. **70,** 7249–7252 (1991).

[90] H. J. Bolink, V. V. Krasnikov, G. G. Malliaras, and G. Hadziioannou, "Effect of Plasticization on the Performance of a Photorefractive Polymer," J. Phys. Chem. **100,** 16356–16360 (1996).

CHAPTER

TWO

Photoconductivity Studies on Molecularly Doped Poly (methyl methacrylate) and Poly(2- methacryloyl -1-(4-azo-1'-phenyl) aniline-co-styrene)

2.1 Introduction

Semiconducting organic materials are being investigated with high importance due to the potential of such materials in displays, flexible electronic gadgets, solar cells etc. Photoconducting polymers attracted considerable interest following the introduction of Copier 1 series of IBM in which the polymer photoconductor Poly(N-vinyl carbazole) doped with 2,4,7,-trinitro-9-fluorenone was used for the first time.[1] Photogeneration of carriers and good mobility for the generated carriers are among the main requirements of photorefractive effect. The carrier mobility directly determines the speed of grating formation in photorefractive polymers.[2] The storage life depends on the extent of time up to which the generated space charge last. It is believed that traps are responsible for the storage of the space charge[3] and they are also liable to thermal release, a process that will erase the information content.

In this chapter, two photoconducting polymer systems are described. They were studied for possible use in photorefractive polymer systems. The first one was based on a simple approach called molecular doping and

the second was a side chain polymer. Details of these photoconducting systems are given after a brief discussion of different classes of polymer photoconductors.

2.2 Photoconducting polymers - Classification

Based on the structure and/or nature of active units that give rise to photoconductivity, these polymers can be classified broadly into the following groups.

- Molecularly Doped Polymers
- Polymers with pendant or in-chain electronically isolated photoactive groups with large π-electron density.
- Polymers with π-conjugated main chain
- Polymers with σ-conjugated backbone

2.2.1 Molecularly doped polymers

Molecularly doped polymers (MDP) are systems in which the molecules giving rise to carrier generation and transport are incorporated in to an inert polymer matrix (Fig. 2.1). The name 'molecular doping' came from the fact that the doped molecules essentially retain their identity in the host polymer.

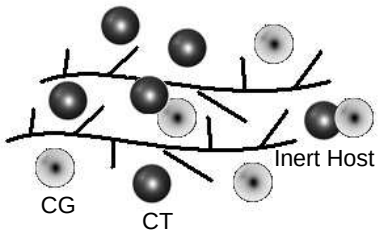

Figure 2.1: Molecularly doped polymers comprise an inert polymer host dispersed with Charge Generating (CG) and Charge Transporting (CT) molecules.

The dopants in molecularly doped polymers have only weak interactions through Van der Waals forces, invalidating the application of classical band transport model to describe the charge transport.[4] Usually the concentration of active molecules in these systems range from 1 to 50% and thus the term doping is different from that employed with inorganic semiconductors.[5]

Molecularly Doped Polymer systems offer the maximum flexibility in design as each component is separately added to the host matrix.[6] There are reports of using this design approach in the fabrication of optoelectronic devices like electroluminescent devices and electro-photographic photoreceptors.[7] The photoconducting material studied first was a molecularly doped polymer. Details of this polymer system are given in Section 2.4.

2.2.2 Polymers with pendant or in-chain photoactive groups

This class of photoconducting polymers have active units responsible for photoconductivity in the main chain or pendant to the main chain as illustrated in Fig. 2.2. The well known photoconductor PVK belongs to this class. There are also many other photoconductive polymers which belong to this class.[8,9]

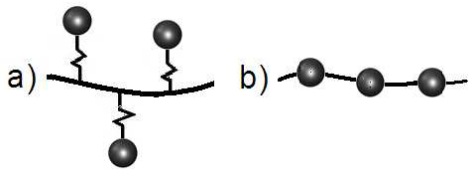

Figure 2.2: Polymers with (a) pendant and (b) in chain photoactive groups.

Most of the photoconducting polymers in this class contain the aromatic amino group as the building block.[10]

2.2.3 Polymers with π-conjugated main chain

Polymers with π conjugated main chain are normally found to be electrically conducting. But there are many reports of photoconductive macro-

molecules with conjugated C=C, C=N, N=N and C≡C bonds. One of the problems associated with this type of molecules is the higher dark conductivity due to the high degree of delocalization of electrons.[10]

2.2.4 Polymers with σ-conjugated backbone

Polymers with σ-electron conjugation were also reported to be photoconducting. Polysilanes are widely studied as the silicon backbone with σ-electron conjugation permits delocalization of electrons along the chain.[11]

2.3 Photoconducting polymer systems studied

Two photoconducting polymer systems are presented in this section. First system belongs to the class of molecularly doped polymers explained in Section 2.2. The second system comprises a new co-polymer synthesized in the lab. The molecule was photoconducting in the visible region of the spectrum. Results obtained when it was doped with a sensitizer molecule are also presented.

2.4 Molecularly doped poly (methyl methacrylate)

There are many types of polymer photoconductors as described in Section 2.2. In this work, we first investigated a molecularly doped polymer system. This class offers the maximum control over the properties as each component (charge generators and transporting units) can be incorporated in to the polymer matrix to the desired level. The maximum extent possible is determined by the phase separation or crystallization of the doped molecules. Charge transport in molecularly doped systems was subjected to numerous investigations[6,12,13] and the mechanism of transport was accepted to be hopping through a manifold of localized states whose energetic distribution is gaussian.[14] The activation energy needed for hopping is a function of electric field and molecular separation.[6] It is considered that

the electric field has an effect of lowering the energy required to hop from one localized state to the other.[12]

Photoconductivity measurements were done in the sandwich cell configuration.[15] In this method, the active material is sandwiched between two electrodes. One of the electrodes must be transparent so that the sample could be illuminated by photons of suitable wavelength. In this study, Indium Tin Oxide (ITO) coated glass plates were used as the substrate so that ITO served as the transparent electrode. The other electrode was vacuum deposited silver. The noble metal Ag could form unreacted contacts to organic molecules,[16] and the rate of evaporation of silver was kept low to avoid damage to the film surface.

2.4.1 Preparation of sandwich cells

Molecularly doped poly(methyl methacrylate) (PMMA) comprises aniline (AN) as electron donor and 2,4,6-trinitrophenol (TNP) as electron acceptor. AN (SD Fine Chemicals, India) was purified by distillation and TNP (SD Fine Chemicals, India) by two fold recrystallization using ethanol. Concentration of TNP was kept low to reduce chances of phase separation and AN was added in excess to make 1 : 100 mole ratio between the components TNP and AN. The samples were labeled according to the dopant ratio present in the PMMA host as follows, S0 (TNP alone), S1 (AN alone), S11 (TNP: AN = 1:1) and S100 (TNP: AN = 1:100). The samples were prepared by drop-casting a 7 wt% solution of the components in spectroscopic grade chloroform onto ITO coated glass plates. The ITO plates used in this work had a layer thickness of 2000 $\mathring{A}$ and a sheet resistance of 10 $\Omega/\Box$.

The solution was filtered using a 0.2 μm Teflon filter prior to casting. The breakdown electric field of the films without this filtering process was $\sim$ 20 V/μm whereas films prepared after filtration could withstand fields up to $90V/\mu$m. After drying at 28 ± 1^0 C for 12h, the samples were transferred to a vacuum desiccator and kept at $\sim 10^{-2}$ Torr. A drying period of total 48 h (at 28^0 C) was given for complete solvent removal. Thickness was determined using a Dektak 6M Stylus profiler. Thickness

could be adjusted to be in the range 15 - 30 μm by varying the viscosity and amount of solution transferred to the ITO. Finally, silver electrodes of area 5x5 mm^2 were vacuum deposited on to the films to complete the sandwich structure. The sandwiched samples in the present case were 16 μm thick.

2.4.2 Optical absorption spectra

The optical absorption spectra of the samples were recorded using a Jasco V-570 spectrophotometer. The absorption spectrum (Fig. 2.3) showed both red shift in the absorption band and an increase in absorbance. These changes, termed as bathochromic and hyperchromic shifts respectively, in the absorption spectrum of S11 compared to S0 or S1 indicated the formation of a charge transfer (CT) complex between TNP and PA. This is similar to the CT complex formation in PVK: TNF photoconductive system.[17] A CT complex is usually formed between an electron donating and electron accepting type molecules.[18]

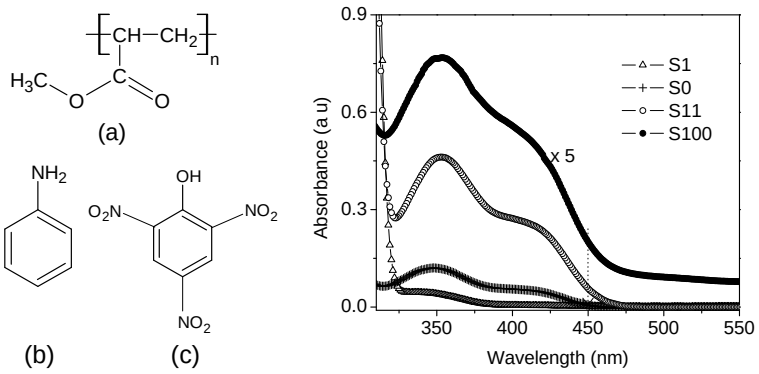

Figure 2.3: Structure of the molecules (a) PMMA (b) AN and (c) TNP and absorption spectra showing bathochromic and hyperchromic shifts.

The spectra of S11 and S100 were similar but there was an increase in absorbance. Absorbance showed a strong dependence on the concentration of the donor molecules. Due to the strong electrostatic interaction between the donor AN molecules and TNP (the acceptor) molecules, multimolecu-

lar assembly of AN molecules around TNP might be formed similar to a solvent cage. This could be the reason for the dependence of absorbance on the concentration of AN.[15]

2.4.3 Temperature dependence of conductivity

Electrical measurements were carried out with ITO biased negative so that the probability of injection of holes could be reduced. The temperature dependent current-voltage measurements (in dark) were done as explained in Section 1.6.2.

Variation of dark conductivity with temperature was noted for the samples. The Arrhenius plots of S1, S11 and S100 are shown in Fig. 2.4 for a limited temperature range.

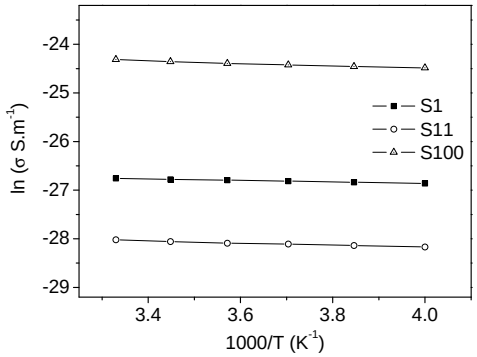

Figure 2.4: Arrhenius plots of the samples S1, S11 and S100. A change in conductivity could also be understood.

The electrical conductivity of S11 sample was less compared to S100 and S1. This could be due to the fact that in S11, the major units were AN:TNP complexes, which release less number of free carriers while S100 and S1 hosted excess donor type molecules. S11 showed an Arrhenius behavior with activation energy of 0.20 eV. In S1, the activation energy was 0.16 eV. This type of increase in activation energy on complex formation was observed in other systems also.[19] Sample S100 was also similar but the activation energy was slightly increased to 0.22 eV.

As thermal activation was involved, the conduction mechanism could be either thermionic emission or hopping conduction.[20] The I-V plots were linear ($I \propto V$) ruling out the possibility of thermionic emission where, a behavior of the type $I \propto V^{1/2}$ would be observed.[20] So the dominant conduction mechanism in the material appeared to be temperature assisted hopping between localized states, similar to other molecularly doped systems.[6]

2.4.4 Photocurrent in molecularly doped PMMA

Spectrally resolved photocurrent (action spectra) measurements were done using the modulated photocurrent setup explained in Section 1.6.4. The spectral light intensity distribution of the illuminating source was shown in Fig. 1.12, the intensity was slightly less than 1mW/cm^2. The photocurrent action spectra of the samples S0, S11 and S100 are shown in Fig. 2.5.

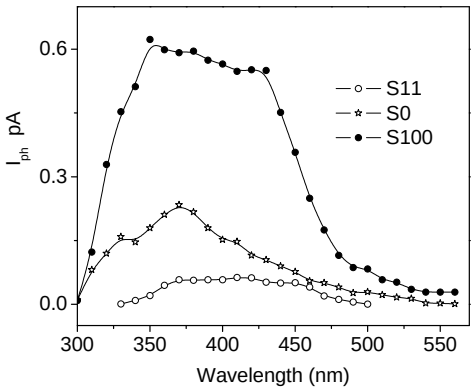

Figure 2.5: Action spectra of S0, S11 and S100 (30 Hz, 26.6$V/\mu m$).

In S11, the photocurrent yield was very small. In sample S100, the photocurrent was higher with considerable increase of current in the visible region. There was no photocurrent for S1, small current for S11 and increased current for S100 and S0. The photoaction spectrum of S100 was similar to the absorption spectrum of S11. Generation of carriers by AN can be neglected as this molecule do not absorb in the visible region. These facts show that the generation of carriers in S100 was by the CT units,

with excess AN acting as transport units. The increased photocurrent yield was obtained for the sample S100, which incorporated both charge generators and transporting units. This sample was further studied for the field and intensity dependence of photocurrent.

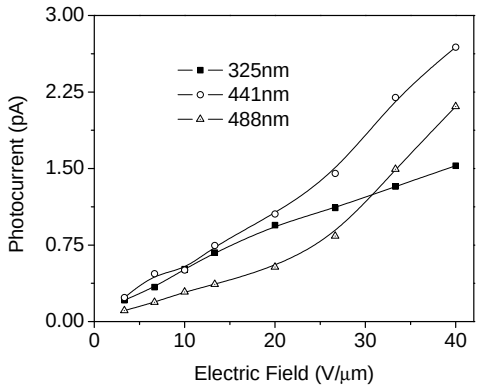

Figure 2.6: Photocurrent as a function of applied electric field at different photon energies at 30 Hz.

Photocurrent showed a power-law behavior of the form $I_{ph} \propto E^{\beta}$ with respect to the electric field (Fig 2.6), with the exponent having lower values at higher photon energies.

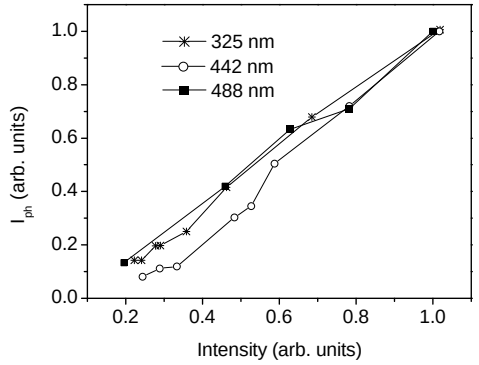

Figure 2.7: Intensity dependence of photocurrent at an applied field of $26.6V/\mu m$, 30 Hz.

The value of $\beta = 0.78$ for 3.82 eV (325nm), 1.2 for 2.81 eV (441.6nm)

and 1.8 for 2.54 eV (488nm) showed the increasing dependence of I_{ph} on electric field for low-energy photons. Dependence of the photocurrent on intensity of illumination was also studied at three different photon energies (Fig. 2.7). Intensity dependence was linear and yielded good fits to the power-law, $I_{ph} \propto W^{\gamma}$ with $\gamma = 0.99$ for 3.82 eV, 1.11 for 2.81 eV and 1.12 for 2.54 eV. The maximum value of the light intensity used was 6.3 mW/cm^2. Linearity of photocurrent with light intensity indicated the absence of bimolecular charge carrier recombination and space charge effects. It also indicated the absence of heating effects.[21]

The steady state photocurrent measurement showed (Fig. 2.8) the change in current through the sample on laser irradiation. The photoconductive sensitivity of the MDP was calculated using equation 1.16.

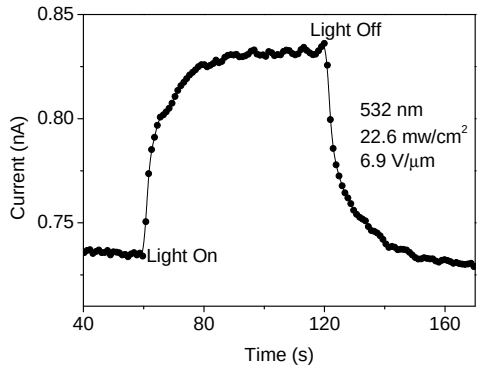

Figure 2.8: Variation of current through the sandwich cell S100 on light exposure.

The photoconductive sensitivity of this system was of the order of 10^{-13} S cm/W, estimated from DC photocurrent measurements. The PMMA composite with a ratio of 1:100 between TNP and AN was found to be a photoconductor. But the use of this composite was limited as the value of sensitivity was low. Also, phase separation of the components may arise when another molecule is added to impart electro-optic functionality to the photoconductor. Thus possibilities of more stable systems with less number of components were looked at and a photoconducting polymer, which was photoconductive with a higher sensitivity was studied. The

next section gives the details of this single component photoconductor and the results of the studies done.

2.5 Poly(2-methacryloyl-1-(4-azo-1'-phenyl)aniline -co-styrene)

The molecule, Poly(2-methacryloyl-1-(4-azo-1'-phenyl)aniline-co-styrene), which was labeled as (PAz), could be synthesized by a free radical co-polymerization of the monomers 2-methacryloyl-1-(4-azo-1'-phenyl) aniline and styrene.[22] The number average molecular weight (M_n) was 4987 and weight average molecular weight (M_w) was 12326, as estimated using size exclusion chromatography. The polydispersity index (M_w/M_n) was 2.47. The glass transition temperature (T_g) of the polymer was determined using differential scanning calorimetry (DSC) and found to be 65.4^o C. Structure of the polymer is shown in Fig. 2.9.[22]

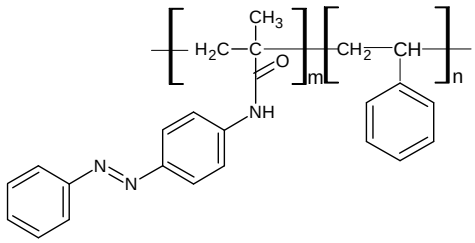

Figure 2.9: Structure of Poly(2-methacryloyl-1-(4-azo-1'-phenyl)aniline-co-styrene)

The main chain of the polymer is non-conjugated but there are electron rich pendant groups attached to this chain. It showed photoconductivity in the pristine as well as doped states. The molecule C_{60} was used as a sensitizer for this polymer. Some properties of this sensitizer are given in Section 1.4.6.

2.5.1 Cyclic voltammetry

The semiconducting properties of molecular semiconductors are highly dependent on the position of the Highest Occupied and Lowest Unoccupied molecular orbitals (HOMO and LUMO).[23,24] The value of LUMO energy level can be estimated from the reduction potential of the molecule. The HOMO level is usually obtained by adding the value of optical gap to the value of LUMO. Cyclic Voltammetry was done to estimate the reduction potential of the polymer as explained in Section 1.6.5. The potential was cycled between 0 to -2 V at a constant sweep rate of 25 mV/s. The cyclic voltammogram of PAz is shown in Fig. 2.10

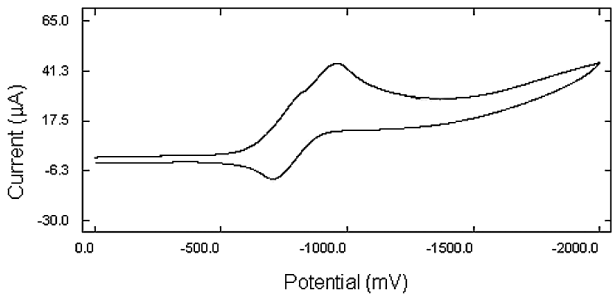

Figure 2.10: Cyclic voltammogram of PAz.

The onset of reduction was at -626 mV. The corresponding LUMO position was estimated to be 3.77eV. Considering the optical gap as the separation between the HOMO and LUMO levels, the HOMO was estimated to be at 5.75eV. The optical gap was estimated to be 1.98 eV.

2.5.2 Preparation of sandwich cells

Photoconductivity measurements were done in the sandwich cell configuration. Spectroscopic grade chloroform was used to prepare an 8 wt% solution of PAz. 1% dioctyl phthalate (DOP) was also added to this solution to increase the adhesion of the polymer to ITO coated substrates. After filtering through a 0.45 μm Nylon filter, the solution was drop cast

onto ITO coated glass plates. After drying at 28 ± 1^0C for 12 h, the samples were transferred to a vacuum desiccator and kept at $\sim 10^{-2}$ Torr. A drying period of total 48 h (at 28^0C) was given for complete solvent removal. Thickness was determined using a Dektak 6M Stylus profiler. Thickness could be adjusted by varying the viscosity and amount of solution transferred to the ITO. Electrodes were deposited on to the films by thermal evaporation of silver to get the sandwich structure. The active area of the device was 36 mm^2. The sandwiched samples in the present case had a thickness of 15 μm. The cell was labeled as ITO/PAz:DOP/Ag.

Sensitized polymer sandwich cells were also prepared by the above method. The concentration of the sensitizer C_{60} was $4.5\text{x}10^{-6}$ moles in an 8 wt% solution (7ml) of PAz. The structure of the cell was ITO/PAz: C_{60}:DOP/Ag.

2.5.3 Optical absorption and fluorescence spectra

Absorption spectrum of a solution of the polymer in chloroform and that of a 1.9 μm thick film cast from chloroform solution are shown in Fig. 2.11. Owing to the good absorption in the visible region, the color of the polymer was dark brown.

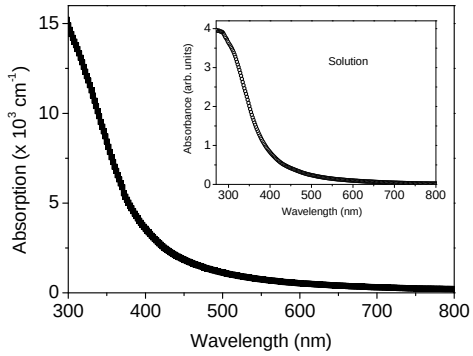

Figure 2.11: Absorption spectra of PAz in film form (on quartz). Inset shows the spectrum of a chloroform solution of PAz.

Absorption spectra of PAz, when doped with C_{60}, showed only a slight

modification (Fig. 2.12). There was no new bands present in the new absorption spectra, instead, it could be considered as a simple overlapping of both the spectra. Similar to the case of MEH-PPV/C_{60} composites, this could be due to weak mixing of the ground state electronic wave functions.[25]

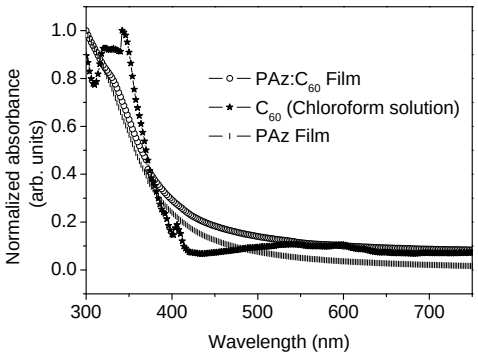

Figure 2.12: Absorption spectra of PAz after sensitizing with C_{60} along with the spectra of individual molecules.

The fluorescence emission of PAz was also recorded for excitation at 400nm. This is shown in Fig. 2.13. In the solid state, the emission intensity was very low and slightly shifted towards longer wavelengths.

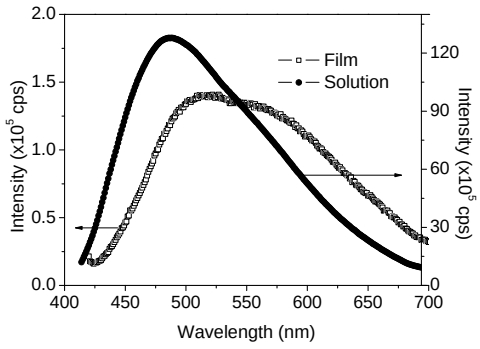

Figure 2.13: Fluorescence spectra of PAz with excitation at 400 nm.

The fluorescence emission was recorded for the C_{60} doped polymer also.

The emission intensity was reduced by $\approx 40\%$ when doped with C_{60}. This fluorescence quenching in C_{60} doped polymers is reported in the literature as a result of an ultra-fast electron transfer reaction.[26] Fluorescence quenching effect of the dopant is shown in Fig. 2.14. The emission intensity of both doped and undoped films were normalized to the maximum emission intensity of the undoped film for easy comparison.

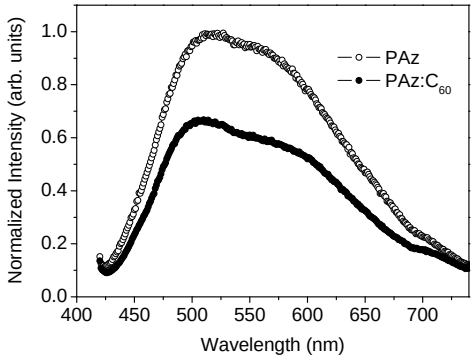

Figure 2.14: Fluorescence quenching action of C_{60}. Excitation was at 400nm.

2.5.4 Photocurrent measurements

Modulated photocurrent method was used to study the spectral response of PAz. Both undoped and C_{60} doped polymers were subjected to the study. Fig. 2.15 and 2.16 show the spectral distribution of photocurrent in ITO/PAz:DOP/Ag and ITO/PAz:C_{60}:DOP/Ag respectively. Photoconductivity was observed in the entire visible region for this molecule. Higher photocurrent was observed above $\sim$ 550nm. It is known that in polymer photoconductors, the primary excited species are singlet and triplet excitons with binding energy of the order of 0.5 eV.[27] It is the dissociation of these species that lead to carrier generation.[28] The photocurrent generation in this polymer could also be by the dissociation of excitons, which otherwise undergo recombination, in the presence of electric field or impurities.[27,29,30]

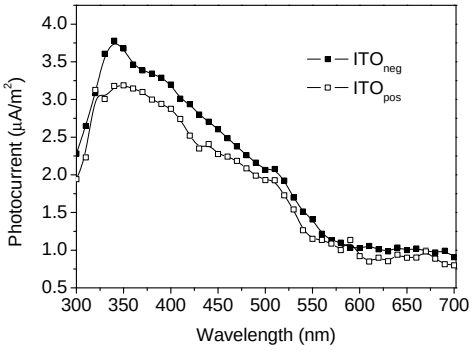

Figure 2.15: Photocurrent action spectrum of ITO/PAz:C_{60}:DOP/Ag cell, (10 V/μm, 30 Hz).

Photocurrent showed a small dependence on the polarity of the electrodes. This could be due to changes in charge injection. Fluorescence quenching observed in the case of C_{60} doping indicate either energy transfer or charge transfer, which are competing processes in donor-acceptor systems.[28]

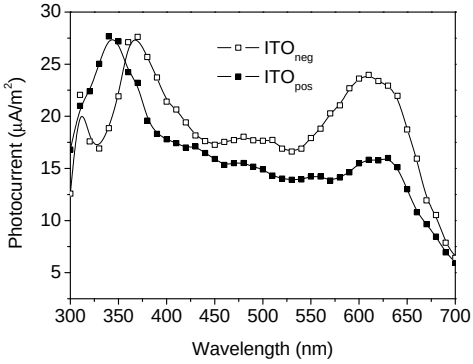

Figure 2.16: Photocurrent action spectrum of ITO/PAz:C_{60}:DOP/Ag cell (10 V/μm, 30 Hz).

Doping of PAz with C_{60} increased the overall photocurrent yield along with higher photocurrent at lower photon energies. The increased photocurrent and the fluorescence quenching upon doping with C_{60} might be due to an efficient charge transfer instead of energy transfer between the polymer and the dopant. Steady state photocurrent measurement was

done using a diode laser operating at 650nm as explained in Section 1.6.3. Fig. 2.17 shows the variation of current through the sandwich device ITO/PAz:C_{60}:DOP/Ag on laser irradiation.

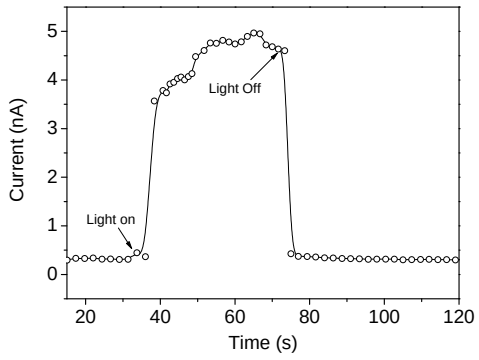

Figure 2.17: Variation of current through the sandwich cell ITO/PAz:C_{60}:DOP/Ag on light exposure (at 3.5V/μm). Irradiation was from a diode laser (650nm, 1mW).

The sudden increase and decrease in current on laser irradiation and cutoff showed that the response of PAz to light was fast. Also, the initial and final values of dark current were of the same order. These facts indicate that the change in conductivity was not due to any light induced chemical reactions. The change in current on irradiation was not due to any heating effects caused by the beam as the absorption of the film at this wavelength was weak and the intensity of the beam was small. The fluctuations in steady state current was due to the instability of the diode laser output. The photoconductive sensitivities of the polymer when doped with C_{60} were 17.6, 16.6 and 22.9 x 10^{-12} Scm/W at 440, 530 and 630nm respectively, based on modulated photocurrent measurements. This value of photoconductive sensitivity is comparable to typical values reported in the literature.[31]

2.6 Summary and conclusions

In this chapter two photoconducting polymer systems were studied, of which one was a simple molecularly doped photoconductor and the other

was a polymer with electron rich pendant units. Temperature dependence of conductivity of molecularly doped PMMA showed that the conduction was supported by hopping of carriers between localized states. The photoconductive sensitivity was found to be of the order of 10^{-13} S cm/W only. Also, a multi-component system like molecularly doped PMMA may not be able to withstand phase separation when other molecules are added to the system to impart electro-optic functionality.

Photoconductivity was established in Poly(2-methacryloyl-1-(4-azo-1'-phenyl)aniline-co-styrene) using spectrally resolved photocurrent measurement and DC photocurrent study. The photoconductive sensitivity of this molecule in the undoped state was of the order of 10^{-12} S cm/W and it depends on the irradiation wavelength. Presence of the molecule C_{60} extended the response of this molecule to longer wavelengths along with a higher photocurrent yield. The sensitivity with C_{60} was an order of magnitude higher.

Based on literature reports, the photoconductive sensitivity observed in Poly(2-methacryloyl-1-(4-azo-1'-phenyl)aniline-co-styrene) was sufficient for photorefractive effect.[31–33] So it appeared that the molecule Poly(2-metha cryloyl-1-(4-azo-1'-phenyl)aniline-co-styrene) sensitized with C_{60} was a good choice as a photoconductor for photorefractive composites.

References

[1] K.-Y. Law, "Organic Photoconductive Materials: Recent Trends and Developments," Chem. Rev. **93,** 449–486 (1993).

[2] J. Shakos, A. Cox, D. West, K. West, F. Wade, T. King, and R. Blackburn, "Processes limiting the rate of response in photorefractive composites," Opt. Commun. **150,** 230–234 (1998).

[3] S. Ducharme, J. C. Scott, R. J. Twieg, and W. E. Moerner, "Observation of the Photorefractive Effect in a Polymer," Phys. Rev. Lett. **66,** 1846–1849 (1991).

[4] A. Peled, L. B. Schein, and D. Glatz, "Hole mobilities in films of a pyrazoline:polycarbonate molecularly doped polymer," Phys. Rev. B. **41,** 10835–10844 (1990).

[5] J. Sworakowski and J. Ulański, "Electrical properties of organic materials," Annu. Rep. Prog. Chem., Sect. C. **99,** 87–125 (2003).

[6] M. Stolka, J. F. Yanus, and D. M. Pai, "Hole transport in solid solutions of a diamine in polycarbonate," J. Phys. Chem. **88,** 4707–4714 (1984).

[7] D. W. Dongge Ma, Z. Hong, X. Zhao, X. Jing, and F. Wang, "Bright blue electroluminescent devices utilizing poly(N-vinyl carbazole) doped with fluorescent dye," Synth. Met. **91,** 331–332 (1997).

[8] R. Oshima, T. Uryu, and M. Seno, "Improved hole mobility of polyacrylate having a carbazole chromophore," Macromolecules **18,** 1043–1045 (1985).

[9] T. Sasakawa, T. Ikeda, and S. Tazuke, "Improved hole drift mobility in excimer-free polymers containing a dimeric carbazole unit," Macromolecules **22,** 4253–4259 (1989).

[10] M. Stolka, "Photoconductive Polymers," In *Special Polymers for Electronics and Optoelectronics*, J. A. Chilton and M. T. Goosey, eds., pp. 284–285 (Chapman & Hall, London, 1995).

[11] R. G. Kepler, J. M. Zeigler, L. A. Harrah, and S. R. Kurtz, "Photocarrier generation and transport in σ bonded polysilanes," Phys. Rev. B. **35,** 2818–2822 (1987).

[12] L. B. Schein, A. Peled, and D. Glatz, "The electric field dependence of the mobility in molecularly doped polymers," J. Appl. Phys. **66,** 686–692 (1989).

[13] I. I. Fishchuk, A. K. Kadashchuk, A. Vakhnin, Y. Korosko, H. Bässler, B. Souharce, and U. Scherf, "Transition from trap-controlled to trap-to-trap hopping transport in disordered organic semiconductors," Phys. Rev. B. **73,** 115210–115221 (2006).

[14] T. Nagase and H. Naito, "Localized-state distributions in molecularly doped polymers determined from time-of-flight transient photocurrent," J. Appl. Phys. **88,** 252–259 (2000).

[15] V. C. Kishore, R. Dhanya, C. S. Kartha, K. Sreekumar, and R. Joseph, "Photoconductivity in molecularly doped poly(methyl methacrylate) sandwich cells," J. Appl. Phys. **101,** 063102–063105 (2007).

[16] Y. Hirose, A. Kahn, V. Aristov, P. Soukiassian, V. Bulovic, and S. R. Forrest, "Chemistry and electronic properties of metal-organic semiconductor interfaces: Al, Ti, In, Sn, Ag, and Au on PTCDA," Phys. Rev. B **54,** 13748–13758 (1996).

[17] T. K. Däubler, R. Bittner, K. Meerholz, V. Cimrová, and D. Neher, "Charge carrier photogeneration, trapping, and space-charge field formation in PVK-based photorefractive materials," Phys. Rev. B. **61,** 13515–13527 (2000).

[18] A. M. A. El-Sayed, H. F. M. Mohamed, and A. A. A. Boraei, "Positron annihilation studies of some charge transfer molecular complexes," Radiat. Phys. Chem. **58,** 791–795 (2000).

[19] P. Pal and T. N. Misra, "Charge transfer compleses of polyenes: spectroscopic, dark and photoconductive studies," J. Phys. D: Appl. Phys. **23,** 218–222 (1990).

[20] W. Wang, T. Lee, and M. A. Reed, "Mechanism of electron conduction in self assembled alkanethiol monolayer devices," Phys. Rev. B. **68,** 035416–035422 (2003).

[21] K. S. Narayan, B. E. Taylor-Hamilton, R. J. Spry, and J. B. Ferguson, "Photoconducting properties of a ladder polymer," J. Appl. Phys. **77,** 3938–3941 (1995).

[22] R. Dhanya, "Development of Photorefractive Polymers: Synthesis and Characterization of Polymers with Donor-π-Acceptor Groups," Ph.D. Thesis (Cochin University of Science and Technology, India, 2008).

[23] H. Wang, Q. Sun, Y. Li, D. Liu, X. Wang, and X. Li, "A luminescent copolymer containing PPV-based chromophores and flexible tri(ethylene oxide) spacers," React. Funct. Polym. **52,** 61–69 (2002).

[24] J. H. Kim and H. Lee, "Enhancement of efficiency in luminescent polymer by incorporation of conjugated 1,3,4-oxadiazole side chains as hole-blocker/electron-transporter," Synth. Met. **143,** 13–19 (2004).

[25] C. H. Lee, G. Yu, D. Moses, K. Pakbaz, C. Zhang, N. S. Sariciftci, A. J. Heeger, and F. Wudl, "Sensitization of the photoconductivity of conducting polymers by C_{60}: Photoinduced electron transfer," Phys. Rev. B **48,** 15425–15433 (1993).

[26] L. Smilowitz, N. S. Sariciftci, R. Wu, C. Gettinger, A. J. Heeger, and F. Wudl, "Photoexcitation spectroscopy of conducting-polymer-C_{60} composites: Photoinduced electron transfer," Phys. Rev. B **47,** 13835–13842 (1993).

[27] V. I. Arkhipov and H. Bässler, "Exciton dissociation and charge photogeneration in pristine and doped conjugated polymers," Phys. Stat. Sol. (a) **201,** 1152–1187 (2004).

[28] M. T. Lloyd, Y.-F. Lim, and G. G. Malliaras, "Two-step exciton dissociation in poly(3-hexylthiophene)/fullerene heterojunctions," Appl. Phys. Lett. **92,** 143308–143311 (2008).

[29] V. I. Arkhipov, H. Bässler, M. Deussen, E. O. Göbel, R. Kersting, H. Kurz, U. Lemmer, and R. F. Mahrt, "Field-induced exciton breaking in conjugated polymers," Phys. Rev. B. **52,** 4932–4940 (1995).

[30] C. L. Braun, "Electric field assisted dissociation of charge transfer states as a mechanism of photocarrier production," J. Chem. Phys. **80,** 4157–4161 (1984).

[31] S.-H. Park, K. Ogino, and H. Sato, "Synthesis and characterization of a main-chain polymer for single component photorefractive materials," Synth. Met. **113,** 135–143 (2000).

[32] S. M. Silence, C. A. Walsh, J. C. Scott, and W. E. Moerner, "C_{60} sensitization of a photorefractive polymer," Appl. Phys. Lett. **61,** 2967–2969 (1992).

[33] L. Wang, Y. Zhang, T. Wada, and H. Sasabe, "Photorefractive effect in a photoconductive electro-optic carbazole trimer," Appl. Phys. Lett. **69,** 728–730 (1996).

CHAPTER

THREE

Photoconductivity Studies on Polybenzoxazines

3.1 Introduction

Molecularly doped photoconductors are liable to phase separation when more components are added for additional functionality.[1,2] This is a potential drawback for their application to photorefractivity where components will be present for inducing electro-optic functionality and for reducing the glass transition temperature of the photorefractive composite. Although the approach to molecularly doped photoconducting system is rather simple, for practical applications more stable systems are required. If the polymer backbone as such is photoconducting, the stability can be improved. Also, this has an added advantage that the polymer itself takes part in the grating formation whereas in molecularly doped systems, the host polymer has the role of an inert matrix and it does not actively participate in charge transport or generation.[3]

In this chapter, three polybenzoxazines are studied for possible use in photorefractive polymers. Though non-conjugated, these polymers possess electronically isolated electron rich units in its main chain. There are reports on methods for tailoring chemical[4,5] and physical properties[6] of this class, but polybenzoxazines have not been studied for optoelectronic applications so far. The polymers were doped with electron acceptor molecules

mentioned in Section 1.4.6 to study the possibility of getting an enhancement in photocurrent. It is to be noted that the systems presented in this chapter are only photoconducting, no dipolar molecules were added with an intention to induce photorefractivity. The aim was to identify molecules with good photoconductivity and spectral response. C_{60} and two more electron acceptor molecules 7,7,8,8-tetracyanoquinodimethane (TCNQ) and 2,4,6-trinitrophenol (TNP) were tried as photosensitizers.

3.2 Preparation of sandwich cell Structure

Sandwich cells of the polymer for electrical measurements were prepared as follows. 8 wt% solution of the polymer was prepared in chloroform which also contained 1 wt% dioctyl phthalate (DOP), which was found to increase the stability of the polymer on ITO substrates. The solution was filtered through a 0.2 μm teflon filter and casted onto clean ITO plates. The casted samples were allowed to dry overnight at room temperature (28 ± 1^0C) and then transferred to a vacuum desiccator and kept at $\sim 10^{-2}$ Torr. A drying period of 48 h was given for maximum solvent removal. Film thickness was determined using a stylus profiler (Dektak 6M) and those with nearly 15-20 μm were selected for the deposition of top electrode.

To sensitize the polymer with electron acceptors, the molecules given in Section 1.4.6 were used. TCNQ, TNP and C_{60} were used as dopants. The concentration of these molecules was kept to $\sim 10^{-5}$ mol/l.

Top electrode was given by vapor deposition of silver in a vacuum chamber. To avoid damage to the film surface, the rate of deposition of silver was kept low. The active area of the device, defined by the silver contact was in the range 36-42 mm^2. As silver could form unreacted contacts with organic molecules,[7] complications due to chemically induced interfacial states could be discarded. The general structure of the sandwich cell was ITO/Polymer:DOP:Dopant/Ag. Synthesis of these molecules are given elsewhere.[8] Following sections gives the details of the polymers and the results obtained.

3.3 Poly(6-tert-butyl-3,4-dihydro-2H-1,3 - benzoxazine)

Poly(6-tert-butyl-3,4-dihydro-2H-1,3-benzoxazine), labeled as P1, is a non-conjugated polymer with an electron rich phenyl ring. The structure of the molecule is shown in Fig. 3.1. The t-butyl substituent on this ring is expected to increase the density of electrons in the ring. Non-bonding electrons are available on the nitrogen and oxygen. As such, the polymer could be regarded as comprising electronically isolated electron rich groups. The glass transition temperature of the polymer was 46^0C, determined using DSC. The molecule is soluble in organic solvents such as toluene, chloroform and chlorobenzene. It has good film forming properties and the films are transparent.

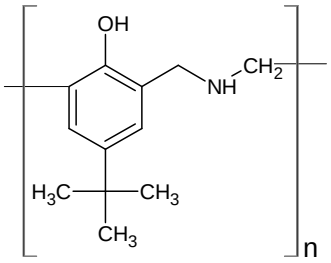

Figure 3.1: Poly(6-tert-butyl-3,4-dihydro-2H-1,3-benzoxazine), (P1).

The number average molecular weight (M_n) of P1 was 403 and weight average molecular weight (M_w) was 1080, which were estimated using size exclusion chromatography. The polydispersity index (M_w/M_n) was 2.7.

3.3.1 Optical absorption spectrum

The optical absorption spectrum of P1 in solution and in film form on quartz substrate are shown in Fig. 3.2. The onset of absorption in the visible was near 490 nm. The absorption coefficient (α) was evaluated using the relation α = (A/L) ln(10) with A as the measured absorbance and L as the film thickness in cm.

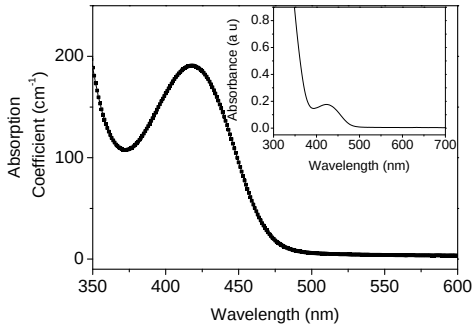

Figure 3.2: Optical absorption spectrum of the polymer P1 in solid (film on quartz) form. Inset shows the absorption spectrum of a chloroform solution of P1.

The first absorption band in the visible (375-475nm) region correspond most probably to a weak $n - \pi^*$ transition[9] which also give rise to strong fluorescence. It involve the excitation of the non-bonding orbital electrons on the hetero atom to the π^* molecular orbital extending over the conjugated part in the polymer. The nature of the transition ($n - \pi^*$ or $\pi - \pi^*$) was clarified by studying the effect of polarity of solvent on this transition. It was based on the hydrogen bonding effect, which induce a blue shift in the absorption band corresponding to an $n - \pi^*$ transition.[10–12]

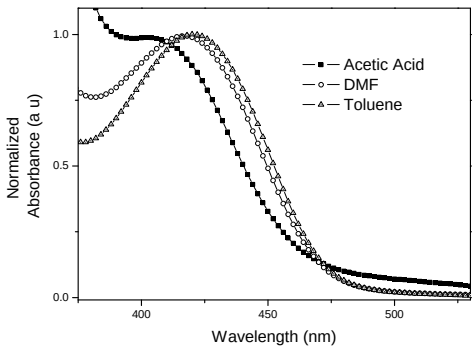

Figure 3.3: Blue shift in the absorption band with polarity of the solvent.

The solvent effect on the band was studied using solvents Acetic acid, Dimethylformamide (DMF) and Toluene. Fig. 3.3 shows the blue shift

of this absorption band when the solvent was changed from least polar (toluene) to highly polar (acetic acid) thereby confirming the transition to be $n - \pi^*$.

3.3.2 Fluorescence quenching

The polymer showed fluorescence when excited with light of energy greater than the optical gap. The fluorescence spectrum of the polymer was studied with and without electron acceptors. Emission from the molecule was quenched when electron acceptor molecules (TCNQ, TNP and C_{60}) were present. The quenching of fluorescence intensity when P1 was doped with the same concentration of electron acceptors is shown in Fig. 3.4.

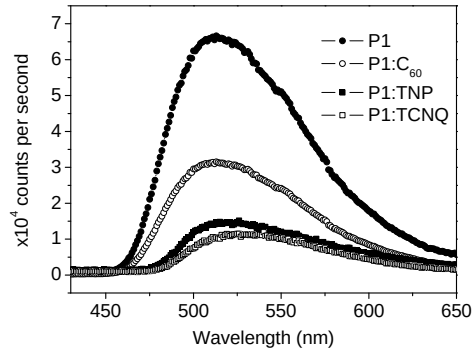

Figure 3.4: Fluorescence quenching effect of TCNQ, TNP and C_{60}. Excitation was at 400nm.

The fluorescence quenching could be either due to electron transfer or due to energy transfer. The strength of energy transfer depends on the Förster radius which in turn depends on the relative overlap between emission band of polymer and the absorption band of the acceptor.[13] If the emission band of the polymer and the absorption band of the dopant are not overlapping, the possibility of quenching through an energy transfer can be ruled out.[14,15] The absorption spectra of the electron acceptor molecules in chloroform were given in section 1.4.6. The absorption spectra of TNP and TCNQ were not overlapping with the emission spectrum of P1. Thus the possibility of energy transfer appeared to be low. Absorption spectrum

of C_{60} overlaps with the emission spectrum of P1. There are literature reports about the ultra-fast electron transfer reaction in C_{60} doped polymers and resulting fluorescence quenching.[16] Transient fluorescence experiments may be required for conclusive statements about electron transfer.

3.3.3 Cyclic voltammetry

Cyclic Voltammetry was used to estimate the reduction potential of the polymer as explained in Section 1.6.5. The cyclic voltammogram of P1 is shown in Fig. 3.5.

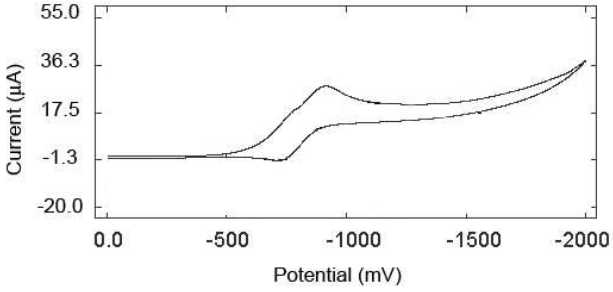

Figure 3.5: Cyclic voltammogram of P1.

The onset of reduction was at -540 mV. The corresponding LUMO position was estimated to be 3.86 eV. Assuming the optical gap as the separation between the HOMO and LUMO levels, the HOMO was estimated to be 6.27eV. The optical gap was estimated to be 2.41 eV. It is to be noted that the single particle LUMO position would be higher by the exciton binding energy,[17] hence there exists an uncertainty up to the value of the exciton binding energy in the above values. Moreover, the solid state values of HOMO and LUMO energy levels usually depend on other factors such as the polarizability of the matrix.[18]

3.3.4 Temperature dependence of conductivity

Measurement of the current-voltage characteristics with temperature permitted the study of the temperature dependence of conductivity (σ) of

the samples. Figure 3.6 shows the dependence of the dc conductivity on temperature.

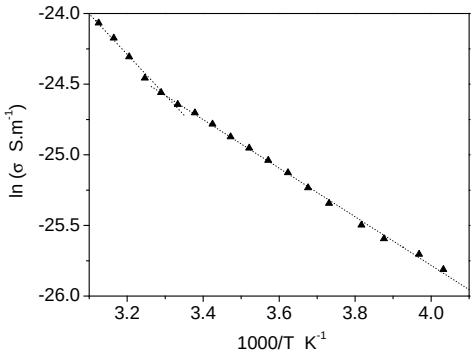

Figure 3.6: Arrhenius plot showing the temperature dependence of the dc conductivity of sandwich cells of P1 (ITO/P1:DOP/Ag). Dotted lines are linear fits to the data.

The temperature dependence of σ showed the semiconducting behavior with two activation energy regions. The near room temperature region showed an activation energy of 0.26 eV while the lower temperature region showed an activation energy of 0.20 eV. Both these values were calculated from the slope of the graph in the regions of interest.

3.3.5 Modulated photocurrent measurement

The spectral dependence of the photocurrent was studied using the modulated photocurrent technique explained in section 1.6.4. The photocurrent action spectrum was measured for different electric fields. The spectra are given in Fig. 3.7 for both polarities of ITO.

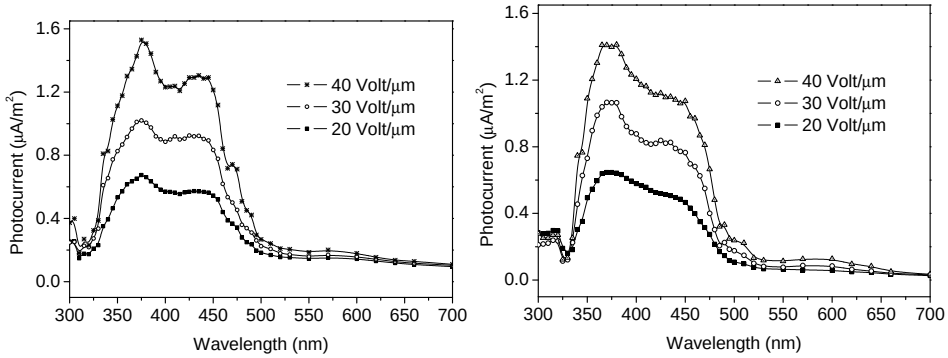

Figure 3.7: Photocurrent action spectra of sandwich cells of P1 (ITO/P1:DOP/Ag) for ITO_+ (left) and ITO_- (right).

The spectra were similar with respect to the biasing given to the electrodes. When light is absorbed by an organic semiconductor, the primary product is an exciton. It is the dissociation of this exciton which initiate charge generation. If the exciton density created by light was dissimilar at the top and bottom contacts, the spectra would depend on the polarity of the electrodes and the efficiency with which the electrode dissociates the exciton. Such a behavior was absent, which was primarily due to the low absorption in the film. Due to weak absorption, illumination could be considered uniform throughout the bulk and thus a uniform density of excitons was expected.[19]

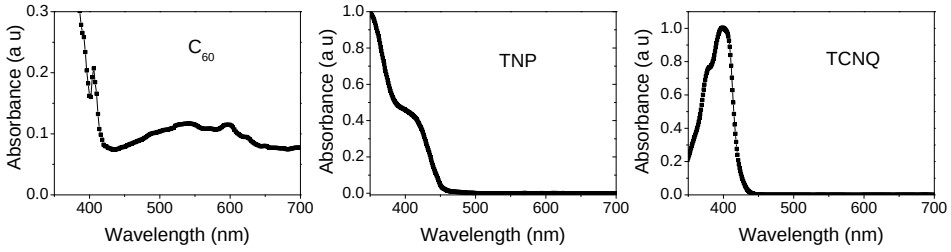

Figure 3.8: Optical absorption spectra of the electron acceptor molecules C_{60}, TNP and TCNQ in chloroform.

The photocurrent action spectra were recorded for the films doped with electron accepting molecules TNP, TCNQ and C_{60} also. Optical absorp-

tion spectra of these sensitizer molecules were given in section 1.4.6. It is reproduced here as Fig. 3.8.

3.3.5.1 Effect of TNP

Absorption of TNP was strong in the 400nm region (Fig.3.8). The spectrum of P1 doped with TNP showed an increase in absorption in the 425nm region of the absorption spectrum of P1.

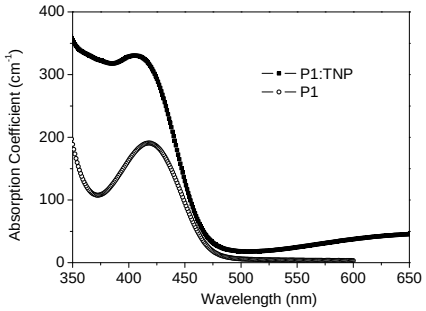

Figure 3.9: Absorption spectrum of P1 doped with TNP.

Fig. 3.10 shows the photocurrent action spectra of the sandwich cell ITO/P1:TNP:DOP/Ag for both polarities of ITO.

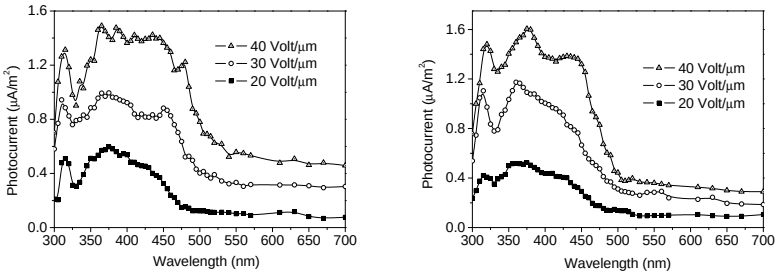

Figure 3.10: Photocurrent action spectra of sandwich cells of P1 doped with TNP for ITO_+ (left) and ITO_- (right).

TNP was not a good photosensitizer for P1 as the spectral response of

films of P1 doped with TNP did not show an appreciable increase in photocurrent.

3.3.5.2 Effect of TCNQ

Optical absorption of TCNQ is at its maximum near 400nm region (Fig.3.8). This molecule is considered to be a strong electron acceptor. The charge transfer complexes of TCNQ were subjected to numerous studies.[20,21] The absorption spectrum of P1 doped with TCNQ is shown in Fig. 3.11. The spectrum was similar to the undoped film except an increase in absorbance. Also, the absorption in the near infra red region was increased with the characteristic bands of TCNQ. But the photocurrent in this region remained unchanged.

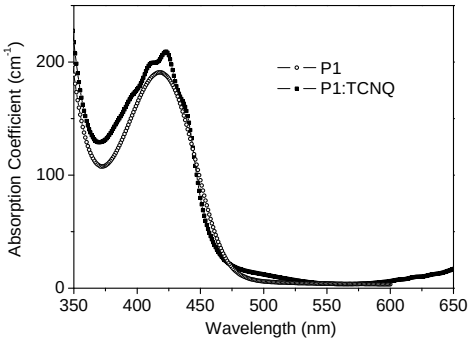

Figure 3.11: Absorption spectrum of P1 doped with TCNQ.

The figure (Fig. 3.12) shows the action spectra of sandwich cells with TCNQ as the dopant. But there was no significant increase in the photocurrent when doped with TCNQ.

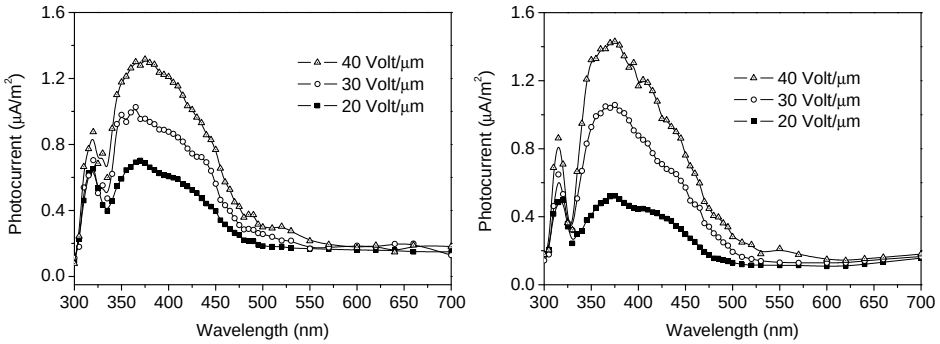

Figure 3.12: Photocurrent action spectra of sandwich cells of P1 doped with TCNQ for ITO_+ (left) and ITO_- (right).

TCNQ was also not able to act as a good sensitizer for P1. The order of photocurrent remained the same.

3.3.5.3 Effect of C_{60}

C_{60} has the ability to increase the hole mobility in hole transport layers.[22] It can also serve as a good photosensitizer for photorefractive polymers.[23] Optical absorption of this molecule span the entire visible spectrum. Absorption spectrum of P1 doped with C_{60} is shown in Fig. 3.13.

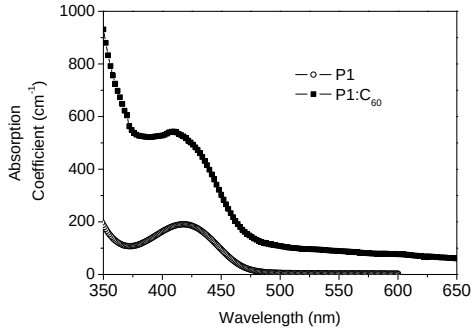

Figure 3.13: Absorption spectrum of P1 doped with C_{60}.

Absorption spectrum of the C_{60} doped state of P1 did not show the formation of any new bands. The spectrum was only a simple overlap of

the spectra of both molecules thereby indicating weak mixing of ground state electronic wave functions.[24] The photocurrent action spectrum of P1 doped with C_{60} is shown in Fig. 3.14. Doping the polymer with C_{60} yielded higher photocurrents along with an increase in photocurrent near the red region of the spectrum.

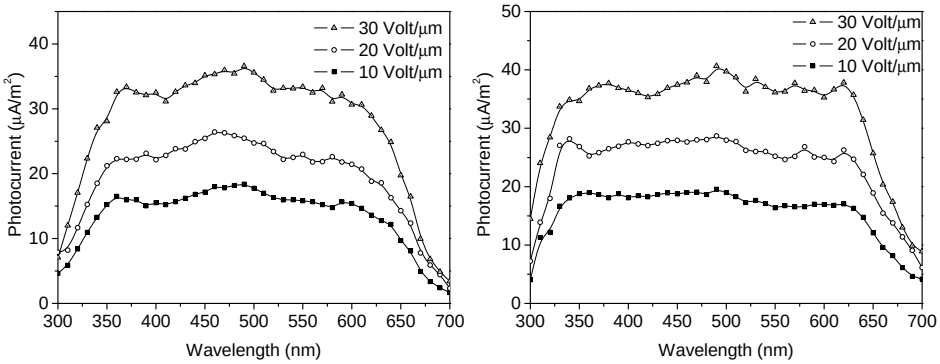

Figure 3.14: Photocurrent action spectra of sandwich cells of P1 doped with C_{60} for ITO_+ (left) and ITO_- (right).

C_{60} doped P1 showed photoconductivity in the entire visible region of the spectrum. Fig. 3.15 shows a comparison between the photocurrent values for positive and negative biasing to ITO.

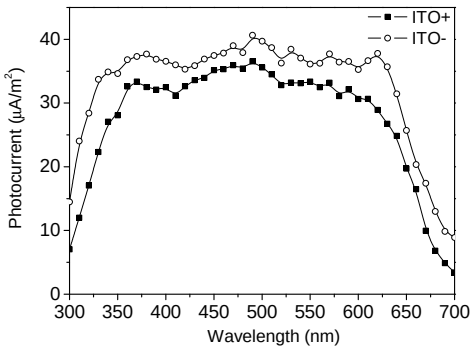

Figure 3.15: Comparison of the action spectra showing the bias dependence of photocurrent for 30V/μm.

Biasing given to ITO had a small effect on the magnitude of the measured photocurrent. Photocurrent was more when ITO was negatively biased with respect to the other electrode. This behavior and its possible reason are discussed in section 3.4.5.1.

3.3.6 Photoconductive sensitivity

Photoconductive sensitivity (S) of the doped polymer is the material parameter of interest. It was estimated using equation 1.16. The photoconductive sensitivity for selected wavelengths are shown in Table 3.1

Table 3.1: Photoconductive sensitivity of the sandwich cells of P1 for different wavelengths (@30V/μm, ITO$_-$).

Wavelength (nm)	Photoconductive Sensitivity 10^{-14}(S cm W^{-1})			
	C_{60}	TNP	TCNQ	Undoped
440	1336	28	23	28
490	1487	13	9	8
530	1488	10	5	4
630	2034	14	7	5

Photoconductive sensitivity of the order of 10^{-12} S cm W^{-1} was reported for C_{60} sensitized photorefractive polymers.[25] Photoconductive sensitivity observed in P1 doped with C_{60} at 30V/μm was of the order of sensitivity values required for observing photorefractive effect in polymers.[26] A value of 1.07 x 10^{-11}(S cm W^{-1}) was reported for a PVK:C_{60} based photorefractive polymer.[27] Thus P1:C_{60} may be used as a photoconducting host provided the photoconductive sensitivity is not reduced when electro-optic functionality is incorporated by other molecules.

3.4 Poly(6-tert-butyl-3-methyl-3,4-dihydro-2H-1,3 - benzoxazine)

Structure of Poly(6-tert-butyl-3-methyl-3,4-dihydro-2H-1,3-benzoxazine), labeled as P2, is shown in Fig. 3.16. The polymer P2 was a slightly modified form of P1. A methyl group was linked to the nitrogen in the monomer unit of P1 to get P2. The electron donating nature of this unit is expected to shift the HOMO level towards higher energy.[28] Higher HOMO level favor hole injection from the ITO electrode,[29] which further result in a higher exciton dissociation rate.

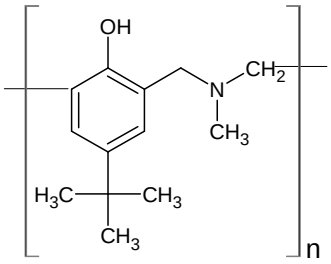

Figure 3.16: Poly(6-tert-butyl-3-methyl-3,4-dihydro-2H-1,3-benzoxazine), (P2).

The glass transition temperature of this polymer was 49^0 C. The number average molecular weight (M_n) was 239 and weight average molecular weight (M_w) was 971, as estimated using size exclusion chromatography. The polydispersity index (M_w/M_n) was 4.

3.4.1 Optical absorption spectrum

The optical absorption spectrum of the polymer is shown in Fig. 3.17 for both film and solution. Film thickness was 1.2 μm, solution concentration was 0.001g/ml in chloroform and path length was 1 cm.

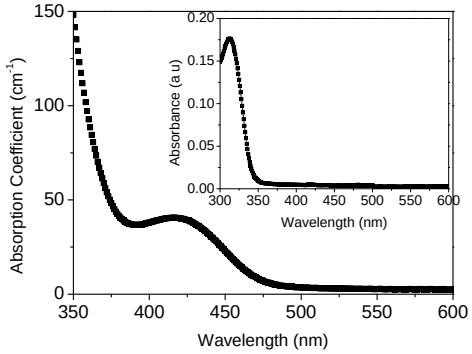

Figure 3.17: Absorption spectra of the polymer P2 in solid (film on quartz). Inset shows the absorption spectrum of a chloroform solution of P2.

Similar to the case with P1, this polymer also showed the characteristic blue shift of the absorption band with increasing polarity of solvent. Fig. 3.18 shows this behavior. Thus the low intensity absorption band was due to an n-π^* transition.

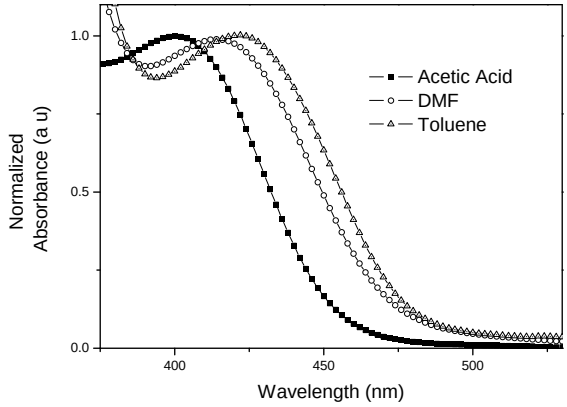

Figure 3.18: Blue shift in the absorption band with increasing polarity of the solvent.

3.4.2 Fluorescence quenching

Fluorescence from the polymer was quenched in the presence of electron accepting molecules. TNP, TCNQ and C_{60} were tried as photo-sensitizers

for P2 also. Thus the effect of these molecules on the fluorescence intensity was studied. Fig. 3.19 shows the reduction in intensity observed when the film of P2 was doped with electron acceptor molecules.

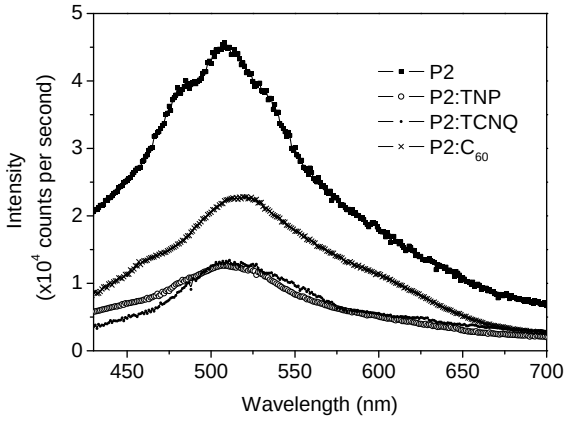

Figure 3.19: Fluorescence quenching effect of TNP, TCNQ and C_{60} on P2.

As earlier, observation of fluorescence quenching alone could not be considered as a solid evidence for an electron transfer. But there was an increase in photocurrent yield as will be seen in Section 3.4.5.1. This hints at the possibility of an electron transfer process.

3.4.3 Cyclic voltammetry

The cyclic voltammogram of P2 is shown in Fig. 3.20. The onset of reduction was at -620 mV. The corresponding LUMO position was estimated to be 3.78 eV and HOMO was 6.41 eV. The optical gap was 2.63 eV.

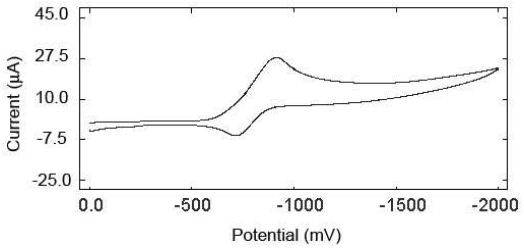

Figure 3.20: Cyclic voltammogram of P2.

Above values do not include the correction for the exciton binding energy. The exciton binding energy in polymers is of the order of 0.5 eV.[30]

3.4.4 Temperature dependence of conductivity

The temperature dependence of electrical conductivity of P2 is shown in Fig. 3.21. Two activation energies were extracted from the slopes of the graph.

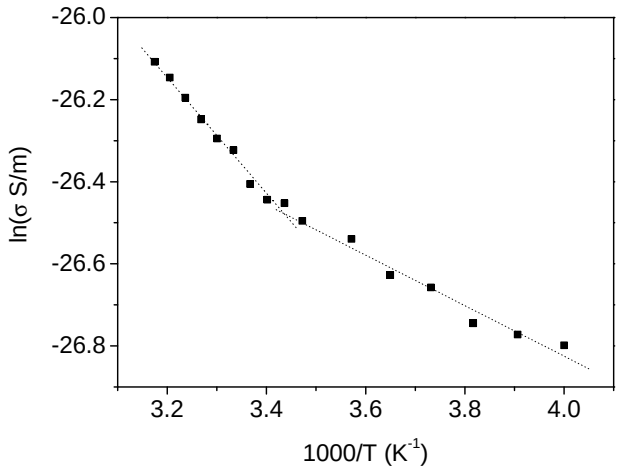

Figure 3.21: Temperature dependence of the dark conductivity of P2. The line is a linear fit to the data.

The below room temperature region gave an activation energy of 121($\pm$5) meV and the lower temperature region gave an activation energy of 52($\pm$4) meV.

3.4.5 Modulated photocurrent measurement

The photocurrent action spectrum of P2 is shown in Fig. 3.22 for different electric fields. The photocurrent was more for ITO biased positive showing that the ITO could inject more holes into the polymer than silver. The work function of the electrodes were almost the same (-4.8eV for ITO and -4.7eV for silver). The barrier for hole injection from ITO to the polymer might be smaller by 0.1eV, resulting in slightly higher current when ITO

was biased positive. The value of 0.1 eV was so small that this much asymmetry in injection barrier could not cause a significant change in the shape of the photocurrent action spectrum as revealed by the similarity in action spectra for both polarities. As the reversal of biasing resulted in only a small decrease in the photocurrent, the photocurrent was not only due to electrode sensitized dissociation of excitons, but also from the dissociation in the bulk, the latter being the higher.[31]

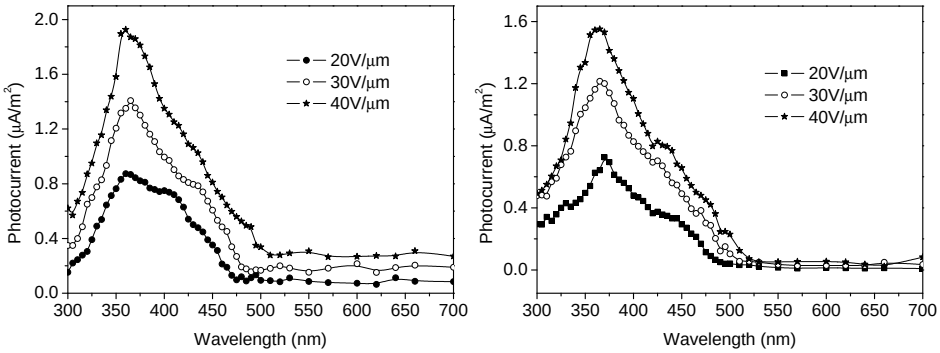

Figure 3.22: Photocurrent action spectra of sandwich cells of P2 for ITO_+ (left) and ITO_- (right).

Generally, in organic semiconductors, photoconductivity is not through a direct generation of carriers, but through the formation and subsequent dissociation of an exciton. The exciton can dissociate at impurity sites, interfaces with asymmetric ionization potentials or it can be dissociated by a strong electric field.[30,32]

A close examination of the photocurrent action spectra revealed a small shift of the action spectra onset to lower energies at higher electric fields. This could be due to the enhanced dissociation of the less hot excitons (vibrationally relaxed)[33] as the additional energy required for dissociation could also be supplied in the form of electric field.

3.4.5.1 Effect of TNP

The absorption spectrum of P2 doped with TNP is shown in Fig. 3.23. Significant increase in absorption was observed in the spectrum when doped with TNP.

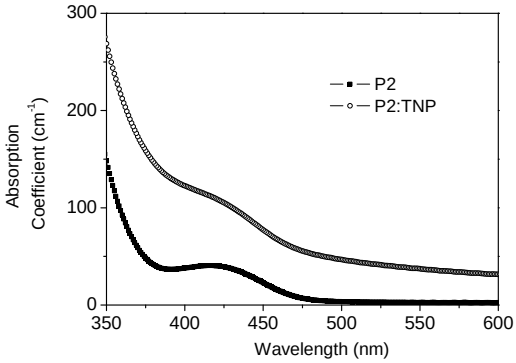

Figure 3.23: Absorption spectra of the films of P2 and its doped form with TNP.

Exciton dissociation can also happen at an interface where there is an ionization potential mismatch.[34] This effect is very important in the case of organic photovoltaic devices and has been the idea behind bulk heterojunction solar cells.[35] The effect of TNP on the action spectrum was studied for both polarities of ITO. The electron acceptor (TNP) doped samples showed an increased photocurrent yield along with a shift in the onset of photoaction spectrum. The spectra are shown in Fig. 3.24.

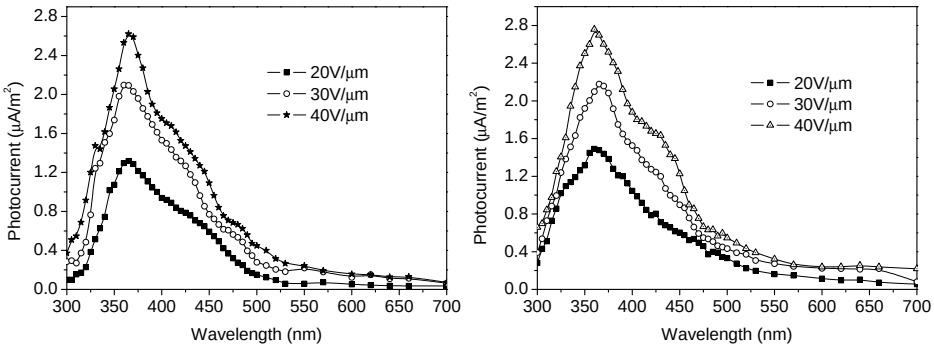

Figure 3.24: Photocurrent action spectra of sandwich cells of P2 doped with TNP for ITO_+ (left) and ITO_- (right).

TNP increased the photocurrent to the values obtained by doubling the field in undoped case. This time the photocurrent was more for the case with ITO biased negative. The reason might be related to the increased absorbance in the film on doping with TNP. After doping there was a significant increase in the absorption coefficient of the host polymer. The excitations were more near the ITO and low near the silver electrode due to the self absorption in the film. Thus the number of excitons near the ITO will be very much higher than near silver. Such a higher density of excitons increases the possibility of exciton-exciton annihilation effect resulting in reduced number of free carriers.

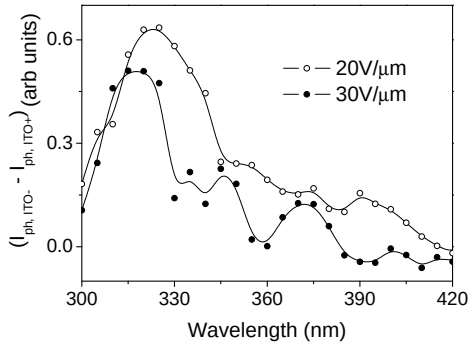

Figure 3.25: Plot of the difference in photocurrents for ITO_{neg} and ITO_{pos} for two electric fields.

The possibility of the existence of this effect in this case was evident from the field dependence of action spectra in the high absorbing region. In Fig 3.25, the difference between the photocurrents for ITO_{neg} and ITO_{pos} is plotted for 20 and 30V/μm. It was seen that the difference decreased when the electric field was increased. It is well understood that bimolecular recombination rate is inversely related to electric field as field induced dissociation start to compete with the former.[36] Koch et. al.,[37] reported that the hole injection properties of virtually any organic-metal interface can be optimized by using strong electron acceptors. They also reported that the extent of increase in hole injection depend on the number of acceptor molecules in direct contact with the metal surface. Thus the low current in the ITO negative case might be due to the increase in hole injection from silver electrode along with bimolecular recombination near ITO.

3.4.5.2 Effect of TCNQ

The absorption spectrum showed a slight hyperchromic shift on doping with TCNQ as shown in Fig. 3.26.

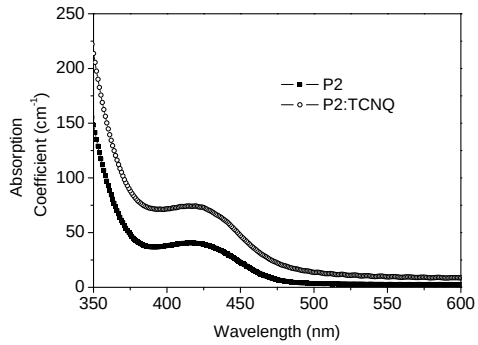

Figure 3.26: Absorption spectra of the films of P2 and its doped from with TCNQ.

The photocurrent action spectra of the TCNQ doped sandwich cells of P2 are shown in Fig. 3.27 for both polarities of ITO. TCNQ did not give an increase in photocurrent yield similar to the case with P1.

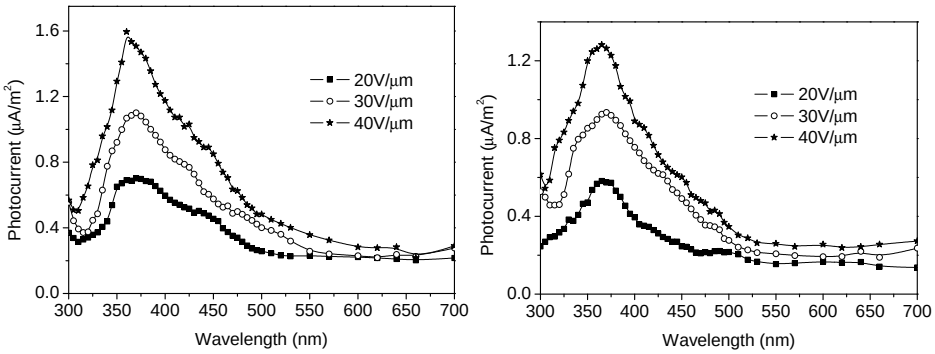

Figure 3.27: Photocurrent action spectra of sandwich cells of P2 doped with TCNQ for ITO_+ (left) and ITO_- (right).

3.4.5.3 Effect of C_{60}

The absorption spectrum of P2 doped C_{60} film is shown in Fig.3.28. Absorbance in the entire visible region was increased.

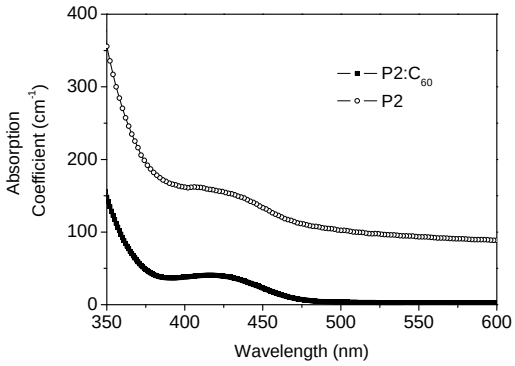

Figure 3.28: Absorption spectra of the films of P2 doped with C_{60}.

Action spectrum of P2:C_{60} is shown in Fig.3.29. Photocurrent was considerably higher when P2 was doped with the molecule C_{60}. Also, the sensitivity in the red region of the spectrum was enhanced, which make P2:C_{60} a photoconductive system sensitive for red lasers.

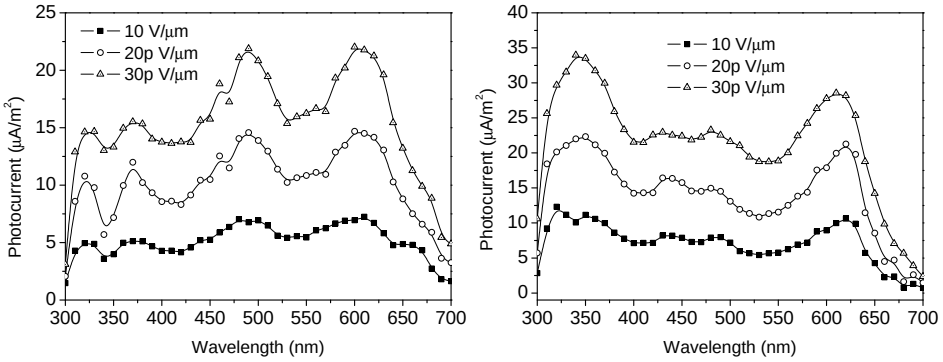

Figure 3.29: Photocurrent action spectra of sandwich cells of P2 doped with C_{60} for ITO_+ (left) and ITO_- (right).

Similar to electron acceptor doped P1, the photocurrent was more when ITO was negatively biased. It could be due to the effects discussed previously, that is, dopant (electron acceptor) assisted increase in hole injection rate and bimolecular recombination. Figure 3.30 shows the bias effect for an applied field of 30V/μm.

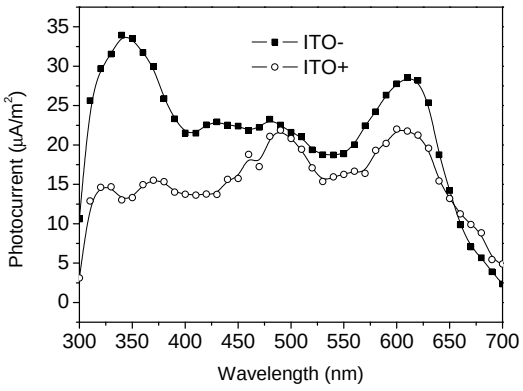

Figure 3.30: Comparison of the action spectra showing the bias dependence of photocurrent for 30V/μm.

3.4.6 Photoconductive sensitivity

The sensitivity of the polymer to light, expressed as the photoconductive sensitivity (S) was estimated based on the modulated photocurrent measurement. Table 3.2 shows the values of S obtained for P2 along with the values obtained when doped with electron acceptors. Here also C_{60} was the best photosensitizer but the values of photoconductive sensitivity were slightly less than the values obtained in the case of P1:C_{60}.

Table 3.2: Photoconductive sensitivity of the sandwich cells of P2 for different wavelengths (@30V/μm, ITO$_-$).

Wavelength (nm)	Photoconductive Sensitivity 10^{-14}(S cm W^{-1})			
	C_{60}	TNP	TCNQ	Undoped
440	816	36	19	20
490	825	17	12	4
530	726	12	8	1
630	1445	12	12	1

3.5 Poly(6-tert-butyl-3-phenyl-3,4-dihydro-2H-1,3 - benzoxazine)

Structure of the polymer is shown in Fig. 3.31. In this polymer, which was labeled as P3, a phenyl group was attached to the nitrogen.

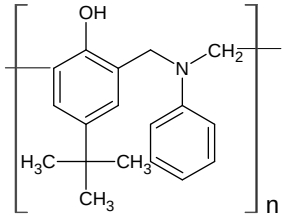

Figure 3.31: Poly(6-tert-butyl-3-phenyl-3,4-dihydro-2H-1,3-benzoxazine), (P3).

The glass transition temperature of this polymer was 52^0C. The number average molecular weight (M_n) was 268 and weight average molecular weight (M_w) was 900, as estimated using size exclusion chromatography. The polydispersity index (M_w/M_n) was 3.3.

3.5.1 Optical absorption spectrum

Absorption spectra of the polymer is shown in Fig. 3.32. Compared to P1 and P2, the absorption coefficient of P3 was considerably increased. This may be due to the increase in the conjugation in the monomer of the polymer.

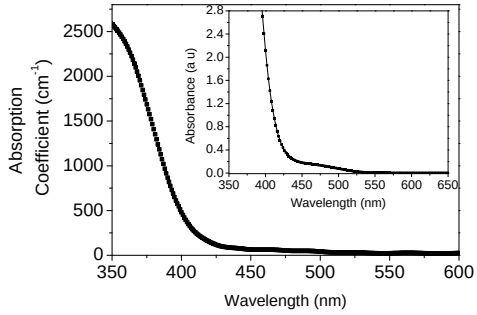

Figure 3.32: Absorption spectra of the polymer P3 in solid (film on quartz). Inset shows the absorption spectrum of a chloroform solution of P3.

The low intensity absorption band in the visible region was studied using the blue shift method described earlier. The observed blue shift is shown in Fig. 3.33.

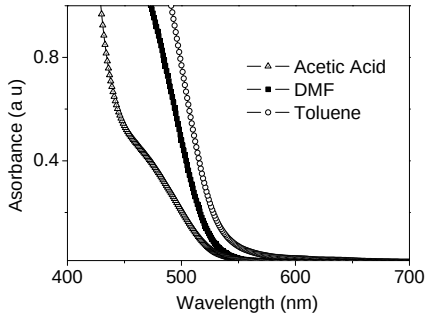

Figure 3.33: Blue shift in the absorption band with increasing polarity of solvent.

The blue shift band was of very low intensity, it was clearly seen in solution form or thick film form.

3.5.2 Fluorescence quenching

In the case of P3, the molecule C_{60} showed the highest degree of fluorescence quenching. Fig. 3.34 shows the quenching of fluorescence in P3 films by the electron acceptor molecules.

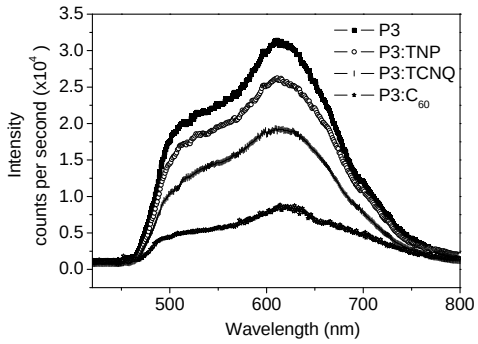

Figure 3.34: Fluorescence quenching effect of TNP, TCNQ and C_{60} on P3.

3.5.3 Cyclic voltammetry

Cyclic Voltammetry was done to estimate the reduction potential of the polymer as explained in Section 1.6.5. The cyclic voltammogram of P3 is shown in Fig. 3.35.

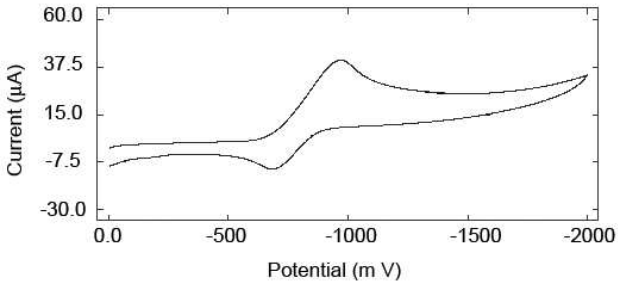

Figure 3.35: Cyclic voltammogram of P3.

The onset of reduction was at -640 mV. The corresponding LUMO position was estimated to be 3.76 eV. The actual LUMO position may be higher by the exciton binding energy ($\approx$ 0.45eV).[17] HOMO was estimated to be 6.09 eV. The optical gap was taken to be 2.33 eV. The HOMO and LUMO energy levels of P3 are very near to the reported energy levels of C_{60}, which are 6.2eV and 3.6eV respectively.[22]

3.5.4 Temperature dependence of conductivity

The temperature dependence of electrical conductivity is shown in Fig. 3.36. The variation was Arrhenius type with more than one activation energy. Two activation energies were determined assuming the form $\sigma = \sigma_0 e^{-E_a/kT}$ for the variation of electrical conductivity. Here σ_0 is a prefactor value of the conductivity, E_a, the activation energy, T, the absolute temperature and k, the Boltzmann constant.

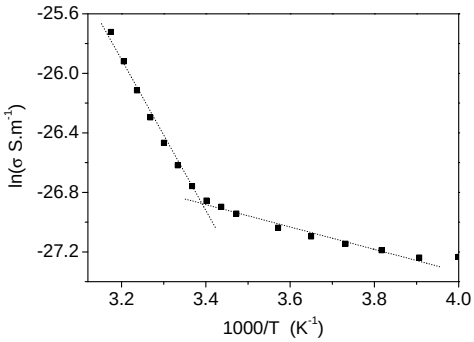

Figure 3.36: Temperature dependence of the dark conductivity of P3. Dotted lines are linear fits.

The below room temperature activation energy was 430 meV and the lower temperature activation energy was 64 meV. This indicated that the conduction mechanism near room temperature and at lower temperatures were different.

3.5.5 Modulated photocurrent measurement

The photocurrent action spectra of P3 are shown in Fig. 3.37 for different electric fields.

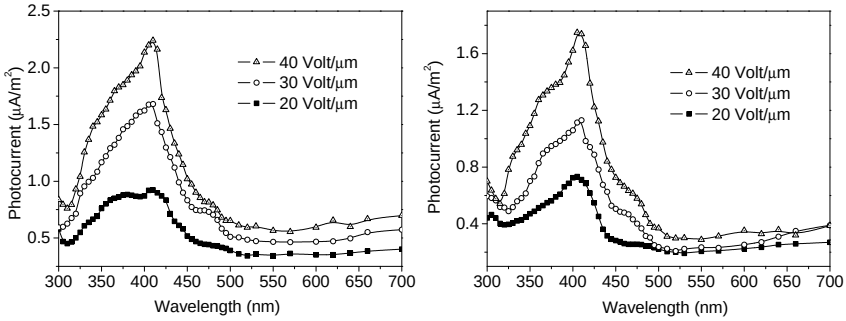

Figure 3.37: Photocurrent action spectra of sandwich cells of P3 for ITO_+ (left) and ITO_- (right).

The photocurrent was higher when the ITO electrode was positively biased. This increase in the photocurrent might be due to the difference in charge injection efficiencies of both the electrodes when appropriately biased.

3.5.5.1 Effect of TNP

Doping P3 with TNP increased its absorption coefficient slightly in the ultra-violet region. Photocurrent spectra with TNP as the sensitizer are shown in Fig. 3.38.

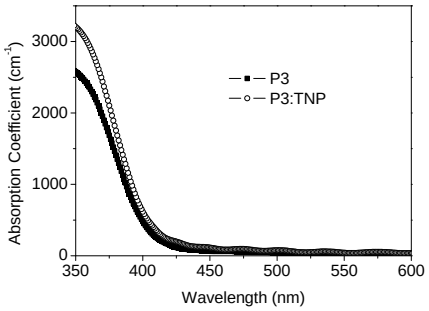

Figure 3.38: Absorption spectra of the films of P3 with and without TNP.

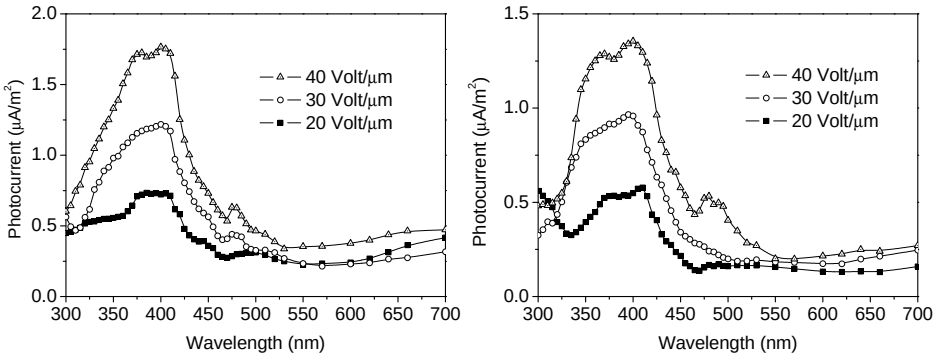

Figure 3.39: Photocurrent action spectra of sandwich cells of P3 doped with TNP for ITO_+ (left) and ITO_- (right).

No significant increase in photocurrent was observed for TNP doped P3. Also, the polarity dependence of photocurrent remained the same.

3.5.5.2 Effect of TCNQ

Absorption spectrum of P3 doped with TCNQ is shown in Fig. 3.40. Possibly due to the low concentration of the dopant, the spectrum of P3 showed no significant modifications, except an increase in absorbance.

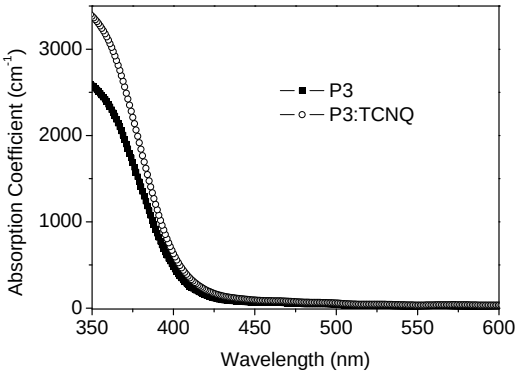

Figure 3.40: Absorption spectra of the films of P3 and its doped form with TCNQ.

Photocurrent action spectra of P3 with TCNQ as dopant are shown in

Fig. 3.41. TCNQ was not a good photosensitizer for P3, the order of photocurrent remained the same.

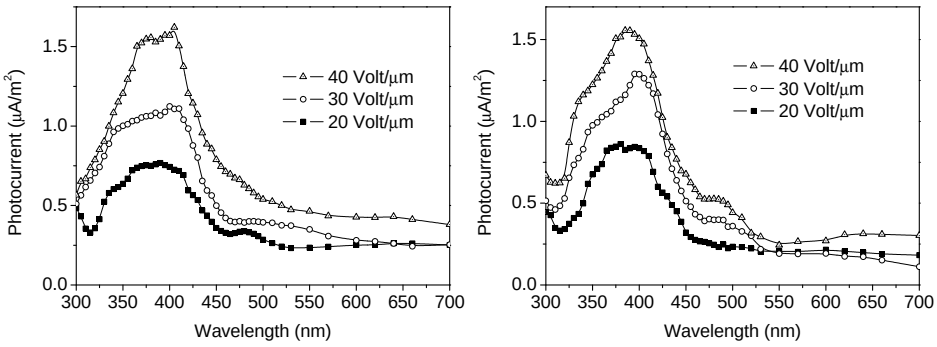

Figure 3.41: Photocurrent action spectra of sandwich cells of P3 doped with TCNQ for ITO_+ (left) and ITO_- (right).

3.5.5.3 Effect of C_{60}

Photocurrent measurements were also performed with C_{60} as the sensitizer. The optical absorption spectrum of the doped film is shown in Fig. 3.42.

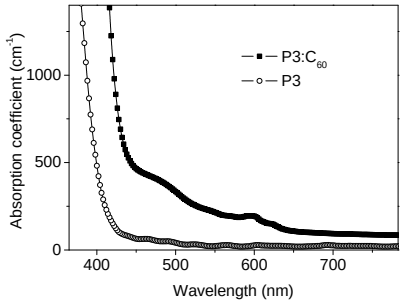

Figure 3.42: Absorption spectra of the films of P3 with and without C_{60}.

There was an increase in the absorption coefficient of the doped film in the entire visible region. The absorption spectrum of the film of P3:C_{60} could be considered as a superposition of the optical absorption spectra of

P3 and C_{60}. Corresponding photocurrent action spectra are given in Fig. 3.43.

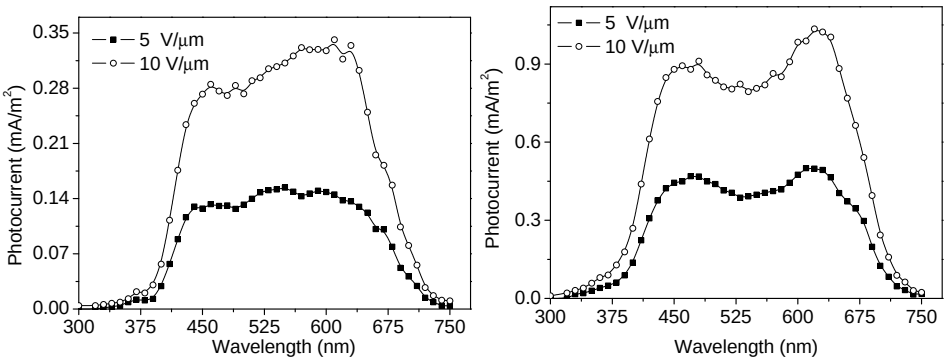

Figure 3.43: Photocurrent action spectra of sandwich cells of P3 doped with C_{60} for ITO_+ (left) and ITO_- (right).

The photocurrent detected in the C_{60} doped case was three orders of magnitude higher than the undoped case. The spectral yield of photocurrent with C_{60} was entirely different, but resembled the optical absorption of C_{60} and the fluorescence spectrum of P3.

The fluorescence from the polymer was efficiently quenched by C_{60} as shown in Fig. 3.34. As the photocurrent was very high, the quenching might be due to the ultra fast electron transfer which is reported to occur from an excited polymer chain to C_{60}.[24] When light is absorbed by an organic semiconductor, the primary product is an exciton. It is the dissociation of this exciton which initiates charge generation. Excitons created by light absorption, which normally radiatively recombine, were getting dissociated by C_{60}. The closeness of the energy levels of the host and the dopant might be the reason for the efficient photocurrent generation. It has already been shown that energetically relaxed excitons (those created with no excess energy from the photons) can only be dissociated at charge transfer centers during the diffusion of excitons.[33]

The magnitude of photocurrent action spectrum was highly dependent on the biasing given to the electrodes. Higher values were obtained when ITO was negatively biased. This could be due to the increase in injection

from silver mediated by the acceptor molecules. Bimolecular recombination effect could also be a reason for the polarity dependent increase in current as discussed in Section 3.4.5.1.

3.5.6 Photoconductive sensitivity

Photocurrent was dependent on the electric field applied across the polymer. The photoconductive sensitivity of P3 doped with C_{60} was very high. Values of S for the sandwich cells are given in Table 3.3.

Table 3.3: Photoconductive sensitivity of the sandwich cells of P3 for different wavelengths (@10V/μm, ITO$_-$).

Wavelength (nm)	Photoconductive Sensitivity 10^{-14}(S cm W^{-1})			
	C_{60}	TNP	TCNQ	Undoped
440	28280	4	7	5
490	28610	3	4	4
530	27433	3	3	3
630	34100	2	3	3

From the above table, it can be seen that P3 with C_{60} as sensitizer is sensitive to most of the common laser wavelengths. The photoconductive sensitivity is sufficiently high for photorefractive effect.[25–27] Other electron acceptor molecule did not give increased photosensitivity.

3.5.7 Time of flight experiment

Carrier mobility could be estimated using the time of flight (TOF) method explained in Section 1.6.1. The photocurrent transient for the undoped P3 film is shown in Fig. 3.44. The transit time of the carriers (electrons, as the ITO was negatively biased) was estimated from the knee in the photocurrent transient.

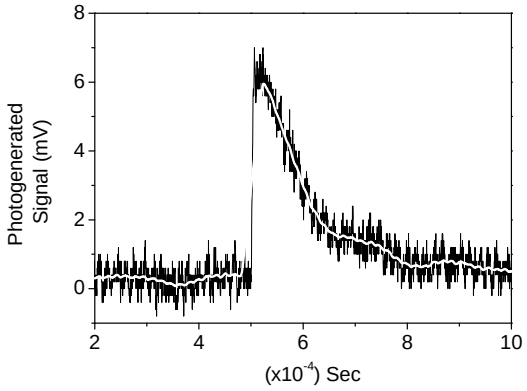

Figure 3.44: Current transient in a TOF experiment done on the sandwich cell of P3. White line is a 100 point adjacent average of the data.

Carrier mobility estimated was 2.77 x 10^{-5} cm^2 V^{-1} S^{-1} at an electric field of 20 V/μm. Transport of carriers was not completely dispersive as a well defined knee was observed in the TOF signal.[22]

3.6 Summary and conclusions

Three polybenzoxazines were studied using different electron acceptors for possible use as sensitive photoconductors for photorefractive polymer systems. The HOMO and LUMO energy levels of the polymers were estimated using cyclic voltammetry. Values of these energy levels are important when considering the applicability of these polymers to other fields such as LEDs or other organic semiconductor based devices. Absorption spectra of all three polymers showed low absorption in the red and green regions of the visible spectrum.

Fluorescence emission from the polymers were found to reduce in the presence of dopants. The photocurrent is expected to increase if this fluorescence quenching is related to an efficient dissociation of the initially created excitons, which normally under go radiative recombination, in to free carriers. Three different electron acceptors were used as dopants, but a quenching associated with an increase in photocurrent was observed only in the case of C_{60} doping.

Photocurrent measurements were done in the sandwich cell configuration on the three polymers. Measurements were done with and without a sensitizer. While the molecule C_{60} acted as a very good sensitizer for all three polybenzoxazines, the electron acceptors 2,4,6-trinitrophenol (TNP) and 7,7,8,8-tetracyanoquinodimethane (TCNQ) were not able to enhance the photocurrent. The increase in photocurrent when the polymers were doped with C_{60} could be due to an electron transfer reaction. The electron transfer from an excited polymer to C_{60} occurs in the picosecond time scales.[16,24] This is shorter than the lifetime of excited states (10^{-8}S) which cause fluorescence. The quenching and the corresponding increase in photocurrent might be due to this ultra-fast electron transfer.

The photoconductive sensitivity was estimated and was found to be sufficient to observe photorefractive effect, based on literature reports.[25–27] The molecule Poly(6-tert-butyl-3-phenyl-3,4-dihydro-2H-1,3-benzoxazine) showed the highest sensitivity when doped with C_{60}.

References

[1] B. Kippelen, K. Tamura, N. Peyghambarian, A. B. Padias, and H. K. Hall, "Photorefractivity in a functional side-chain polymer," Phys. Rev. B. **48,** 10710–10718 (1993).

[2] C. Zhao, C.-K. Park, P. N. Prasad, Y. Zhang, S. Ghosal, and R. Burzynski, "Photorefractive Polymer with Side-Chain Second-Order Nonlinear Optical and Charge-Transporting Groups," Chem. Mater. **7,** 1237–1242 (1995).

[3] K. Yokoyama, K. Arishima, T. Shimada, and K. Sukegawa, "Photorefractive Effect in a Polymer Molecularly Doped with Low-Molecular-Weight Compounds," Jpn. J. Appl. Phys. **33,** 1029–1033 (1994).

[4] H. Ishida and D. Sanders, "Regioselectivity of the ring-opening polymerization of monofunctional alkyl-substituted aromatic amine-based benzoxazines," Polymer **42,** 3115–3125 (2001).

[5] Y.-J. Lee, J.-M. Huang, S.-W. Kuo, J.-K. Chen, and F.-C. Chang, "Synthesis and characterizations of a vinyl-terminated benzoxazine monomer and its blending with polyhedral oligomeric silsesquioxane (POSS)," Polymer **46,** 2320–2330 (2005).

[6] T. Takeichi and T. A. Tsutsumi, "High Performance Polybenzoxazines as Novel Thermosets," High Perform. Polym. **18,** 777–797 (2006).

[7] Y. Hirose, A. Kahn, V. Aristov, P. Soukiassian, V. Bulovic, and S. R. Forrest, "Chemistry and electronic properties of metal-organic semiconductor interfaces: Al, Ti, In, Sn, Ag, and Au on PTCDA," Phys. Rev. B **54,** 13748–13758 (1996).

[8] R. Dhanya, "Development of Photorefractive Polymers: Synthesis and Characterization of Polymers with Donor-π-Acceptor Groups," Ph.D. Thesis (Cochin University of Science and Technology, India, 2008).

[9] C. N. Banwell and E. M. McCash, *Fundamenals of Molecular Spectroscopy*, 4 ed. (Tata McGraw-Hill, New Delhi, 1997), pp. 186–193.

[10] G. J. Brealey and M. Kasha, "The Role of Hydrogen Bonding in the n $\rightarrow \pi^*$ Blue-shift Phenomenon," Abstracts of OSU International Symposium on Molecular Spectroscopy 1946-1959 **77,** 4462–4468 (1955).

[11] K. Yoshihara and D. R. Kearns, "Spectroscopic Properties of Lower-Lying Excited States of Fluorenone," J. Chem. Phys. **45,** 1991–1999 (1966).

[12] H. McConnell, "Effect of Polar Solvents on the Absorption Frequency of n$\longrightarrow \pi$ Electronic Transitions," J. Chem. Phys. **20,** 700–704 (1952).

[13] J. Cabanillas-Gonzalez, T. Virgili, G. Lanzani, S. Yeates, M. Ariu, J. Nelson, and D. D. C. Bradley, "Photophysics of charge transfer in a polyfluorene/violanthrone blend," Phys. Rev. B. **71,** 014211–014219 (2005).

[14] C. Im, J. M. Lupton, P. Schouwink, S. Heun, H. Becker, and H. Bässler, "Fluorescence dynamics of phenyl-substituted poly(phenylene vinylene)trinitrofluorenone blend systems," J. Chem. Phys. **117,** 1395–1402 (2002).

[15] D. Veldman, J. J. Bastiaansen, B. M. Langeveld-Voss, J. Sweelssen, M. M. Koetse, S. C. Meskers, and R. A. Janssen, "Photoinduced charge and energy transfer in dye-doped conjugated polymers," Thin Solid Films **511-512,** 581–586 (2006).

[16] L. Smilowitz, N. S. Sariciftci, R. Wu, C. Gettinger, A. J. Heeger, and F. Wudl, "Photoexcitation spectroscopy of conducting-polymer-C_{60} composites: Photoinduced electron transfer," Phys. Rev. B **47,** 13835–13842 (1993).

[17] C. Im, W. Tian, H. Bässler, A. Fechtenkötter, M. D. Watson, and K. Müllen, "Photoconduction in organic donor-acceptor systems," J. Chem. Phys. **119,** 3952–3957 (2003).

[18] R. W. Lof, M. A. van Veenendaal, B. Koopmans, H. T. Jonkman, and G. A. Sawatzky, "Band gap, excitons, and Coulomb interaction in solid C_{60}," Phys. Rev. Lett. **68,** 3924–3927 (1992).

[19] D. Ray, M. P. Patankar, N. Periasamy, and K. L. Narasimhan, "Photoconduction in Alq3," J. Appl. Phys. **98,** 123704–123711 (2005).

[20] A. Arena, A. M. Mezzasalma, S. Patanè, and G. Saitta, "Investigation of the novel charge transfer complex Cd-TCNQ," J. Mater. Res. **12,** 1693–1697 (1997).

[21] F. Yakuphanoglu and M. Arslan, "The fundamental absorption edge and optical constants of some charge transfer compounds," Opt. Mater. **27,** 29–37 (2004).

[22] J. Y. Lee and J. H. Kwon, "Enhanced hole transport in C_{60}-doped hole transport layer," Appl. Phys. Lett. **88,** 183502–183504 (2006).

[23] Y. Zhang, Y. Cui, and P. N. Prasad, "Observation of photorefractivity in a fullerene-doped polymer composite," Phys. Rev. B **46,** 9900–9902 (1992).

[24] C. H. Lee, G. Yu, D. Moses, K. Pakbaz, C. Zhang, N. S. Sariciftci, A. J. Heeger, and F. Wudl, "Sensitization of the photoconductivity of conducting polymers by C_{60}: Photoinduced electron transfer," Phys. Rev. B **48,** 15425–15433 (1993).

[25] S. M. Silence, C. A. Walsh, J. C. Scott, and W. E. Moerner, "C_{60} sensitization of a photorefractive polymer," Appl. Phys. Lett. **61,** 2967–2969 (1992).

[26] L. Wang, Y. Zhang, T. Wada, and H. Sasabe, "Photorefractive effect in a photoconductive electro-optic carbazole trimer," Appl. Phys. Lett. **69,** 728–730 (1996).

[27] S.-H. Park, K. Ogino, and H. Sato, "Synthesis and characterization of a main-chain polymer for single component photorefractive materials," Synth. Met. **113,** 135–143 (2000).

[28] G. Daminelli, J. Widany, A. D. Carlo, and P. Lugli, "Tuning the optical properties of thiophene oligomers toward infrared emission: A theoretical study," J. Chem. Phys. **115,** 4919–4923 (2001).

[29] F.-I. Wu, P.-I. Shih, M.-C. Yuan, A. K. Dixit, C.-F. Shu, Z.-M. Chung, and E. W.-G. Diau, "Novel distyrylcarbazole derivatives as hole-transporting blue emitters for electroluminescent devices," J. Mater. Chem. **15,** 4753–4760 (2005).

[30] V. I. Arkhipov and H. Bässler, "Exciton dissociation and charge photogeneration in pristine and doped conjugated polymers," Phys. Stat. Sol. (a) **201,** 1152–1187 (2004).

[31] V. C. Kishore, R. Dhanya, K. Sreekumar, R. Joseph, and C. S. Kartha, "Spectral distribution of photocurrent in poly(6-tert-butyl-3-methyl-3,4-dihydro-2H-1,3-benzoxazine)," Synth. Met. p. in press (2008).

[32] V. I. Arkhipov, H. Bässler, M. Deussen, E. O. Göbel, R. Kersting, H. Kurz, U. Lemmer, and R. F. Mahrt, "Field-induced exciton breaking in conjugated polymers," Phys. Rev. B. **52,** 4932–4940 (1995).

[33] V. I. Arkhipov, E. V. Emelianova, and H. Bässler, "On the role of spectral diffusion of excitons in sensitized photoconduction in conjugated polymers," Chem. Phys. Lett. **383,** 166–170 (2004).

[34] E. R. Bittner, J. G. S. Ramon, and S. Karabunarliev, "Exciton dissociation dynamics in model donor-acceptor polymer heterojunctions. I. Energetics and spectra," J. Chem. Phys. **122,** 214719–214728 (2005).

[35] P. W. M. Blom, V. D. Mihailetchi, L. J. A. Koster, and D. E. Markov, "Device Physics of Polymer:Fullerene Bulk Heterojunction Solar Cells," Adv. Mater. **19,** 1551–1566 (2007).

[36] M. Obarowska and J. Godlewski, "Electric field dependence of the bimolecular recombination rate of the charge carriers," Synth. Met. **109,** 219–222 (2000).

[37] N. Koch, S. Duhm, J. P. Rabe, A. Vollmer, and R. L. Johnson, "Optimized Hole Injection with Strong Electron Acceptors at Organic-Metal Interfaces," Phys. Rev. Lett. **95,** 237601–237605 (2005).

CHAPTER

FOUR

Estimation of the First Hyperpolarizability of a Series of p-Nitroaniline Derivatives

4.1 Introduction

The electro-optic effect can be brought about in a polymer matrix by the addition of non-centrosymmetric dipolar molecules. These molecules possess high second order susceptibilities and are sometimes called nonlinear optical chromophores.[1] The molecular second order susceptibility is also termed as the first hyperpolarizability β_{ijk}, where i, j and k refers to molecular axes. The synthesis and study of molecules with large first order hyperpolarizabilities is important due to the potential applications of such molecules in nonlinear optics. Many components for optical signal processing and communication devices can be made out of materials possessing high electrooptic coefficients.[2]

This chapter gives the details of the molecules studied for nonlinear optical properties. The molecular parameters including ground state dipole moment, excited state dipole moment and the first hyperpolarizability were estimated. The aim was to make a selection of molecules with comparatively higher values for the figure of merit explained in Section 1.5.3.

The estimation of the first hyperpolarizability was done using the two level microscopic model of β_{ijk}. The techniques available to measure this

important parameter are second harmonic generation,[3] electric field induced second harmonic generation (EFISH)[4] and hyper-Raleigh scattering.[5] An estimation of first hyperpolarizability can be done using the simplified two level model also.[6] This method requires the excited state dipole moment, which can be estimated using solvatochromism and the ground state dipole moment which can be estimated using the Debye-Guggenheim method. Solvatochromism involves studying the effect of solvent polarity on the molecule's absorption and fluorescence spectra.

4.2 Molecules studied

All molecules were synthesized in our lab and the details are given elsewhere.[7,8] The structure of the molecules studied are given in Fig. 4.1, 4.2 and 4.3. The main difference between the molecules was in the number of alkyl spacers connecting the acceptor group and the donor group.

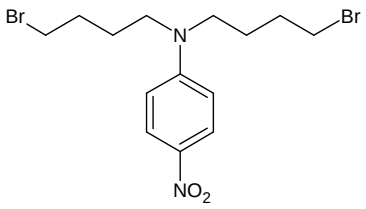

Figure 4.1: N,N-bis(4-bromobutyl)-4-nitrobenzenamine (1a).

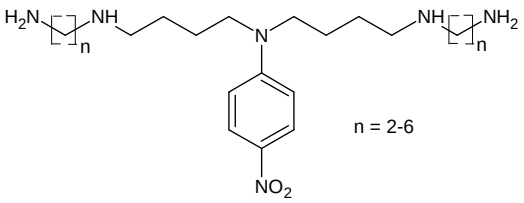

Figure 4.2: N,N-bis(4-[(n-aminoalkyl)amino]butyl)-4-nitrobenzenamine. Molecules with this general structure were labeled as 2a, 2b, 2c, 2d and 2e.

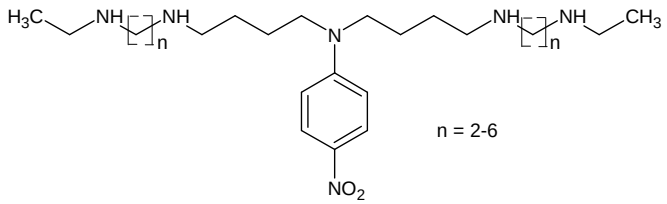

Figure 4.3: N, N-bis(4-[n-(ethyl amino)alkyl amino]butyl)-4-nitrobenzenamine. Molecules with this general structure were labeled as 3a, 3b, 3c and 3d.

The number of alkyl units was varied from n = 2 to 6, correspondingly there were a total of 10 molecules under study. In the second set, n = 5 was not available for studies. Table 4.1 shows the labeling of the molecules adopted during the experiments.

Table 4.1: Details of the molecules

n	IUPAC Name	No.
	N,N-bis(4-bromobutyl)-4-nitrobenzenamine	1a
2	N,N-bis(4-[(2-aminoethyl)amino]butyl)-4-nitrobenzenamine	2a
3	N,N-bis(4-[(3-aminopropyl)amino]butyl)-4-nitrobenzenamine	2b
4	N,N-bis(4-[(4-aminobutyl)amino]butyl)-4-nitrobenzenamine	2c
5	N,N-bis(4-[(5-aminopentyl)amino]butyl)-4-nitrobenzenamine	2d
6	N,N-bis(4-[(6-aminohexyl)amino]butyl)-4-nitrobenzenamine	2e
2	N,N-bis(4-[2-(ethylamino)ethylamino]butyl)-4-nitrobenzenamine	3a
3	N,N-bis(4-[3-(ethylamino)propylamino]butyl)-4-nitrobenzenamine	3b
4	N,N-bis(4-[4-(ethylamino)butylamino]butyl)-4-nitrobenzenamine	3c
6	N,N-bis(4-[6-(ethylamino)hexylamino]butyl)-4-nitrobenzenamine	3d

4.3 Determination of ground state dipole moment (μ_g)

The figure of merit of nonlinear optical chromophores is highly dependent on the ground state dipole moment and the first hyperpolarizability of the molecule.[9] The refractive index modulation achievable in a photorefractive guest host system depends on the figure of merit[10] and in turn on the dipole moment of the material. As described in Section 1.5, the tendency of the molecules to align antiparallel is determined by the ground state dipole moment. Thus an idea about the magnitude of this molecular property is useful when deciding the poling requirements to induce non-centrosymmetry. The ground state dipole moment can be determined by the Debye Guggenheim method, where the actual measurement is the static dielectric constant of a series of solutions of varying weight fraction of the molecule in a non-polar solvent. The value is then extrapolated to infinite dilution to calculate the dipole moment using equation 4.1.[11]

$$\mu_g^2 = \frac{3\varepsilon_0 kT}{N_A} \frac{9}{(\varepsilon^0 + 2)(n_0^2 + 2)} \frac{M}{\rho_0} \left(\frac{\partial \epsilon}{\partial \omega} \right)_o, \tag{4.1}$$

Here M is the molar mass of the molecule, ω is the weight fraction, ε^0, n_0 and ρ_0 are the dielectric constant, refractive index and the density of pure solvent respectively. N_A is the Avogadro number and ε_0 is the permittivity of vacuum. The term $(\partial\epsilon/\partial\omega)_0$ represents the variation of dielectric constant with weight fraction at infinite dilution.

The above equation assumes that the refractive index of a solution of the molecule has negligible dependence on its weight fraction.[11] The refractive index of the solutions were measured using an Atago DRM2 refractometer and the variation with weight fraction was found to be negligibly small, so that the equation can be safely applied. To calculate dielectric constants, several concentrations of the molecules under investigation were prepared in toluene (being a non-polar solvent) and filled between the plates of a parallel plate capacitor with variable plate separation and the capacitance was measured as a function of plate separation

(d) using an HP 4277A LCZ meter operating at 10 KHz. Capacitance of the capacitor was measured in this manner first filling it with the solution under test and later with spectroscopic grade toluene. If C_s is the capacitance with the solution and C_t is the capacitance with toluene, the dielectric constant of the solution can be determined from the ratio of the slopes of the plots of C vs 1/d. The dielectric constant of the solution, ε_s was determined using equation 4.2.

$$\varepsilon_s = \varepsilon_t \frac{K_s}{K_t} \tag{4.2}$$

Here ε_t is the dielectric constant of toluene, K_s is the slope of the plot of C_s with 1/d and K_t is the slope of the plot of C_t with 1/d.

Toluene ($\epsilon_r = 2.379$) was used for the standardization of the measurement. The parameter $\partial\epsilon/\partial\omega$ was extracted from the plot of dielectric constant with weight fraction of the molecule. Plots of the variation of dielectric constant with weight fraction of the solute are shown in Fig. 4.4, 4.5, 4.6, 4.7 and 4.8. Equation 4.1 was used to calculate the ground state dipole moment of the molecule.

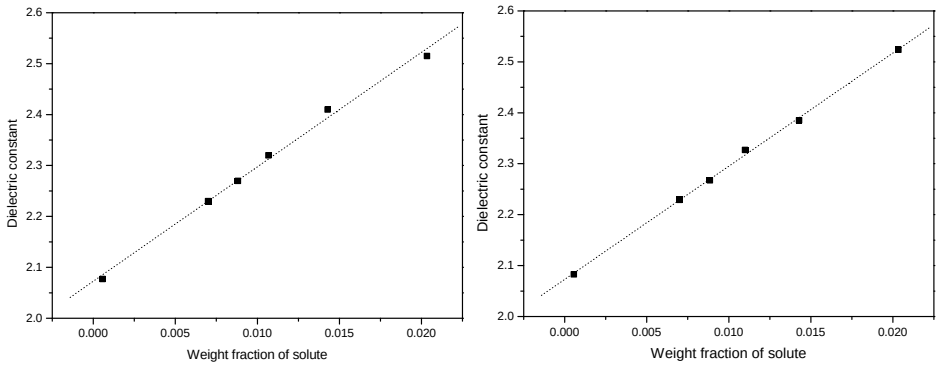

Figure 4.4: Variation of the dielectric constant with weight fraction of 1a and 2a.

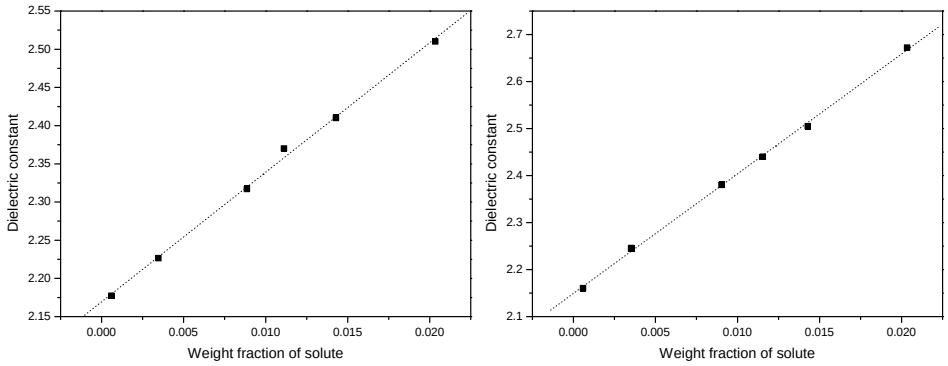

Figure 4.5: Variation of the dielectric constant with weight fraction of 2b and 2c.

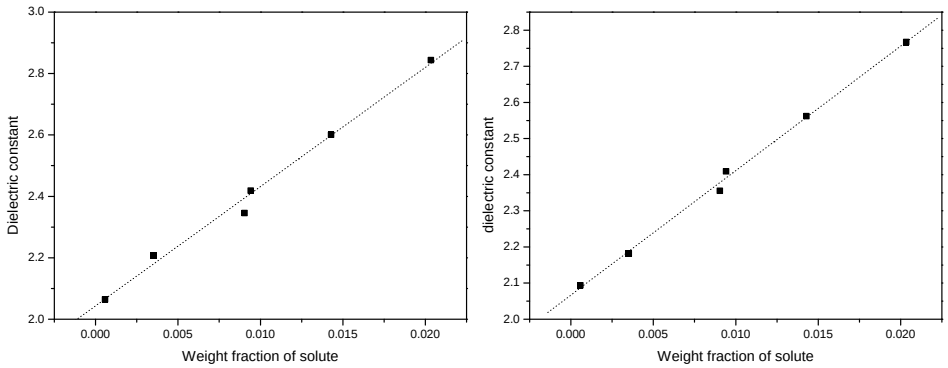

Figure 4.6: Variation of the dielectric constant with weight fraction of 2d and 2e.

The range of weight fractions of the second set of molecules was less than the previous set. As the method assumes the values at infinite dilution, this change in concentration will not affect a comparison of the results.[11]

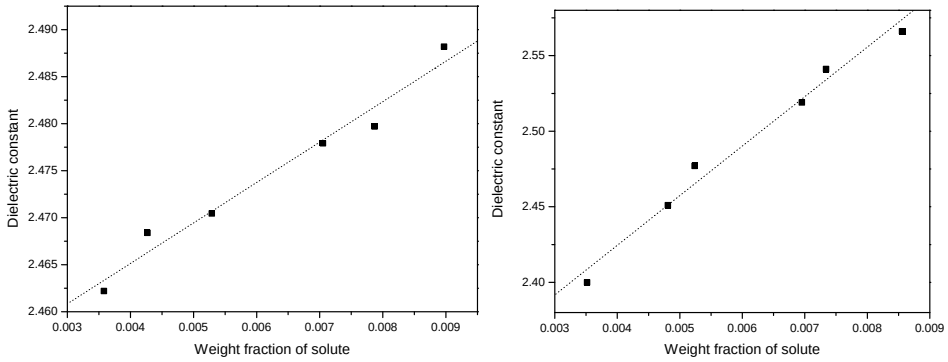

Figure 4.7: Variation of the dielectric constant with weight fraction of 3a and 3b.

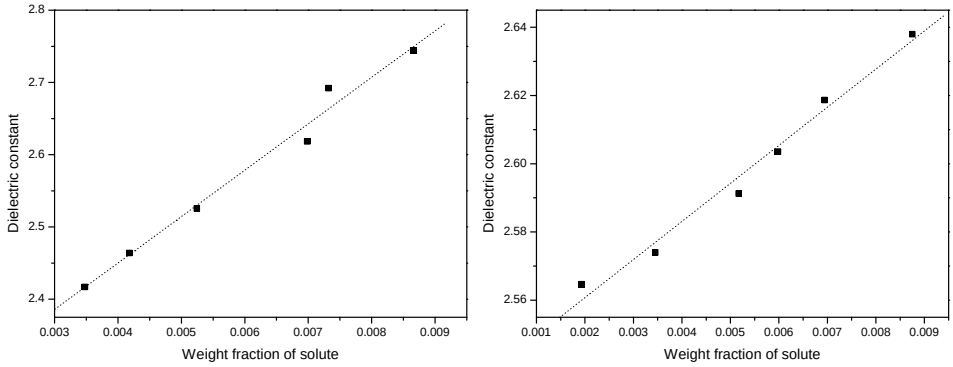

Figure 4.8: Variation of the dielectric constant with weight fraction of 3c and 3d.

The results obtained are given in Table 4.2. A unit conversion can be achieved by noting that 1 Debye = 3.33564x10^{-30} C.m = 10^{-18} esu.

Table 4.2: Ground state dipole moments of the molecules

Molecule	μ_g (D)	Molecule	μ_g (D)
1a	9.78	2e	12.63
2a	8.88	3a	4.43
2b	8.48	3b	11.75
2c	10.20	3c	16.85
2d	8.06	3d	7.47

4.4 Determination of excited state dipole moment (μ_e)

The excited state dipole moment is another quantity which shows the extent of charge transfer after excitation by radiation of sufficient energy. If the difference between the ground and excited state dipole moments is very large, the charge transfer is also very large provided the bond length remains unaltered upon excitation. The determination of excited state dipole moment is very important and there are many methods proposed in the literature. Gas-phase stark effect is one of such methods which involve examination of the splitting of rotational lines due to externally applied electric field.[12] A simple method is to analyze the solvent polarity dependence of the absorption and emission maxima (solvatochromism) of the molecule under consideration to extract μ_e.[9]

4.4.1 The solvatochromic effect

Solvatochromism is the change in the position, intensity, and shape of absorption or emission bands of a molecule due to the change in polarity of the solvent.[13] The spectral shift is caused by the electric field experienced by a molecule embedded in such a solvent. This electric field, called reaction field, arises from the polarization of the surrounding solvent molecules due

to the dipole moment of the solute.[12]

The solvatochromic method was used for the estimation of the first hyperpolarizability of the molecules. Although the accuracy of the method was less compared to more accurate methods like second harmonic generation or hyper Raleigh scattering, the purpose was to screen the synthesized chromophores. For this purpose the experiment was well suited.

4.4.2 Solvatochromic measurements

The solvatochromic estimation of μ_e involves no laser measurements. The absorption and fluorescence spectra in solvents of varying polarity were needed for the analysis. In order to get a gradual variation of the polarity of the solvents, a binary solvent mixture comprising the polar solvent acetonitrile and the non-polar solvent toluene were used for the solvatochromic analysis.[8] A polar molecule has unequal sharing of electrons between the atoms constituting it.

The refractive index and the dielectric constant of the mixture at various proportions were measured to compute the bulk solvent polarity parameter $F(\varepsilon, n)$ defined[14] by equation 4.3.

$$F(\varepsilon, n) = \frac{(2n^2+1)}{(n^2+2)} \left\{ \frac{(\varepsilon-1)}{(\varepsilon+2)} - \frac{(n^2-1)}{(n^2+2)} \right\}, \tag{4.3}$$

here n and ε are the refractive index and the dielectric constant of the mixture respectively. There are mainly two methods proposed in the literature for the analysis of the solvatochromic data.

4.4.2.1 Method 1

In this method, the emission υ_f cm^{-1} and absorption υ_a cm^{-1} bands are analyzed based on the following equations.[15]

$$\upsilon_a - \upsilon_f = m_1 F(\varepsilon, n) + Constant, \tag{4.4}$$

$$\upsilon_a + \upsilon_f = -m_2 \{F(\varepsilon, n) + 2g(n)\} + Constant, \tag{4.5}$$

here g(n) is another parameter given by $g(n) = (3/2)(n^4-1)/(n^2+2)^2$. Equations 4.4 and 4.5 show that the plots of $\upsilon_a - \upsilon_f$ and $\upsilon_a + \upsilon_f$ with $F(\varepsilon, n)$

and $[F(\varepsilon, n) + 2g(n)]$ would be linear with slopes m_1 and m_2 respectively. These slopes are further given by,

$$m_1 = 2\frac{(\mu_e - \mu_g)^2}{hca^3} \tag{4.6}$$

$$m_2 = 2\frac{(\mu_e^2 - \mu_g^2)}{hca^3}, \tag{4.7}$$

where h is the Planks constant and c is the velocity of light. a is the Onsager cavity radius which can be calculated using the density (d) and the molecular weight (M) of the molecule using the relation $a^3 = (3M/4\pi dN_A)$.[16] Values of m_1 and m_2 can be obtained from the plots of $\upsilon_a - \upsilon_f$ and $\upsilon_a + \upsilon_f$ with $F(\varepsilon, n)$ and $[F(\varepsilon, n) + 2g(n)]$.

Even small errors in the estimated value of the cavity radius can lead to very large errors as the value enters as cubed in the above equations. Taking the ratio m_2/m_1 enables the determination of the excited state dipole moment without using the value of a. The excited state dipole moment of the molecule can be expressed in terms of the known value of the ground state dipole moment as $\mu_e = \mu_g(1 + x)/(x - 1)$, where $x = m_2/m_1$.

4.4.2.2 Method 2

In the second method, the analysis is based on the dimensionless solvent polarity parameter E_N^T proposed by Reichardt,[13] which is given by equation 4.8.

$$E_N^T = \frac{E_T(solvent) - 30.7}{32.4}, \tag{4.8}$$

where $E_T(solvent) = 28591/\lambda_{max}(\text{nm})$, and λ_{max} corresponds to the peak wavelength in the red region of the intramolecular charge transfer absorption of the molecule 2,6-diphenyl-4-(2,4,6-triphenyl-N-pyridino) phenolate.[13] This molecule, also called Reichardt's dye, shows a large solvatochromic effect. The absorption maxima of the dye in solvent mixtures of varying polarity were experimentally determined and used for the calculation of E_N^T. This reduced the error due to the presence of impurities in the

mixture as each solvent mixture was separately analyzed for its polarity value before use.

The plots of E_N^T and $F(\varepsilon, n)$ versus the weight fraction of Acetonitrile in the mixture is shown in Fig. 4.9. The plots were nonlinear when the percentage of toluene was higher, thus for the analysis of the data, only solvent mixtures showing a linear variation of the polarity parameters were used. Detailed physical properties of the toluene-acetonitrile mixture is available in the literature.[17]

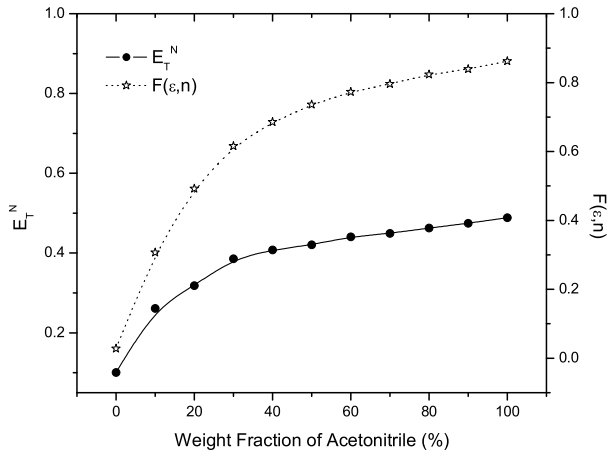

Figure 4.9: Variation of the polarity parameters with weight fraction of Acetonitrile

For the determination of the excited state dipole moment μ_e, the Stoke's shift $\upsilon_a - \upsilon_f$ was calculated from the absorption and fluorescence spectra. Here υ_a and υ_f denote the absorption and fluorescence band maxima respectively, in cm^{-1}. The Stoke's shift $(\upsilon_a - \upsilon_f)$ was analyzed as a function of the polarity of the solvent. Variation of $(\upsilon_a - \upsilon_f)$ with E_T^N was linear with more than 98 % correlation to a linear fit. The variation of the Stoke's shift with E_T^N is shown in Fig. 4.10 for the molecules 1a, 2a, 2b, 2c, 2d and 2e. For the other set of molecules the variation is given in Fig. 4.11.

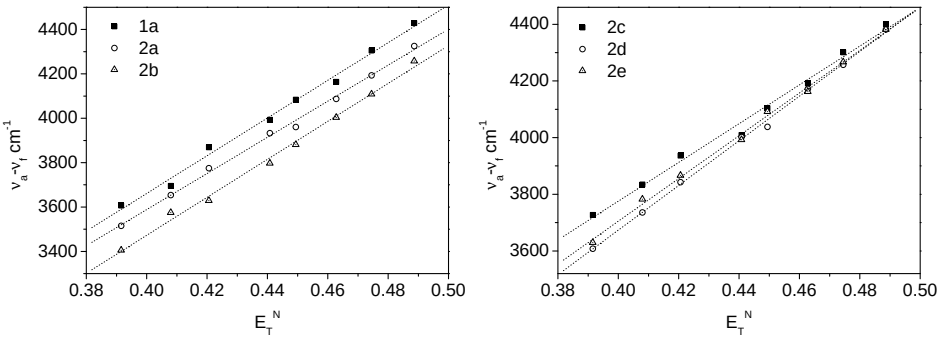

Figure 4.10: Graphs showing the linear variation of Stoke's shift with E_T^N for 1a, 2a, 2b, 2c, 2d and 2e.

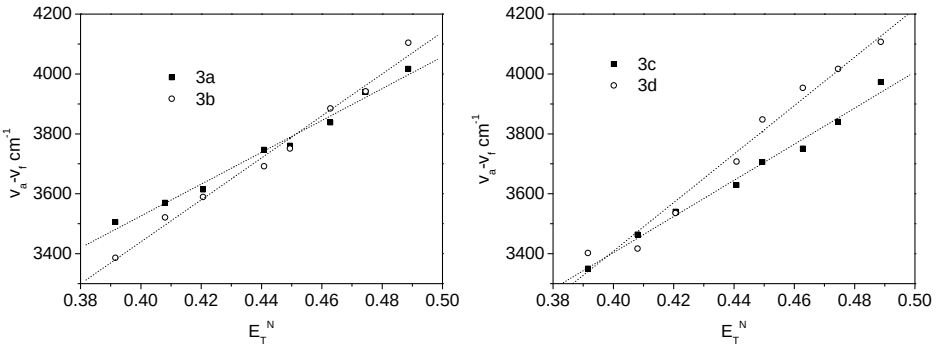

Figure 4.11: Graphs showing the linear variation of Stoke's shift with E_T^N for 3a, 3b, 3c and 3d.

The Stoke's shift is related to the difference in dipole moments and the Onsager radii of the molecule and the dye by equation 4.9.

$$\upsilon_a - \upsilon_f = 11307.6 \left(\frac{\Delta\mu^2 a_D^3}{\Delta\mu_D^2 a^3} \right) E_T^N + Constant \tag{4.9}$$

Here $\Delta\mu = \mu_e - \mu_g$ is the difference between the ground and excited state dipole moments of the molecule being studied and $\Delta\mu_D$ is that of Reichardt's dye. In the expression, the Onsager radii of both the dye (a_D) and the molecule (a) enters as a ratio and thus the error due to the uncertainty in the value of a is minimized. As the values of a_D and $\Delta\mu_D$

were known (6.2$\mathring{A}$ and 9D respectively[13]), the excited state dipole moment of the material under study could be evaluated from the plot of $\upsilon_a - \upsilon_f$ with E_N^T. Results of the calculation are given in Table 4.3.

Table 4.3: Excited state dipole moments of the molecules estimated from the solvatochromic analysis.

Molecule	μ_e (D)	Molecule	μ_e (D)
1a	14.96	2e	19.07
2a	14.53	3a	9.50
2b	14.55	3b	17.58
2c	15.88	3c	22.56
2d	24.12	3d	14.67

4.5 Estimation of the first hyperpolarizability (β)

Based on the solvatochromic measurements described above, one can estimate the first hyperpolarizability of the molecule with the two level microscopic model of β.[6,18] In this model, the contributions from all excited states other than the first excited state are neglected.[6] The following equation gives the value of β in terms of experimentally measurable quantities.

$$\beta = \frac{3\omega_{eg}^2(\mu_e - \mu_g)\mu_{eg}^2}{2\hbar^2(\omega_{eg}^2 - 4\omega^2)(\omega_{eg}^2 - \omega^2)} \tag{4.10}$$

here $\omega_{eg} = 2\pi c/\lambda_{max}$ and μ_{eg} = the transition moment, calculated from the area under the absorption band.[6] The area was determined by doubling the area of half of the absorption band if the spectrum was not symmetric about the peak frequency.[11]

The solvatochromic method gives only one dominant component of the tensor quantity β_{ijk}. It is assumed that the molecules have the donor and acceptor groups located such that the charge transfer takes place primar-

ily along the axis of the permanent ground state dipole moment of the molecule.[6] Thus Eq. 4.10 gives β_{xxx} (or β_{CT}) (charge transfer).

Photorefractive materials can be used for beam amplification in the two beam coupling geometry. Chromophores for such photorefractive guest host systems must not be absorbing at the operating wavelength to get an effective two beam coupling gain.[19] The molecules described here have only low absorption in the visible region of the spectrum. All molecules showed an increase in dipole moment on excitation by light. This showed that there was a higher degree of charge transfer taking place. The results are given in Table 4.4.

Table 4.4: Compilation of the results obtained on the different molecules

Molecule	λ_{max} (nm)	β (10^{-30}) esu	$9\mu_g\beta(10^{-46})$ esu
1a	387	3.77	3.32
2a	393	3.22	2.57
2b	395	2.84	2.17
2c	397	2.64	2.42
2d	398	5.16	3.74
2e	399	4.07	4.63
3a	400	2.87	1.14
3b	400	3.97	4.20
3c	401	2.77	4.20
3d	402	5.56	3.74

4.6 Summary and conclusions

The purpose of the work outlined was to evaluate the nonlinear optical properties of the synthesized molecules so as to select those possessing high values of photorefractive figure of merit. The ground and excited state dipole moments were determined which gave insight into the possibility of

light induced charge transfer in these molecules. It could be seen that, on excitation by light, the charge redistribution was such that it resulted in a higher value for the dipole moment. The estimate of the ground state dipole moment gave the relative tendency of the investigated molecules to align antiparallel in pairs in the bulk so that a net second order nonlinear optical effect could be absent. This molecular parameter was kept in mind when deciding the requirement of poling for the photorefractive samples.

The solvatochromic method assumes that the molecule is spherical and this method is suitable to small molecules. The estimation of (β_{ijk}) suffers from errors associated with the Onsager radius and the size of the molecule though some of them can be circumvented by appropriate processing of the data. Measures were taken to reduce the errors by using solvents of maximum purity and they were characterized as described in Section 4.4.2.2, each time before use. As the aim was to screen the molecules to find the ones with maximum value for (β_{ijk}), errors can be neglected even if it is as high as 20%.

It is reported that the length of the alkyl spacer connecting the donor to the acceptor moiety has major effect on the value of (β_{ijk}).[20] This approach of increasing the value of β has the advantage that the absorption maxima of the molecule is not getting changed as there is no change in the effective conjugation length of the material. The main aim of the present work was to study the possibility of the synthesized molecules for application to photorefractive polymers as the absorption of these molecules do not fall well in to the visible region. This was stimulated by the fact that for highly efficient photorefractive applications, the molecule for electro-optic functionality should not absorb at the operating wavelength. There was only small change in the absorption peak of the these materials, as shown in Table 4.4, but a steady increase in hyperpolarizability was not achieved. A small increase in the figure of merit was observed.

The chromophores with odd number of alkyl spacers showed higher (β_{ijk}) values. It is reported that the lower values for even number of alkyl units can be due to a centrosymmetric arrangement of the molecules.[20,21] A deep investigation of this interesting effect was not attempted. The

molecules with high values for the product $\mu\beta$ were selected for the preparation of photorefractive guest host systems. The experimental techniques for the evaluation of the electro-optic coefficients are described in Chapter 5 along with the results obtained.

References

[1] D. M. Burland, R. D. Miller, and C. A. Walsh, "Second-Order Nonlinearity in Poled-Polymer Systems," Chem. Rev. **94,** 31–75 (1994).

[2] B. E. A. Saleh and M. C. Teich, *Fundamentals of Photonics* (John Wiley & Sons, Inc., New York, 1991), pp. 697–698.

[3] S. K. Lor, H. Hiraoka, P. Yu, L.-T. Cheng, and G. K. L. Wong, "Second harmonic characteristics of Disperse Red 1 doped polysulfones," J. Mater. Res. **10,** 2693–2696 (1995).

[4] C. Zhang, A. S. Ren, F. Wang, J. Zhu, and L. R. Dalton, "Synthesis and Characterization of Sterically Stabilized Second-Order Nonlinear Optical Chromophores," Chem. Mater. **11,** 1966–1968 (1999).

[5] M. A. Pauley, C. H. Wang, and A. K. Y. Jen, "Hyper-Rayleigh scattering studies of first order hyperpolarizability of tricyanovinylthiophene derivatives in solution," J. Chem. Phys. **102,** 6400–6405 (1995).

[6] M. S. Paley and J. M. Harris, "A Solvatochromic Method for Determining Second-Order Polarizabilities of Organic Molecules," J. Org. Chem. **54,** 3774–3778 (1989).

[7] R. Dhanya, "Development of Photorefractive Polymers: Synthesis and Characterization of Polymers with Donor-π-Acceptor Groups," Ph.D. Thesis (Cochin University of Science and Technology, India, 2008).

[8] V. C. Kishore, R. Dhanya, K. Sreekumar, R. Joseph, and C. S. Kartha, "On the Dipole Moments and First-order hyperpolarizability of N,N-bis(4-bromobutyl)-4-nitrobenzenamine," Spectrochim. Acta Part A: Mol. Biomol. Spectrosc. p. in press (2007).

[9] A. V. Vannikov and A. D. Girishina, "The Phtorefractive Effect in Polymeric Systems," Russ. Chem. Rev. **72,** 471–488 (2003).

[10] S. R. Marder, B. Kippelen, A. K. Y. Jen, and N. Peyghambarian, "Design and synthesis of chromophores and polymers for electro-optic and photorefractive applications," Nature (London) **388,** 845–851 (1997).

[11] C. Bosshard, G. Knöpfle, P. Prêtre, and P. Günter, "Second-order polarizabilities of nitropyridine derivatives determined with electric-field-induced second-harmonic generation and a solvatochromic method: A comparative study," J. Appl. Phys. **71,** 1594–1605 (1992).

[12] J. R. Lombardi, "Solvatochromic Shifts: A Reconsideration," J. Phys. Chem. A **102,** 2817–2823 (1998).

[13] C. Reichardt, "Solvatochromic Dyes as Solvent Polarity Indicators," Chem. Rev. **94,** 2319–2358 (1994).

[14] K. Guzow, M. Szabelski, J. Karolczak, and W. Wiczk, "Solvatochromism of 3-[2-(aryl)benzoxazol-5-yl]alanine derivatives," J. Photochem. Photobiol. A: Chem. **170,** 215–223 (2005).

[15] Y. Nadaf, B. Mulimani, M. Gopal, and S. Inamdar, "Ground and excited state dipole moments of some exalite UV laser dyes from solvatochromic method using solvent polarity parameters," J. Mol. Struct. (Theochem) **678,** 177–181 (2004).

[16] P. Suppan, "Excited-state dipole moments from absorption/fluorescence solvatochromic ratios," Chem. Phys. Lett. **94,** 272–275 (1983).

[17] G. Rltroulls, N. Papadopoulos, and D. Jannakoudakls, "Densities, Viscosities, and Dielectric Constants of Acetonitrile + Toluene at 15, 25, and 35^oC," J. Chem. Eng. Data **37,** 146–148 (1986).

[18] R. L. Sutterland, *Handbook of Nonlinear Optics* (Marcel Dekker, Inc., New York, 1996), pp. 256–257.

[19] K. Meerholz, B. L. Volodin, Sandalphon, B. Kippelen, and N. Peyghambarian, "A photorefractive polymer with high optical gain and diffraction efficiency near 100%," Nature **371,** 497–499 (1994).

[20] A. Datta, S. K. Pati, D. Davis, and K. Sreekumar, "Odd-Even Oscillations in First Hyperpolarizability of Dipolar Chromophores: Role of Conformations of Spacers," J. Phys. Chem. **109,** 4112–4117 (2005).

[21] S. K. Asha, K. Kavita, P. K. Das, and S. Ramakrishnan, "Relaxation Behavior of Twin Nonlinear Optical Chromophores: Effect of the Spacer Length," Chem. Mater. **11,** 3352–3358 (1999).

CHAPTER

FIVE

Study of Electro-optic Effect

5.1 Introduction

Polymers showing nonlinear optical properties is the subject of intense research due to their applicability to integrated optical devices and high speed electro-optic modulators.[1–3] These devices rely on the refractive index modulations induced by a DC or AC electric field. If the refractive index modulation is proportional to the applied electric field, it is called linear electro-optic effect or Pockels effect. If the refractive index change is proportional to the square of the field, it is termed as the quadratic electro-optic effect or Kerr effect.[4]

In photorefractive materials, the refractive index modulation is due to a space charge field induced electro-optic effect.[5] The electro-optic response is possible in a polymer if it contains chromophores possessing nonlinear optical properties or anisotropy of the linear polarizability.[6] These chromophores can be a part of the polymer chain[7] or dispersed in the polymer.[8] It can also be part of a charge transporting polymer, in which case the polymer is said to be bifunctional.[9] The method of making the chromophore bound to the polymer offer higher stability but generally involves complicated synthesis procedures. The simplest method is dispersing molecules with the required nonlinear properties in to a polymer

host.[5] Diffraction efficiency of $\sim$ 95 % was reported for a photorefractive composite prepared by this method.[5]

Being a second order nonlinear effect, the linear electro-optic effect requires non-centrosymmetry in the bulk. The centrosymmetry of the system must be broken to achieve an effective macroscopic second order nonlinearity.[10] As explained in Section 1.5.2, chromophores used for photorefractive applications usually possess a rod like shape. These can be aligned in the polymer host by the application of an electric field.[11] If the field was applied keeping the composite near the glass transition temperature of the host, the alignment will be more efficient. This process is termed as electric poling. Poling breaks the centrosymmetry of the system by aligning the nonlinear optical chromophores in the direction of the field and the medium is said to have attained polar order. If the field is removed, the molecules will tend to rotate back to their equilibrium positions due to thermal agitation there by reducing any second order effects. Proposed methods to prevent the rotational relaxation include cross-linking,[12] use of high T_g hosts as well as chiral designs.[13] In low T_g photorefractive composites, the refractive index modulation is higher due to the orientational birefringence effect caused by the field induced alignment of rod shaped chromophore molecules.[14,15]

This chapter deals with the details and results of electro-optic studies. One of the polymer systems studied was based on a guest-host approach, in which the optically transparent polymer poly(methyl methacrylate) and selected paranitroanline derivatives studied in chapter 4 were used. The second was a single component polymer Poly(3-methacrloyl-1-(4'-nitro-4-azo-1'-phenyl)phenyl alanine-co-methyl methacrylate), which has a structure similar to other electro-optic co-polymer systems reported in the literature.[16] A discussion of the origin of nonlinear optical effects and the experimental techniques was given in Section 1.5.

5.2 Electro-optic polymer systems

Electro-optic response for photorefractive effect can be achieved in many ways. The first and easiest is the guest host approach, in which molecules showing the required nonlinear optical properties are dispersed in a suitable photoconductive host. Numerous photorefractive polymer systems belong to this category.[5,17–19] Many of the reported photorefractive systems are solid solutions of nonlinear optical molecules (chromophores) in the photoconducting host PVK which was sensitized with TNF.[5] Selection of chromophores is usually done based on the figure of merit discussed in Section 1.5.3.

To achieve macroscopic second order susceptibility, guest-host systems with high T_g must be poled near or above the T_g of the host.[20,21] Drawbacks of this class of polymers include phase separation and crystallization of chromophores and loss of polar order with aging and temperature.

To better stabilize the nonlinear optical properties of the polymer, functionalized nonlinear optical polymers were introduced.[7,22] These polymers may be used as host for charge generating and transporting molecules or can be blended with a photoconducting polymer to achieve the requirements for photorefractive effect in a single system. The review by Burland et. al.,[21] describes various types of nonlinear polymer systems in detail, which are of possible use in photorefractive systems as well.

5.3 Polymer systems studied

Three paranitroaniline molecules were selected based on the studies done in chapter 4 and dispersed in poly(methyl methacrylate) to make guest-host systems. The molecules were N,N-bis(4-[(6-aminohexyl)amino]butyl)-4-nitrobenzenamine (C1), N,N-bis(4-[3-(ethylamino)propylamino]butyl)-4-nitrobenzenamine (C2) and N,N-bis(4-[4-(ethylamino) butylamino]butyl)-4-nitrobenzenamine (C3).

The other system was a co-polymer of 3-methacrloyl-1-(4'-nitro-4-azo-1'-phenyl) phenylalanine and methyl methacrylate. This type of polymers

are widely studied due to their stability compared to guest-host systems. The co-polymer approach helps in getting the required nonlinear response of a polymer and the good film forming ability of another polymer into the co-polymer.

5.3.1 Preparation of samples

Electro-optic measurements were done on sandwiched samples. In the case of guest-host PMMA, the molecules were dissolved in a chloroform solution of 8 wt% PMMA. The concentration of the chromophores was limited to 15 wt% due to the lack of optical quality in films containing more than this quantity. Patterned ITO plates were used as substrate for casting the above solution. After drying for 48 h, another patterned ITO plate was placed on the film using teflon sheets as spacer. Both the ITO's were clamped together using metallic clips and heated to 100^0C so that the polymer layer softens. The sandwiched sample was cooled and the ITO's were glued together using a thermally stable adhesive. The thickness of the samples were ~ 48 μm.

A similar procedure was employed for preparing the samples using Poly(3-methacrloyl-1-(4-nitro-4-azo-1-phenyl)phenylalanine-co-methyl methacrylate).

5.4 Guest-Host PMMA

Three molecules possessing comparatively higher value for the product $\mu\beta$ were selected for the electro-optic studies. Their structures are given in Fig. 5.1.

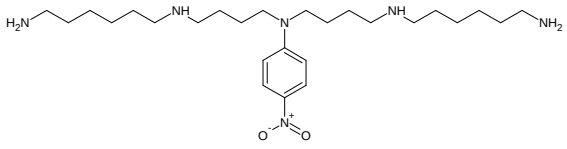

N,N-bis(4-[(6-aminohexyl)amino]butyl)-4-nitrobenzenamine - C1

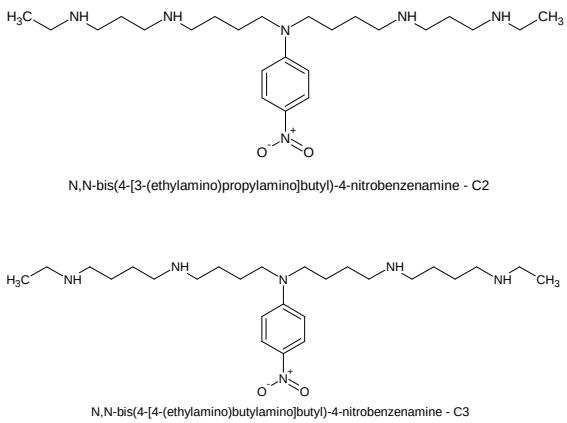

Figure 5.1: Molecular structures of the chromophores selected for the electro-optic study.

The molecules were dispersed in PMMA at appropriate weight ratios. A doping concentration of higher than 20% resulted in films of less optical clarity. Also, at higher chromophore loading, chances of electrostatic interaction increases which tends to align the molecules in a centrosymmetric fashion thereby reducing the electro-optic response.[23–25]

5.4.1 Optical absorption

Absorption spectra of the chromophores in chloroform are shown in Fig. 5.2 Absorption was weak in the visible region of the spectrum.

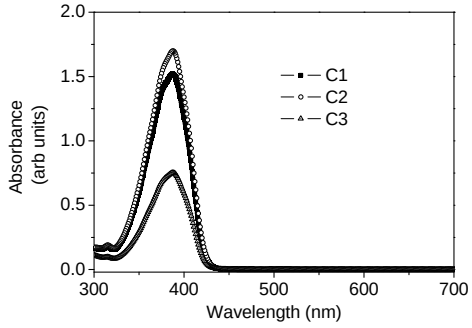

Figure 5.2: Absorption spectra of the chromophores C1, C2 and C3.

The ground state dipole moment of the chromophores were evaluated and given in Chapter 4. All molecules possessed high ground state dipole moments. Thus, to achieve a non-centrosymmetric arrangement in the bulk, poling of the sample was necessary.

5.4.2 Electrical poling

Poling must be attempted by maintaining an electric field across the sample while keeping the sample near its glass transition. Thus glass transition temperatures of the doped PMMA were determined using a differential scanning calorimeter (Q-100, TA Instruments). All guest host systems prepared in PMMA showed similar glass transition temperatures. The DSC traces are shown in Fig. 5.3.

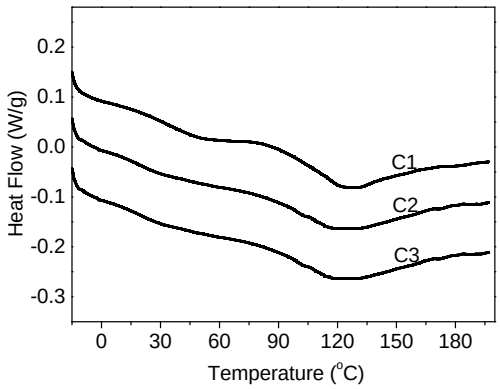

Figure 5.3: DSC traces of PMMA doped with the chromophores C1, C2 and C3.

The glass transition temperature was 100.8^o C for C1, 99.3^{o}C for C2, and 99^{o}C for C3 doped PMMA. Thus the poling temperature was selected to be near 100^{0}C. For poling electro-optic systems, corona poling (see Section 1.6.7) is mainly used which allow very high fields and less current flow through the sample. As this technique was experimentally not feasible, poling was done on the sandwiched samples by keeping them at the poling temperature and applying a DC voltage to the ITO electrodes. As temperature increased, DC current through the sample also increased, care was

taken to avoid electric breakdown of the sample by increased DC current flow. The poling field was 10V/μm and was kept at this value to minimize current. Poling was continued for 2h and the sample was cooled slowly to room temperature while maintaining the field.

5.4.3 Electro-optic measurements

Experiments were done as explained in Section 1.6.6. On the un-poled samples no meaningful measurements could be made, possibly due to the high ground state dipole moments of the chromophores, which tend to cancel a macroscopic second order susceptibility. Measurement of the modulated signal was done as a function of poling temperature and time after poling. The temperature dependence of the modulated signal is shown in Fig. 5.4. Higher modulation was obtained for samples poled near the glass transition temperature of the system.

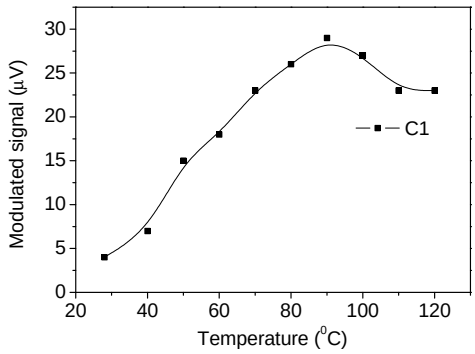

Figure 5.4: Temperature dependence of electro-optic modulated signal for PMMMA:C1 system.

The electro-optic coefficient r_{33} was calculated from the measured signals as explained in Section 1.6.6. The modulated signal was studied with time after poling and it was found to be stable for at least 6h after an initial decrease. The temporal stability of the poling depends on many factors, mainly the glass transition temperature of the composite.[26,27] The temporal behavior of the electro-optic signal after electric field poling is

shown in Fig. 5.5.

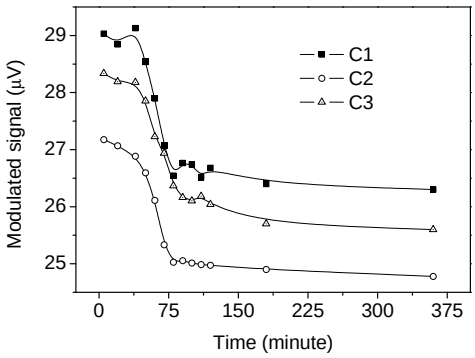

Figure 5.5: Temporal variation of the measured electro-optic modulated signal after poling for C1, C2 and C3 doped PMMA.

The polar order showed an initial fast decay followed by a relatively stable region. This might be due to the rotational relaxation of the chromophores in the host. This kind of decay of the second order response is common to guest-host systems.[27] The electro-optic coefficients of the presently studied guest-host systems are given in Table 5.1.

Table 5.1: Electro-optic coefficients of guest-host systems with PMMA as host and C1, C2 and C3 as chromophores.

Dopant	T_g ^{0}C	r_{33} (pm/V)
C1	100	2.7
C2	99	1.7
C3	99	1.9

Electro-optic signals in the sandwich cell geometry can also get contributions from the piezo-electric effects. Field induced change in thickness can cause additional path length changes. In such cases, the refractive index change exhibit a quadratic dependence on the applied field.[28] In the present experiments we could not detect any signals at twice the modulation frequency, implying absence/less importance of quadratic electro-optic

effects. The absence of signals on un-poled samples may also be due to the absence of signals produced by field induced thickness changes.

Thus the molecules studied in Chapter 4 were able to show an electro-optic effect when doped in to PMMA. It has been shown that the free-volume surrounding the dopants, which determines the rotational freedom of the dopants, has major influence on the response of the system.[27] Thus the response of these molecules in a photoconductive host was expected to change from the measured values.

5.5 Poly(3-methacrloyl-1-(4'-nitro-4-azo-1'-phenyl) phenylalanine-co-methyl methacrylate)

The guest-host approach, though simple and flexible, suffers from the stability issues related to the nonuniform dispersion of chromophores, their phase separation or crystallization and the lack of thermal stability due to the chromophore reorientation.[21] In order to reduce these drawbacks, chromophores were chemically attached to the polymer back bone. This has the advantage of limited chromophore motion as they are connected to the polymer, lack of phase separation or crystallization of the units and high glass transition temperature. In guest host approach, the glass transition temperature of the polymer may get reduced due to the plasticization action of the doped chromophores. In side chain polymers, the number density of the chromophores is related to the chemical substitution level and can be done to the maximum extent without phase separation.

The molecule studied here, Poly(3-methacrloyl-1-(4'-nitro-4-azo-1'-phen yl)phenylalanine-co-methyl methacrylate) is such a side chain polymer. The structure of the polymer is shown in Fig. 5.6. Synthesis and characterization of the molecule were done in our lab. The details are given elsewhere.[29] The number average molecular weight (M_n) was 3175 and weight average molecular mass (M_w) was 6408.

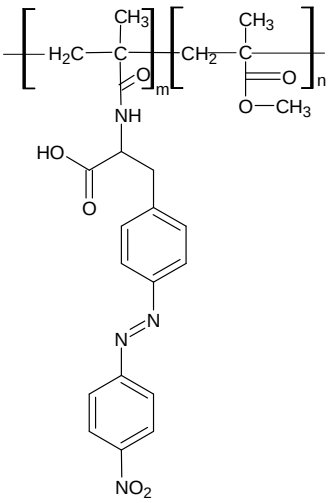

Figure 5.6: Molecular structure of Poly(3-methacrloyl-1-(4'-nitro-4-azo-1'-phenyl)phenylalanine-co-methyl methacrylate).

The absorption spectrum of the polymer is shown in Fig. 5.7 and the differential scanning calorimetry trace is shown in Fig. 5.8. The refractive index of the polymer in film form was measured using an Atago DRM2 refractometer. A value of 1.673 was obtained at 590 nm.

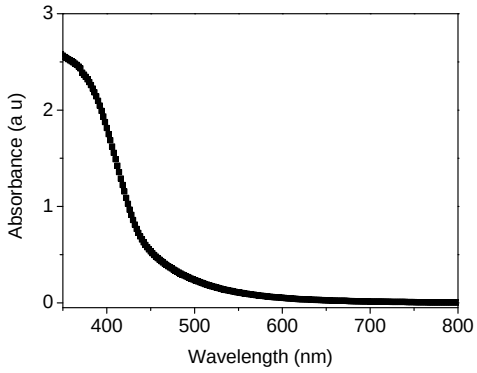

Figure 5.7: Absorption spectrum of Poly(3-methacrloyl-1-(4'-nitro-4-azo-1'-phenyl)phenylalanine-co-methyl methacrylate).

The amino acid L-phenylalanine, used in the synthesis of this molecule is

a chiral molecule. Chirality of this molecule may lead to improved non-centrosymmetry and lack of mirror symmetries[30,31] in the final polymer. Electro-optic measurements were done on the un-poled samples using 632.8 nm light from a He-Ne laser. Absorption of the molecule at this wavelength was small.

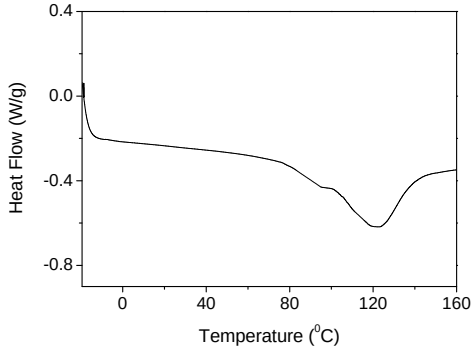

Figure 5.8: Differential scanning calorimetry trace of Poly(3-methacrloyl-1-(4'-nitro-4-azo-1'-phenyl)phenylalanine-co-methyl methacrylate).

The glass transition temperature of the polymer was 96.7^0 C. High T_g of the polymer may be useful when it is used in situation where good thermal stability is required.

5.5.1 Electro-optic effect

Samples for the determination of electro-optic coefficient was prepared as explained in Section 5.3.1. The solvent used was toluene as chloroform was found to yield films of less optical clarity. Thickness of the studied samples were approximately 48 μm, determined using a Stylus profiler. As the film will be subjected to high electric fields, the presence of contaminants was carefully avoided.

The transmission mode ellipsometric measurement explained in Section 1.6.6 was used for the determination of the electro-optic coefficient. The angle of incidence of the beam was 65^0 with respect to the sample normal. This high incident angle facilitated a high propagation distance of the beam through the active layer so that the modulation in intensity was

maximized. The experiment was performed at 1500 Hz with only the AC field present. The field dependence of the modulated signal is shown in Fig. 5.9. The measurement was done at room temperature (27 ± 1^0C).

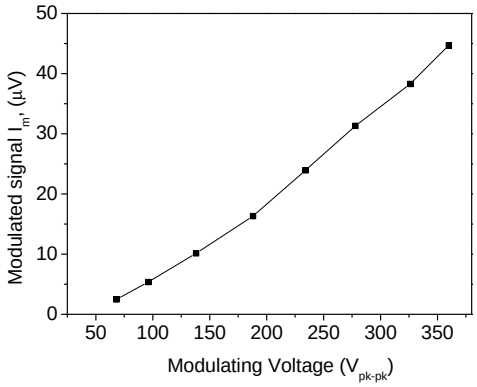

Figure 5.9: Electro-optic modulated signal obtained from the sandwich cell of Poly(3-methacrloyl-1-(4'-nitro-4-azo-1'-phenyl)phenylalanine-co-methyl methacrylate).

Electro-optic coefficient r_{33} was estimated using equation 1.30 and found to be 4.75 pm/V. The observation of electro-optic modulation in un-poled samples indicated that there was a certain degree of non-centrosymmetry in the polymer films. This could be due to the chiral nature of the phenyl alanine unit present in the polymer. It is believed that chirality leads to a non-centrosymmetric arrangement in the bulk, which is referred to as chemical poling.[32] Second order nonlinear optical effects are highly dependent on the chirality of the molecules involved.[33] The observation of electro-optic effect in this polymer alone could not guarantee a chemical poling behavior, circular dichroic studies of the polymer might provide more information in this respect.[33]

5.6 Summary and conclusions

Three p-nitroaniline derivatives were found to show electro-optic effect in poly(methyl methacrylate) matrix. The chromophore loading level was

limited to less than 20% due to lack of optical clarity, possibly due to the increased chromophore-chromophore electrostatic interaction and subsequent crystallization. Contact poled guest-host systems were studied using a modulated ellipsometric setup and they showed a maximum r_{33} value of 2.7 pm/V for the molecule N,N-bis(4-[(6-aminohexyl)amino]butyl)-4-nitrobenzenamine doped to 15 wt% in PMMA, at 632.8 nm. The electro-optic coefficient obtained was sufficient for photorefractive effect.

The second polymer system was a side chain polymer Poly(3-methacrloyl-1-(4'-nitro-4-azo-1'-phenyl)phenylalanine-co-methyl methacrylate). The electro-optic coefficient r_{33} of this polymer was 4.75 pm/V at 632.8 nm. The measurement was done on un-poled samples assuming an inherent polar order due to the structure of the molecular units.

References

[1] J. Zhou, Z. Cao, X. Deng, Q. Shen, W. Wei, Z.-J. Zhang, and S.-X. Xie, "An attenuated total internally reflected light modulator utilizing quadratic electro-optic polymer film," J. Opt. A: Pure Appl. Opt. **8,** 996–998 (2006).

[2] D. Chen, H. R. Fetterman, A. Chen, W. H. Steier, L. R. Dalton, W. Wang, and Y. Shi, "Demonstration of 110 GHz electro-optic polymer modulators," Appl. Phys. Lett. **70,** 3335–3337 (1997).

[3] C. C. Teng, "Traveling-wave polymeric optical intensity modulator with more than 40 GHz of 3-dB electrical bandwidth," Appl. Phys. Lett. **60,** 1538–1540 (1992).

[4] B. E. A. Saleh and M. C. Teich, *Fundamentals of Photonics* (John Wiley & Sons, Inc., New York, 1991), pp. 697–698.

[5] K. Meerholz, B. L. Volodin, Sandalphon, B. Kippelen, and N. Peyghambarian, "A photorefractive polymer with high optical gain and diffraction efficiency near 100%," Nature **371,** 497–499 (1994).

[6] A. V. Vannikov and A. D. Girishina, "The Phtorefractive Effect in Polymeric Systems," Russ. Chem. Rev. **72,** 471–488 (2003).

[7] M. Trollsås *et al.*, "Preparation of a Novel Cross-Linked Polymer for Second-Order Nonlinear Optics," J. Am. Chem. Soc. **118,** 8542–8548 (1996).

[8] M. J. Cho, S. K. Lee, J.-I. Jin, D. H. Choi, and L. R. Dalton, "Electro-optic property of chromophore-terminated trifunctional dendrimer in a guesthost system," Thin Solid Films **515,** 2303–2309 (2006).

[9] Y. Zhang, S. Ghosal, M. K. Casstevens, and R. Burzynski, "Photorefractive composite materials with bi-functional charge transporting second-order nonlinear optical chromophores," J. Appl. Phys. **79,** 8920–8929 (1996).

[10] Sandalphon, B. Kippelen, K. Meerholz, and N. Peyghambarian, "Ellipsometric measurements of poling birefringence, the Pockels effect, and the Kerr effect in high-performance photorefractive polymer composites," Appl. Opt. **35,** 2346–2354 (1996).

[11] L. M. Hayden, G. F. Sauter, F. R. Ore, P. L. Pasillas, J. M. Hoover, G. A. Lindsay, and R. A. Henry, "Second-order nonlinear optical measurements in guest-host and side-chain polymers," J. Appl. Phys. **68,** 456–465 (1990).

[12] G. Xu, J. Si, X. Liu, Q. Yang, P. Ye, Z. Li, and Y. Shen, "Permanent optical poling in polyurethane via thermal crosslinking," Opt. Commun. **153,** 95–98 (1998).

[13] P. Biju and K. Sreekumar, "Nonlinear optical properties of chiral polyesters: a joint experimental and theoretical study," In *Smart Materials, Structures, and Systems*, S. Mohan, B. Dattaguru, and S. Gopalakrishnan, eds., Proceedings of the SPIE **5062,** 116–123 (2003).

[14] Y. Chen, B. Zhang, and F. Wang, "Photorefractive material based on a polymer containing photoconductors and nonlinear chromophores," Opt. Commun. **228,** 341–348 (2003).

[15] W. E. Moerner, A. Grunnet-Jepsen, and C. L. Thompson, "Photorefractive Polymers," Annu. Rev. Mater. Sci. **27,** 585–623 (1997).

[16] M. Goodwin, D. Bloor, and S. Mann, "Nonlinear materials," In *Special Polymers for Electronics and Optoelectronics*, J. A. Chilton and M. T. Goosey, eds., pp. 155–157 (Chapman & Hall, London, 1995).

[17] Y. Chena, Q. Gong, F. Wang, B. Zhang, and Z. Chen, "Synthesis and characterization of photorefractive materials based on polymers containing photoconductors and nonlinear chromophores," Materials Letters **57,** 4372–4377 (2003).

[18] Y. Zhang, C. A. Spencer, S. Ghosal, M. K. Casstevens, and R. Burzynski, "Photorefractive properties of a thiapyrylium-dye-sensitized polymer composite," J. Appl. Phys. **76,** 671–679 (1994).

[19] Y. Zhang, Y. Cui, and P. N. Prasad, "Observation of photorefractivity in a fullerene-doped polymer composite," Phys. Rev. B **46,** 9900–9902 (1992).

[20] S. K. Park, J. Y. Do, J. J. Ju, S. Park, and M.-H. Lee, "A stable host-guest electro-optic polymer system with polyisoimide as a host," React. Funct. Polym. **58,** 93–101 (2004).

[21] D. M. Burland, R. D. Miller, and C. A. Walsh, "Second-Order Nonlinearity in Poled-Polymer Systems," Chem. Rev. **94,** 31–75 (1994).

[22] D. Yu and L. Yu, "Design and Synthesis of Functionalized Polyimides for Second-Order Nonlinear Optics," Macromolecules **27,** 6718–6721 (1994).

[23] G. Koeckelberghs, S. Sioncke, T. Verbiest, I. V. Severen, I. Picard, A. Persoons, , and C. Samyn, "Synthesis and Properties of Chiral Chromophore-Functionalized Polybinaphthalenes for Nonlinear Optics: Influence of Chromophore Concentration," Macromolecules **36,** 9736–9741 (2003).

[24] L. R. Dalton, A. W. Harper, and B. H. Robinson, "The role of London forces in defining noncentrosymmetric order of high dipole momenthigh hyperpolarizability chromophores in electrically poled polymeric thin films," Proc. Natl. Acad. Sci. USA **94,** 4842–4847 (1997).

[25] A. W. Harper, S. Sun, L. R. Dalton, S. M. Garner, A. Chen, S. Kalluri, W. H. Steier, and B. H. Robinson, "Translating microscopic optical nonlinearity into macroscopic optical nonlinearity: the role of chromophore chromophore electrostatic interactions," J. Opt. Soc. Am. B **15,** 329–337 (1998).

[26] M. Tsuchimori, O. Watanabe, and A. Okada, "Temporal Stability of Second-Order Optical Nonlinearity of Polyurethane: Influence of Poling Conditions," Jpn. J. Appl. Phys. **40,** 6396–6400 (2001).

[27] H. L. Hampsch, J. Yang, G. K. Wong, and J. M. Torkelson, "Dopant orientation dynamics in doped second-order nonlinear optical amorphous polymers. 2. Effects of physical aging on poled films," Macromolecules **23,** 3648–3654 (1990).

[28] J. Bouclé, A. Kassiba, M. Makowska-Janusik, J. Sanetra, N. Herlin-Boime, A. Bulou, and S. Kodjikian, "Electro-optic phenomena in guesthost films of PMMA and SiC nanocrystals," Opt. Commun. **246,** 415–420 (2005).

[29] R. Dhanya, "Development of Photorefractive Polymers: Synthesis and Characterization of Polymers with Donor-π-Acceptor Groups," Ph.D. Thesis (Cochin University of Science and Technology, India, 2008).

[30] E. Meijer and B. Feringa, "Chirality in nonlinear optics and optical switching," Mol. Cryst. Liq. Cryst. **235,** 169–180 (1993).

[31] V. Ostroverkhov, O. Ostroverkhova, R. G. Petschek, K. D. Singer, L. Sukhomlinova, and R. J. Twieg, "Prospects for Chiral Nonlinear Optical Media," IEEE J. Sel. Top. Quantum Electron. **7,** 781–792 (2001).

[32] P. Biju and K. Sreekumar, "Nonlinear optical properties of chiral polyesters: a joint experimental and theoretical study," In *Smart Materials, Structures, and Systems*, S. Mohan, B. Dattaguru, and S. Gopalakrishnan, eds., Proceedings of the SPIE **5062,** 116–123 (2003).

[33] B. J. Burke, A. J. Moad, M. A. Polizzi, and G. J. Simpson, "Experimental Confirmation of the Importance of Orientation in the Anomalous Chiral Sensitivity of Second Harmonic Generation," J. Am. Chem. Soc. **125,** 9111–9115 (2003).

CHAPTER

SIX

Observation of Photorefractive Effect in a Polybenzoxazine Based System

6.1 Introduction

The photorefractive effect requires both photoconductivity and electro-optic effect in a single medium. Materials which are photorefractive can be used for a variety of applications ranging from multiplexed reversible data storage[1] to neural networks.[2] Earlier works were focussed on photorefractive inorganic crystals. These are difficult to prepare with required dopant level, as most of the dopants will be expelled during the crystal growth process. Also, in these materials the dielectric constant is higher which reduces the photorefractive figure of merit.[3] Polymer photorefractive systems offer a very flexible alternative as tunability of properties can be achieved very easily using chemical methods and the dielectric constant of these materials are small which permits higher space charge fields. Many polymer photorefractive systems were reported claiming device quality speeds and gain coefficients.[4] Yet, the use of organic photorefractive materials has not come up to the level of a commercial application mainly due to the instability problems with polymers. Diffraction efficiency approaching 100 % and two beam coupling gain coefficient of over 200 cm^{-1} were achieved in photorefractive polymers.[5] Nano-particles were also used

as sensitizers for photorefractive polymers and a maximum gain coefficient of 48 cm^{-1} was reported.[6] Recently an updatable holographic 3D display was demonstrated based on a photorefractive polymer.[7]

Aim of the present study was to identify molecules suitable for photorefractive systems and to develop a photorefractive formulation. In the preceding chapters, studies done to select molecules capable of showing photoconductivity and electro-optic effect are given. Presence of photoconductivity and electro-optic response may not guarantee a photorefractive effect. The only proof comes from the asymmetric energy transfer which will be observed if the gratings formed are truly photorefractive as mentioned in Section 6.3. Molecules were selected based on the studies performed on them to prepare possible photorefractive composites. Experiments and the results are given in the present chapter.

There are so many photorefractive systems reported in the literature. Each of them belong to the classes of photorefractive polymers discussed in Section 1.3. A fully functionalized photorefractive system[8] is considered to be highly stable as the components are chemically linked together. But this requires lengthy and usually complicated synthesis procedures. A flexible method is the guest-host approach which offers a variety of combinations. Guest-host systems with glass transition (T_g) temperature near room temperature have shown high two beam coupling gain coefficients due to the field induced reorientation of the dipolar chromophores.[5,9] Thus we have also decided to start from a guest-host system based on the molecules studied.

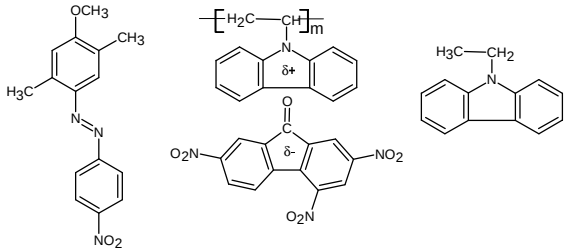

Figure 6.1: The chemical structure of the molecules used in a high efficiency photorefractive composite.

The highest photorefractive diffraction efficiency (near 100%) was obtained for a guest-host system.[5] Fig. 6.1 shows the chemical structure of the molecules used in this system. The molecules depicted are, charge transfer complex of poly(N-vinylcarbazole) with 2,4,7-trinitro-9-fluorenone (middle), 2,5-dimethyl-4-(p-nitrophenylazo)anizole (left) and N-ethylcarbazole. The next section describes the polymer system developed in the present work and the details of the studies carried out.

6.2 Guest host system based on Poly(6-tert-butyl-3-phenyl-3,4-dihydro-2H-1,3-benzoxazine)

As the first requirement is carrier generation at the operating wavelength, the photoconductor, Poly(6-tert-butyl-3-phenyl-3,4-dihydro-2H-1,3-benzo xazine) which was sensitized with C_{60} was selected as the photoconducting host. Electro-optic effect can be brought about in this host by doping with either the molecules or polymer studied in Chapter 5. Unfortunately, these molecules could not be used as none of them showed required transparency when blended with the photoconducting matrix of selection. These molecules may be compatible with some other photoconductive systems. Thus for the preparation of a photorefractive system, the well studied nonlinear optical chromophore Disperse Red 1 (DR1) was used in the above photoconducting host. The structure of the molecules in the system is given in Fig. 6.2.

6.2.1 Preparation of sandwich cells

Preparation of sandwich structures which were transparent required much attention to every detail. The photorefractive polymer has to be subjected to very high electric fields. Thus even traces of impurities lead to electric breakdown and waste of material and time. Patterning of the ITO was necessary to avoid discharge through the edges of ITO plates and sample failure. The plates were patterned by first defining the ITO area to be kept by applying a thick coating of ethylene-propylene diene monomer (EPDM)

rubber. Immersing the coated plates in a mixture of hydrochloric acid and nitric acid at a ratio of 3:1 for 10 minutes removed all uncovered ITO from the plate.[10] Plates were thoroughly cleaned using soap solution and water after the etching process.

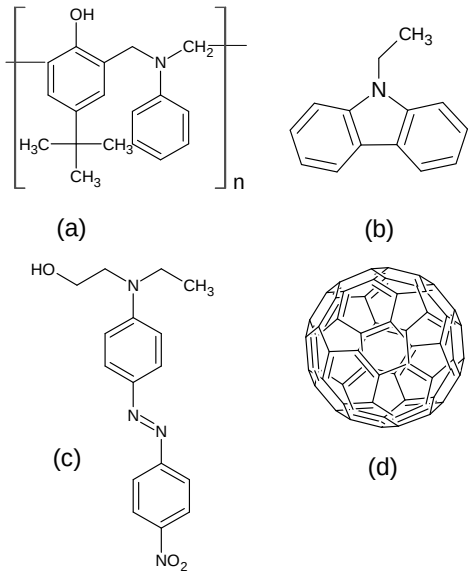

Figure 6.2: Molecular structures of the molecules used for preparing a system showing both photoconductivity and electro-optic effect. (a) Poly(6-tert-butyl-3-phenyl-3,4-dihydro-2H-1,3-benzoxazine), (b) N-ethyl carbazole, (c) 4-[N-ethyl-N-(2-hydroxyethyl)]amino-4-nitroazobenzene (DR1), and (d) C_{60}.

To prepare the device for photorefractive studies, ITO cells were assembled first. For this, one of the the patterned ITO's was given two layers of Teflon (48 μm) covering at the two edges and another ITO was flipped over it as shown in Fig. 6.3, two metallic clips were used at both sides to keep them stuck together. This gave a glass cell with $\sim 48\mu$m inter-electrode separation.

The sample was made to fill between the plates utilizing capillary action. For this, the sample was prepared as a fine powder. The following composition of components was used for preparing a polymer system

with photoconductivity and electro-optic response. Poly(6-tert-butyl-3-phenyl-3,4-dihydro-2H-1,3-benzoxazine) (68 wt%), C_{60} (0.6 wt%), N-ethyl carbazole (18.9 wt%) and DR1 (12.5 wt%), this composition showed good optical clarity. All these were dissolved in 20 ml spectroscopic grade chloroform. The solution was filtered through a 0.45 μm Nylon filter and allowed to solidify. The solid material was crushed and dried for several hours (more than 48 h) in a vacuum ($\sim 10^{-2}$ Torr) oven maintained at 60^0C, which was above the T_g of the polymer. After thorough drying, the material was crushed to powder using a clean spatula.

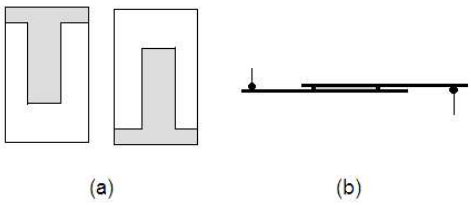

Figure 6.3: (a). Etched pattern of ITO on glass and (b). Side view of sandwich cell for photorefractive studies.

The final step was done by keeping the assembled glass cell on a hot plate and a small amount of the above powder was placed near the opening of the cell. Temperature was raised till the powder melted, after careful examination for bubbles or other objects, the melt was forced to touch the opening of the cell. The melt moved into the cell due to capillary action. Enough time was allowed for completely filling the area between the electrodes. The sample was rapidly cooled by placing it on an ice cube. After cooling, the edges of the plates were sealed using two component resin adhesive and kept for setting. Samples prepared in this method were able to withstand high electric fields (up to 65 V/μm) and they were of high optical clarity. All subsequent measurements were done at room temperature (28 ± 1^0 C).

6.2.2 Optical absorption and glass transition

The optical absorption of the composite was taken using a Jasco V-570 spectrophotometer. Fig. 6.4 shows the absorption spectrum of the system. The absorption coefficient at 632 nm was estimated to be 73 cm^{-1}.

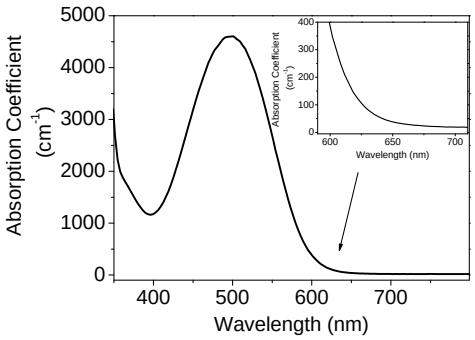

Figure 6.4: Absorption spectrum of the polymer system prepared.

The absorption in the visible region was dominated by the absorption of the Disperse Red 1 dye. The absorption spectrum of the dye in chloroform is shown in Fig. 6.5.

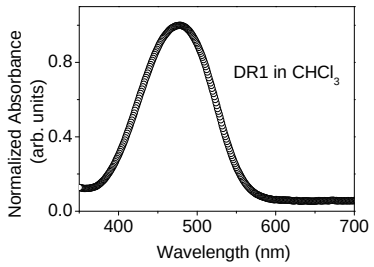

Figure 6.5: Absorption spectrum of Disperse Red 1 in chloroform.

The absorption band in the visible region is due to the strong internal charge transfer (ICT) occurring in the dye.[11] The glass transition temperature of the composite was lowered by the plasticizing action of ECZ to 33^0C. Nonlinear optical chromophores are also capable of plasticizing the

polymer. The differential scanning calorimetry trace of the composite is shown in Fig. 6.6.

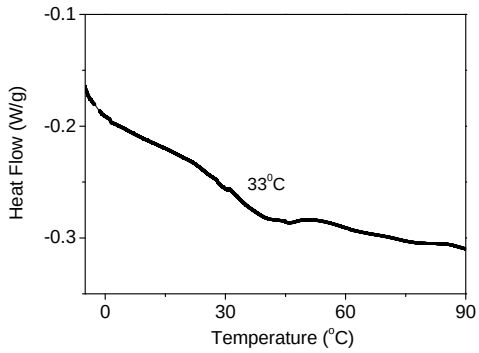

Figure 6.6: Differential scanning calorimetry trace of the prepared composite.

The low T_g of the system facilitated the rotation of the chromophores under an applied electric field, which was expected to give an "orientational enhancement" of gain coefficient.[12] In such a case, the refractive index modulation is not due to Pockels effect, which relies on the molecular first hyperpolarizability and a macroscopic second order susceptibility ($\chi^{(2)}$), alone. Field induced alignment of the chromophores with a polarizability anisotropy lead to a field dependent change in the first order susceptibility ($\chi^{(1)}$).[12] This additional mechanism causes larger refractive index modulations and is operative in low T_g high efficiency photorefractive polymers.[13]

6.2.3 Photoconductivity

The sandwich cell was tested for photoconductivity using the DC photocurrent method. A storage oscilloscope (Tektronix TDS210) used to record the current thought the sample as illumination was given. Illumination source was a 10 mW He-Ne laser at 632.8 nm. The response of the sandwich cell to light is shown in Fig. 6.7.

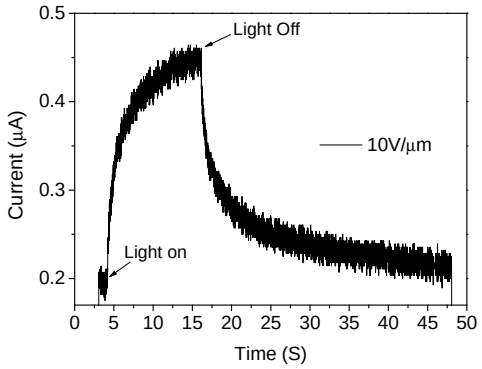

Figure 6.7: Variation of current through the sandwich cell with and without illumination.

The photoconductive sensitivity of the polymer system was evaluated using the steady state photocurrent and was found to be 1.25 x 10^{-10} S cm W^{-1}. The time taken to reach steady state was approximately 10 seconds.

6.2.4 Electro-optic effect

Refractive index modulation in photorefractive materials is due to the electro-optic effect. In the present case, to bring about electro-optic effect, the molecule Disperse Red 1 (DR1) was used. This molecule has a first hyperpolarizability (β) value of 125 x 10^{-30} esu and a ground state dipole moment of 8.72 Debye.[14] The glass transition temperature of the composite was low, which will allow the reorientation of the doped dipolar molecules under the applied electric field. The refractive index modulation could be due to birefringence, Pockels effect and Kerr effect.[13] The birefringence n_p-n_s was calculated by keeping the sample in between two crossed polarizers and measuring the transmitted intensity as a function of applied field as described by Roberto et. al.[15] In this configuration, the sample acts as a retardation plate with field dependent retardation. The detected intensity is given by,[15]

$$I = I_{max} sin^2 \left(\frac{\pi d \triangle n}{\lambda} - \frac{\psi}{2} \right) \tag{6.1}$$

Here I_{max} is the light intensity transmitted through the sample, d is the total optical path length within the sample, λ is the wavelength and ψ is the phase retardation introduced by a quarter wave plate kept before the sample. Measurement of the transmitted intensity was done as a function of applied field and the birefringence ($\triangle n$) was calculated. The quantity n_p-n_s showed a field dependence as shown in Fig. 6.8.

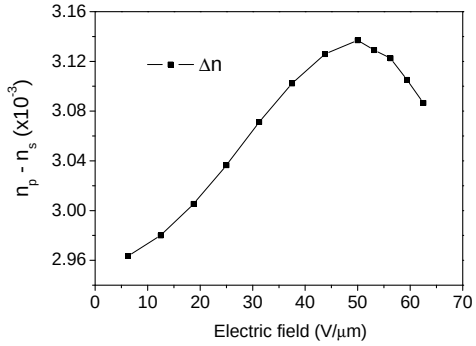

Figure 6.8: Field dependence of birefringence in the polymer system due to the field induced rotation of the dipolar molecules.

The above graph shows that the field induced reorientation of the chromophores was active in the system. The birefringence measured at 62.5 V/μm was 3 x 10^{-3}. In a highly efficient photorefractive system reported, the birefringence was 7.1 x 10^{-3} at an electric field of 81 V/μm.[5]

As contribution from birefringence was found to be dominant, for characterizing the electro-optic response of this low T_g system, the electro-optic response function was used.[16] The experiential setup was same as the one used for the electro-optic characterization described in Section 1.6.6. The response functions are given by,

$$R(\Omega) = \frac{3I_m(\Omega)\lambda G d}{\pi n^3 I_i V_B V_{AC}} \quad and \quad R(2\Omega) = \frac{3I_m(2\Omega)\lambda G d}{\pi n^3 I_i V_{AC}^2} \tag{6.2}$$

Here I_m is the modulated intensity measured as a function of the frequency (Ω) of the applied ac voltage of magnitude V_{AC} and I_i is the transmitted intensity without any fields. I_m were also measured at the second harmonic

of the modulation frequency using the lock-in-amplifier. For a refractive index (n) of 1.67 and incident angle of 45^0, the geometrical factor[16] G was equal to 5. V_B is the constant voltage maintained across the device, which was 1V in the present case, due to the limitations of the modulator. The response functions were evaluated at the modulation frequency R(Ω) and its second harmonic, R(2Ω). Fig. 6.9 shows the electro-optic response functions of the polymer system.

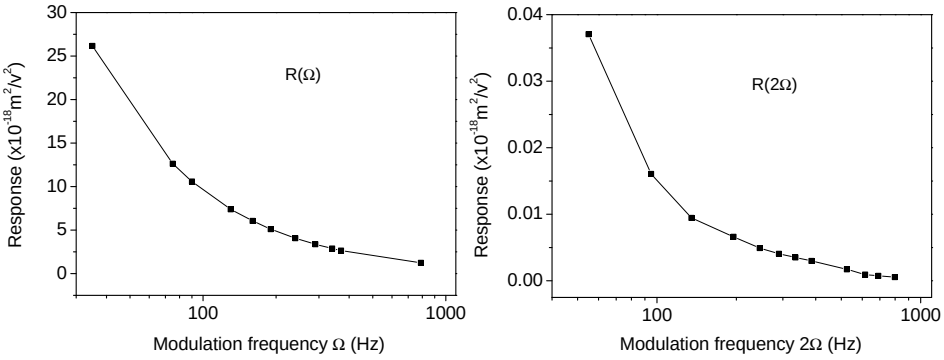

Figure 6.9: The electro-optic response function of the polymer system as a function of the frequency of the applied ac field.

6.3 Test of photorefractive nature of gratings

A polymeric system with photoconductivity and an electrooptic response may not necessarily be photorefractive. Also, the presence of non-photorefractive gratings cannot be ruled out in a photorefractive polymer. Other types of gratings of physical or chemical origin may coexist with a truly photorefractive grating. The proof for the photorefractive nature of the gratings can only be demonstrated with the two beam coupling (TBC) experiment. In TBC experiment, the intensities of the grating writing beams are monitored after the passage through the photorefractive sample. The experimental setup of the two beam coupling experiment is shown in Fig. 6.10

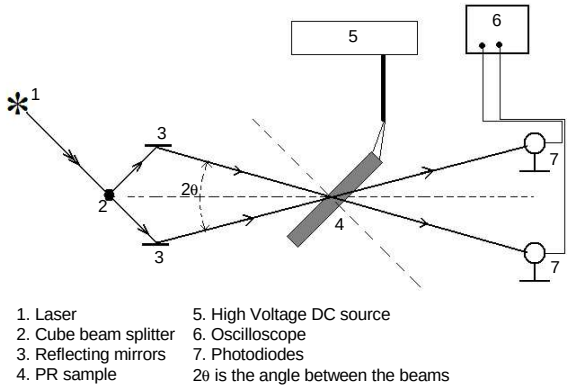

Figure 6.10: The two beam coupling experiment.

The presence of other types of gratings (due to chemical or physical changes) can be understood by monitoring the intensity of the beams. A simultaneous increase (decrease) of both the writing beams must be due to a decrease (increase) of the absorption coefficient of the sample which is in phase with the illumination pattern. Unaltered intensities may be due to the absence of any type of gratings or due to an in phase refractive index grating or a 90^o phase shifted absorption grating.[17] A photorefractive grating will induce an asymmetric energy coupling between the two writing beams. That is, one beam will be amplified and the other attenuated.

6.3.1 Two beam coupling experiment

The experiment was done in the tilted geometry to have a component of the applied electric field along the grating wave vector. Two s-polarized laser beams were made to interfere inside the photorefractive sample. Beam intensities were $\sim$1 W/cm^2 for both the laser beams. Inter-beam angle was 30^0 and the angles between the normal to the sample surface and the interfering beams were 25^0 and 55^0. The intensities of both the beams after traversing the sample were monitored after the application of electric field. The absorption within the sandwiched sample showed an increase with applied field as evidenced by the reduction in intensity of both beams when the electric field was applied. The experiment was performed only

after the field induced change reached a steady value. For fields above 40 V/μm, measurable intensity changes were observed in one beam when the other beam was interrupted. The change in intensity of beam 1 on introducing beam 2 is shown in Fig. 6.11 for 62.5 V/μm.

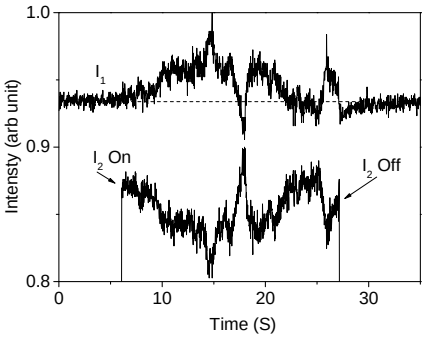

Figure 6.11: The two beam coupling effect. Intensity of Beam 1 increased as Beam 2 was introduced. Electric field was 62.5 V/μm.

Fig. 6.11 shows the two beam coupling effect in the sample proving the system to be photorefractive. It can be seen that the two beam energy transfer persists and reaches a steady state. There were transient energy transfers occurring during the experiment as can be seen in Fig. 6.11, which is reported to be due to local gratings of origin other than photorefractive effect.[12] The gain coefficient was evaluated as described in Section 1.2 using the steady state values of the beam intensities and their interaction length. The gain coefficient can be related to the refractive index modulation ($\triangle n$) and the intensities I_1 and I_2 of the interfering beams by the equation,

$$\Gamma = \frac{4\pi}{\lambda}\frac{\triangle n}{m} sin(\Phi), \tag{6.3}$$

where λ is the wavelength of laser and m is the modulation depth given by $m = 2\sqrt{I_1 I_2}/(I_1 + I_2)$. The quantity Φ is the phase shift between the illumination pattern and the resultant refractive index grating. Determination of phase shift can be done by shifting the interference pattern or the sample at a rate greater than the response tie of the photorefractive

grating and noting the change in intensities of the passing beams[18] but this could not be done experimentally. If the maximum phase shift of 90^0 (occurs only for gratings formed by diffusion of charges) is assumed for the grating, it corresponds to a refractive index modulation of 4.4 x 10^{-5} for a gain coefficient of 8.8 cm^{-1}. Fig. 6.12 shows the variation of the gain coefficient Γ with applied field.

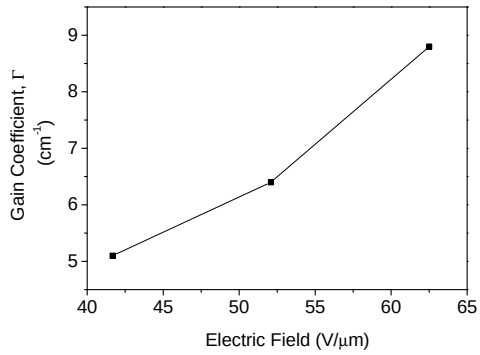

Figure 6.12: Field dependence of the two beam coupling gain coefficient.

6.3.2 Diffraction efficiency

The diffraction efficiency was determined using the four wave mixing geometry as shown in Fig. 6.13. In this, two s-polarized laser beams of power density 1.1 W/cm^2 derived using a beam splitter at the output of a He-Ne laser (30mW, Melles Griot) was used to create an interference pattern inside the sample. Another p-polarized weak laser beam was made to counter propagate one of the writing beams and the diffracted signal was detected using a photodiode. Orthogonal polarization direction of the probe beam reduce its interaction with the interfering beams. The p-polarized beam was chopped using a mechanical chopper and the diffracted beam intensity was measured using a lock-in-amplifier tuned to the chop-

ping frequency.

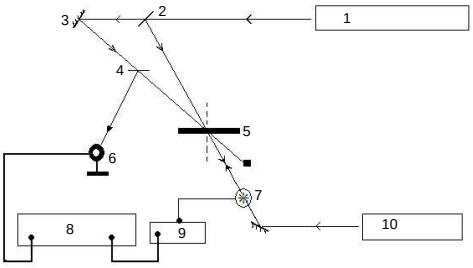

1. He-Ne laser (s-polarized)
2. Beam splitter
3. Mirror
4. Beam splitter
5. Photorefractive cell (power supply not shown)
6. Photodiode
7. Chopper
8. Lock-in-amplifier
9. Chopper controller
10. He-Ne laser (p-polarized)

Figure 6.13: Experimental arrangement for diffraction efficiency measurement in the four wave mixing geometry.

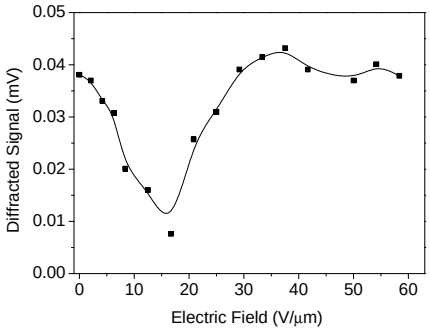

Figure 6.14: Intensity of diffracted signal as a function of applied voltage.

Non-photorefractive gratings were also present as evidenced by the diffraction of the beam in the absence of the external electric field. The diffracted signal from this mixed grating was measured as a function of electric field. The variation of the detected signal with field is shown in Fig. 6.14. The diffraction efficiency was calculated from the intensities as the ratio of diffracted intensity and incident intensity. The maximum diffraction efficiency was found to be 2 x 10^{-3} % and was not due to photorefractive gratings alone.

6.3.3 Response time

The response time of a photorefractive system determines the time required for steady state operation. It depends on many factors including the efficiency of charge generation, mobility of charges and the orientational mobility of the electro-optic chromophores. Photorefractive polymer with response time of 5 ms was reported by Wright et. al. and they concluded that the photoconductivity was the rate determining step.[4,19] Presence of dipolar molecules were also proposed to be the limiting factor of the photorefractive response time.[20]

The grating buildup time, measured in a four wave mixing geometry is considered to be the photorefractive response time. But in the present case, the diffraction efficiency could not be considered as due to photorefractive effect alone. Thus the response time was estimated from the two beam coupling data. The approximate time required to achieve the steady state coupling was determined from Fig. 6.11 as $\sim$ 5 s.

6.4 Summary and conclusions

A photorefractive polymer system was developed which showed a two beam coupling gain of 8.8 cm^{-1} at an electric field of 62.5 V/μm. The two beam coupling gain coefficient was very small compared to the optical absorption coefficient of the system. Hence no net gain was obtained from this system. Photoconductive sensitivity of the system was evaluated at 632.8 nm. Electro-optic response functions of this low T_g photorefractive system was also studied. The two beam coupling effect showed that the developed system was photorefractive. Presence of non-photorefractive gratings was also detected in diffraction efficiency measurements in the four wave mixing configuration.

References

[1] G. J. Steckman, R. Bittner, K. Meerholz, and D. Psaltis, "Holographic multiplexing in photorefractive polymers," Opt. Commun. **185,** 13–17 (2000).

[2] Y. Frauel, G. Pauliat, A. éVilling, and G. Roosen, "High-Capacity Photorefractive Neural Network Implementing a Kohonen Topological Map," Appl. Opt. **40,** 5162–5169 (2001).

[3] B. Kippelen, K. Tamura, N. Peyghambarian, A. B. Padias, and H. K. Hall, "Photorefractivity in a functional side-chain polymer," Phys. Rev. B. **48,** 10710–10718 (1993).

[4] D. Wright, M. A. Díaz-García, J. D. Casperson, M. DeClue, W. E. Moerner, and R. J. Twieg, "High-speed photorefractive polymer composites," Appl. Phys. Lett. **73,** 1490–1492 (1998).

[5] K. Meerholz, B. L. Volodin, Sandalphon, B. Kippelen, and N. Peyghambarian, "A photorefractive polymer with high optical gain and diffraction efficiency near 100%," Nature **371,** 497–499 (1994).

[6] D. J. Suh, O. O. Park, T. Ahn, and H.-K. Shim, "Observation of the photorefractive behaviors in the polymer nanocomposite based on p-PMEH-PPV/CdSe-nanoparticle matrix," Opt. Mater. **21,** 365–371 (2002).

[7] S. Tay *et al.*, "An updatable holographic three-dimensional display," Nature **451,** 694–698 (2008).

[8] Y. Chen, B. Zhang, and F. Wang, "Photorefractive material based on a polymer containing photoconductors and nonlinear chromophores," Opt. Commun. **228,** 341–348 (2003).

[9] A. V. Vannikov and A. D. Girishina, "The Phtorefractive Effect in Polymeric Systems," Russ. Chem. Rev. **72,** 471–488 (2003).

[10] C. J. Huang, Y. K. Sub, and S. L. Wu, "The effect of solvent on the etching of ITO electrode," Mater. Chem. Phys. **84,** 146–150 (2004).

[11] C. Toro, A. Thibert, L. D. Boni, A. E. Masunov, and F. E. Hernández, "Fluorescence Emission of Disperse Red 1 in Solution at Room Temperature," J. Phys. Chem. B **112,** 929–937 (2008).

[12] O. Ostroverkhova and W. E. Moerner, "Organic Photorefractives: Mechanisms, Materials, and Applications," Chem. Rev. **104,** 3267–3314 (2004).

[13] B. Kippelen, Sandalphon, K. Meerholz, and N. Peyghambarian, "Birefringence, Pockels, and Kerr effects in photorefractive polymers," Appl. Phys. Lett. **68,** 1748–1750 (1996).

[14] S. K. Lor, H. Hiraoka, P. Yu, L.-T. Cheng, and G. K. L. Wong, "Second harmonic characteristics of Disperse Red 1 doped polysulfones," J. Mater. Res. **10,** 2693–2696 (1995).

[15] R. Termine, I. Aiello, N. Godbert, M. Ghedini1, and A. Golemme1, "Light-induced reorientation and birefringence in polymeric dispersions of nano-sized crystals," Opt. Express **16,** 6910–6920 (2008).

[16] Sandalphon, B. Kippelen, K. Meerholz, and N. Peyghambarian, "Ellipsometric measurements of poling birefringence, the Pockels effect, and the Kerr effect in high-performance photorefractive polymer composites," Appl. Opt. **35,** 2346–2354 (1996).

[17] W. E. Moerner and S. M. Silence, "Polymeric Photorefractive Materials," Chem. Rev. **94,** 127–155 (1994).

[18] A. Grunnet-Jepsen, C. L. Thompson, and W. E. Moerner, "Measurement of the spatial phase shift in high-gain photorefractive materials," Opt. Lett. **22,** 874–876 (1997).

[19] G. Baüml, S. Schloter, and D. H. U. Hofmann, "Correlation between photoconductivity and holographic response time in a photorefractive guest host polymer," Opt. Comm. **154,** 75–78 (1998).

[20] J. Shakos, A. Cox, D. West, K. West, F. Wade, T. King, and R. Blackburn, "Processes limiting the rate of response in photorefractive composites," Opt. Commun. **150,** 230–234 (1998).

CHAPTER

SEVEN

Summary

7.1 Summary of the work

The photorefractive effect, which was considered an unwanted phenomenon, is now being looked at as a promising candidate for reversible holographic data storage. Researchers around the world are working on challenging problems with photorefractive polymer systems. Commercialization of photorefractive polymers requires reduced response time, low applied fields and high stability. As no single material can provide all these properties, a variety of materials are being studied and reported in the literature.

The aim of this work was to develop photorefractive polymer systems. The experimental techniques required for studying polymer photoconductors were surveyed and setup. Initially, a molecularly doped polymer system was made and studied. Due to the low sensitivity and instability of this system, new polymers were selected and studied. Chapters 2 and 3 deal with the studies done on these polymers. Out of four polymer photoconductors studied, the polymer Poly(6-tert-butyl-3-phenyl-3,4-dihydro-2H-1,3-benzoxazine) sensitized with C_{60}, was found to be highly sensitive in the entire visible region of the spectrum. The photoconductive sensitivity of this polymer was sufficient for photorefractive effect.

In chapter 4, the possibility of solvatochromic effect to elucidate the

first hyperpolarizability of a series of p-nitroaniline derivatives was explored. The electro-optic effect needed for the refractive index modulation was studied in chapter 5. Guest-host systems were made based on PMMA and electro-optic effect was observed. Also, the polymer Poly(3-methacrloyl-1-(4'-nitro-4-azo-1'-phenyl)phenylalanine-co-methyl methacrylate) showed electro-optic modulation without any electrical poling.

A variety of combinations were tried to make a single polymer system capable of showing both photoconductivity and electro-optic effect. Electro-optic molecules studied in Chapter 5 could not be used due to the miscibility problems with the polymer photoconductor Poly(6-tert-butyl-3-phenyl-3,4-dihydro-2H-1,3-benzoxazine) sensitized with C_{60}. The system made with this photoconductor and the molecule disperse red 1 showed photorefractive effect with a gain coefficient of 8.8 cm^{-1} at 62.5 V/μm. Electro-optic and photoconductive properties of this photorefractive system were also examined.

Importance of the present work is that it presented the very first observation of photorefractive effect in Poly(6-tert-butyl-3-phenyl-3,4-dihydro-2H-1,3-benzoxazine), which belong to a less studied class of polymers for optoelectronic applications. The main advantage is that these polymers can be easily synthesized with low cost chemicals. Observation of good photosensitivity in a polybenzoxazine may trigger studies on solar cells based on these polymers. The present study made some important observations on an electro-optic polymer which require deeper studies. The study was a success in the sense that the aim was achieved along with some results which may find applications in other areas also.

7.2 Outlook

This thesis discussed molecules suitable for photorefractive effect. Out of the molecules studied, only one system was used to make photorefractive polymers system. Other molecules, especially, the electro-optic polymer, Poly(3-methacrloyl-1-(4'-nitro-4-azo-1'-phenyl)phenylalanine-co-methyl methacrylate) can be subjected to more detailed studies to explore

the possibilities of using them for electro-optic applications. Though not included in the thesis, the efficient photoconductor, Poly(6-tert-butyl-3-phenyl-3,4-dihydro-2H-1,3-benzoxazine) sensitized with C_{60}, which was described in Chapter 3 showed a low magnitude photovoltaic effect. This hints at the possibility of using this system for organic solar cells also.

The thesis presented the initial observation of photorefractive effect in a polybenzoxazine based polymer system. A detailed analysis of the effect of C_{60}, ECZ and DR1 can be carried out to check for the possibility of a high efficiency photorefractive system.

INDEX